Unbiased Homomorphic System and its Application in Multiplicative Noise Reduction

Debashis Sen

A Thesis

in

The Department

of

Electrical and Computer Engineering

Presented in Partial Fulfillment of the Requirements
for the Degree of Master of Applied Science at
Concordia University,
Montreal, Quebec, Canada

April 2005

Your file Votre référence
ISBN: 0-494-04393-8
Our file Notre référence
ISBN: 0-494-04393-8

ABSTRACT

Unbiased Homomorphic System and its Application in Multiplicative Noise Reduction

Debashis Sen

Noise of a multiplicative nature is encountered in many applications such as coherent imaging, remote sensing and signal processing for communication systems.

This thesis is concerned with the problem of reducing the multiplicative noise corrupting a signal. A generalization of the existing sampled function weighted order (SFWO) filter is proposed by relaxing the symmetry condition for the probability density function (PDF) of the noise to the filter. This generalized SFWO (GSFWO) filter is then used within a homomorphic system to reduce the multiplicative noise. It is shown that the output from such a system is biased, and hence, a suitable bias compensation technique is suggested. An unbiased homomorphic system, whose design is based on the PDF of the corrupting multiplicative noise, is proposed to reduce the noise.

Images and videos generated by coherent imaging systems are always corrupted by speckle, which is a multiplicative noise having a lognormal distribution. A filter called the mean median (MM) filter to reduce additive white Gaussian noise (AWGN) is first proposed and this filter is then used within the unbiased homomorphic system to reduce the speckle in images.

Fast filters to reduce AWGN in videos are also proposed in this thesis. Novel techniques for temporal estimation employing a change detection technique to determine the interframe motion are developed for their use in these filters. A new method is proposed to appropriately combine the spatial and spatiotemporal estimates of the original signal in order to obtain the final output. Finally, the MM-filter along with a novel temporal estimation scheme are used within the unbiased homomorphic system to reduce the speckle in videos.

The effectiveness of the various proposed algorithms is demonstrated and compared with that of some of the existing schemes through extensive simulations.

ACKNOWLEDGEMENTS

I would like to express my profound gratitude to my supervisors, Dr. M. N. S. Swamy and Dr. M. O. Ahmad, for their expert guidance and support that made this research work possible. Exceptional researchers, they have been extremely careful, thorough and extraordinarily patient in their critical review of my thesis. It has been a great privilege to work with them which has resulted in the writing of a few invaluable research papers and reports. I sincerely thank Dr. Eugene I. Plotkin, Dr. Aishy Amer and Dr. Wei-Ping Zhu for insightful discussions on related topics at one point or other during the course of this thesis.

Enormous encouragement and support from my parents have always been the key factor behind every success in my life. I would like to take this opportunity to thank them for their love and sacrifices which have been pivotal to the success of this work. Many thanks are due to my close relatives and friends, especially to Jolly Sandhu, Parjanya Sen, Ranjana Sen, Ayushya Bangur, Harun Prasad, Amitabh & Aditi Barua, Ajit Singh, and Nikhil Gupta for their constant help and encouragement.

This work has been carried out at the Center for Signal Processing and Communications (CENSIPCOM), Concordia University.

Debashis Sen, April 2005

I dedicate this work to my

Mother, Dr. Sampa Sen, Father, Dr. Utpal Sen, and Nation, India.

Contents

List of Figures

List of Tables

List of Symbols

$\Omega(i)$	:	Output of the GSFWO filter
h_j	:	Unnormalized coefficients of the GSFWO filter
$E[\cdot]$	:	Expected value or mean
D, D^{-1}	:	Forward homomorphic transform and its inverse
$\Psi(i)$	:	A signal corrupted by a multiplicative noise
$\Phi(i)$	:	A multiplicative noise
L	:	Equivalent number of looks
$PDF[\cdot]$	:	Probability density function
U$\oplus$V	:	Either U or V
$V(\cdot,\cdot)$	:	Asymptotic variance
ARE_{MM}	:	Asymptotic relative efficiency with respect to MM-filter
$IF(\cdot)$	:	Influence function
γ	:	Coefficients of the MM-filter
$med[\cdot]$	:	Median value
EP	:	Figure of merit evaluating edge preservation
as	:	A signal corrupted by speckle
ns	:	Speckle noise
N, M	:	Number of rows and columns in an image
N_w, M_w	:	Number of rows and columns in a filter window used on an image
a_n	:	The $(n+1)^{th}$ frame of a video corrupted by AWGN

η_n	:	The AWGN corrupting the $(n+1)^{th}$frame of a video
b_n	:	The $(n+1)^{th}$frame of an uncorrupted video
$\hat{b}_n^s$	:	Spatial estimate of the $(n+1)^{th}$frame of an uncorrupted video
$\hat{b}_n^t$	:	Spatiotemporal estimate of the $(n+1)^{th}$ frame of an uncorrupted video
$\hat{b}_n$	:	Final estimate of the $(n+1)^{th}$frame of an uncorrupted video
VAR[$\cdot$]	:	Variance normalized with respect to largest greyscale value, 255.
W_n	:	Weight matrix for temporal filtering with respect to the $(n+1)^{th}$ frame

List of Abbreviations

MSE	:	mean square error
SFWO	:	sampled function weighted order
PDF	:	probability density function
GSFWO	:	generalized sampled function weighted order
MMSE	:	minimum mean square error
MLE	:	maximum likelihood estimate
AWGN	:	additive white Gaussian noise
MM	:	mean median
CDF	:	cumulative distribution function
SAR	:	synthetic aperture radar
MAP	:	maximum aposteriori
ENL	:	equivalent number of looks
MVU	:	minimum variance estimator
ARE	:	asymptotic relative efficiency
MAD	:	median of absolute deviation
FOM	:	figure of merit
LMMSE	:	linear minimum mean square error
AWA	:	adaptive weighted averaging
EBMA	:	exhaustive block matching algorithm
PSNR	:	peak signal to noise ratio

n D	:	n dimension
PSNRi	:	improvement in peak signal to noise ratio
DCT	:	discrete cosine transform
SMSER	:	signal to mean square error ratio
SMSERi	:	improvement in signal to mean square error ratio

Chapter 1

Introduction

Various kinds of noise get associated with a signal during the process of production, transmission and archiving of the signal. Noise is random in nature and has different attributes depending on its origin. The analysis and characterization of the signal as well as the performance of the techniques used for processing the signal are hindered by the presence of noise. Noise corrupting the signals can be broadly classified into signal independent and signal dependent noise.

Noise of an additive nature is a signal independent noise. Linear as well as nonlinear filters are used for reducing the additive noise [1, 2, 3]. Linear filters are easy to design and implement due to their mathematical simplicity and the existence of some desirable properties such as linearity. Linear filters that minimize the mean square error (MSE) between the desired response and the actual output of the filter can usually be found in closed form. For example, sample mean filter, which is a linear filter, is optimal in minimizing the MSE between the desired and the actual output, when used to diminish random additive white noise with a Gaussian distribution [1, 4].

In many instances, such as in the case of noise being non-additive or non-Gaussian, it might not be possible to find an acceptable linear filter. In such cases, nonlinear filters might be found useful. A comprehensive review of nonlinear filters for reducing additive non-

Gaussian noise is given in [2]. Order statistic filters, morphological filters and polynomial filters are a few examples of nonlinear filters. Order statistic filters are one of the most popular classes of nonlinear filters for reducing non-Gaussian noise and are based on theory of robust statistics [1]. Ranked-order filters, L-filters, alpha trimmed mean filters are a few examples of order statistic filters. L-filter gets its name from 'linear combination of order statistics' and many useful nonlinear estimators can be obtained by varying the coefficients of L-filter. Optimal coefficients of L-filter, which minimizes the MSE between the desired response and the actual output of the filter, can be obtained for a given noise distribution as described in [2].

Unfortunately, the design and implementation of nonlinear filters is not as easy as its linear counterparts. In [5], a new class of order statistic filter called *sampled function weighted order* (SFWO) filter has been proposed to reduce additive white noise. The performance of the SFWO filters is very close to the optimal L-filters, but its design is much easier.

Noise of a multiplicative nature is a signal dependent noise. Linear filters perform poorly while reducing multiplicative noise compared to the nonlinear filters. Homomorphic filter, which is a nonlinear filter, is one of the oldest and most popular filters for reducing corruption by a multiplicative noise [1].

1.1 Homomorphic Filters

In many applications of digital signal processing, both the desired and the undesired components of a signal are found to be mixed in nonlinear way. A signal corrupted by noise of a multiplicative nature is an example of such a mixture. Homomorphic filters [1] are a special class of nonlinear filters that can be used to reduce this undesired component of the signal.

The basic idea is to use a suitable nonlinear function to transform such a signal into ad-

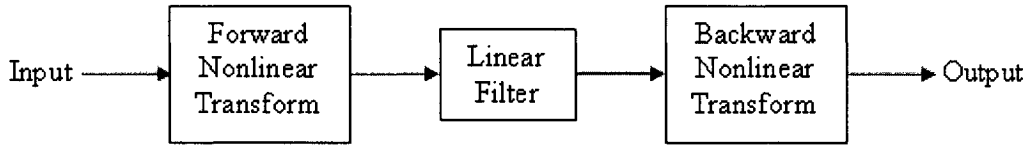

Figure 1.1: The classical homomorphic system

ditively combined ones and then to process the resulting signal using a linear filter. Then, the inverse of the nonlinear function is applied to the output of the linear filter. Thus, a linear filter, which is easier to design, is used between the forward and backward nonlinear transforms to reduce the nonlinearly related undesired components. The classical homomorphic system is shown in Figure 1.1. The nonlinear transforms used within a homomorphic system is also called the homomorphic transforms. When the noise is of a multiplicative nature, the forward and backward homomorphic transforms are respectively the natural logarithm and exponentiation.

1.2 Reduction of Multiplicative Noise using a Homomorphic System

There are many applications like radar imaging, ultrasonic imaging, and digital signal processing for communication systems, where multiplicative noise with different distributions are encountered. As mentioned earlier, a homomorphic system, which consists of a linear filter in between the natural logarithm and exponential transforms, could be used to reduce the multiplicative noise. As the natural logarithm transforms the multiplicative noise to an additive noise, the purpose of the linear filter is to reduce the additive noise. But, as mentioned earlier, the linear filter would perform satisfactorily only when the additive noise has a Gaussian distribution, which is the case when the original multiplicative noise has a lognormal distribution.

A nonlinear filter, which may be more useful in reducing an additive noise of non-

Gaussian nature, could be used instead of a linear filter within the homomorphic system. The SFWO filter proposed in [5] is a nonlinear filter with a simple design procedure; it could be used within the homomorphic system to reduce noise of a multiplicative nature. But, the design of the SFWO filter assumes the probability density function (PDF) of the additive noise to be symmetric, which unfortunately might not be the case after the application of the forward nonlinear transform to the original signal corrupted by a multiplicative noise. In addition, the design of the SFWO filter makes an assumption that the signal is of constant amplitude within a filter window, which may not always be true. For example, this assumption is not valid in the case of an image signal containing an edge within a filter window.

1.3 Scope and Organization of the Thesis

There are many filters that have been proposed to reduce additive white noise, based on the type of the PDF of the noise, for example, the optimal L-filters and the SFWO filters. In order to reduce noise of a multiplicative nature, a filter whose design is based on the PDF of the noise would be desirable. To the best knowledge of the author, such a problem has not been dealt with. This thesis looks into the problem of designing a filter to reduce the noise of a multiplicative nature, based on the type of noise distribution. This thesis is also concerned with the reduction of speckle, in images and videos, speckle being a multiplicative noise whose PDF approximately follows a lognormal distribution [6].

The organisation of the thesis is as follows. In Chapter 2, we first briefly review some of the existing nonlinear filters such as the ranked order filter, L-filter and SFWO filter from the point of view of reducing an additive noise. The design of all these filters assumes that the PDF of the noise is symmetric. We generalize the SFWO filter by relaxing the symmetry condition for the PDF of the noise. Next, a homomorphic system is presented to reduce noise of a multiplicative nature by replacing the linear filter in Figure 1.1 by the

proposed generalized SFWO (GSFWO) filter. It is shown that the output from the homomorphic system is biased; hence, a suitable bias compensation technique is introduced after carrying out the exponentiation to get the unbiased estimate. Finally, the performance of the proposed unbiased homomorphic system to reduce the multiplicative noise in images is studied and compared with that of a few other existing filters.

In Chapter 3, reduction of speckle in images using a homomorphic system is considered. As mentioned earlier, the speckle is a multiplicative noise, whose PDF approximately follows a lognormal distribution [6]; it gets converted to an additive Gaussian noise after the natural logarithm operation. In such a case, the unbiased homomorphic system proposed in Chapter 2 reduces to the classical homomorphic system followed by the bias compensation as shown in Figure 1.2, where the linear filter is the sample mean filter. The design of the sample mean filter, which is optimal in both the minimum mean square error (MMSE) sense and the maximum likelihood estimate (MLE) sense when used to diminish a random additive white Gaussian noise (AWGN) [1, 4], assumes that the uncorrupted signal to the filter is of constant amplitude within the filter window. For this reason, we propose a nonlinear filter, which is referred to as the *mean median* (MM) filter to reduce the additive Gaussian noise corrupting the signal to the filter. The performance of the proposed MM-filter to reduce additive Gaussian noise in images is studied and compared with that of the sample mean filter and the edge-adaptive Wiener filter [7]. Next, an unbiased homomorphic system is presented to reduce the speckle by replacing the linear filter in Figure 1.2 by the proposed MM-filter. Finally, the performance of the MM-filter-based unbiased homomorphic system to reduce speckle in images is studied and compared with that of a few existing ones.

When the reduction of speckle in videos using a homomorphic system is considered, a filter suitable to reduce AWGN would be used between the forward and backward nonlinear transforms. In Chapter 4, we propose two fast filters to reduce AWGN in videos, where the interframe motion is measured using a change detection technique between frames, instead

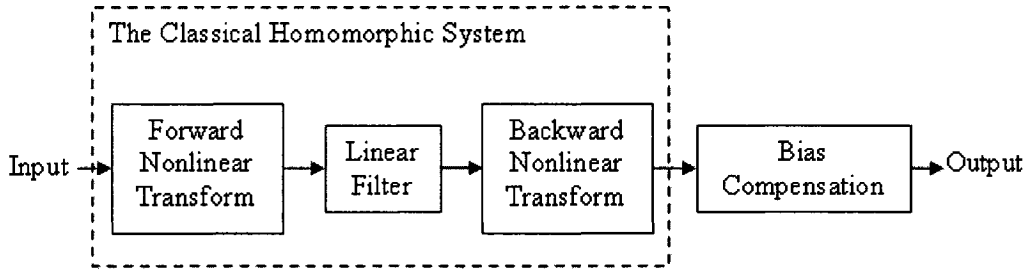

Figure 1.2: An unbiased homomorphic system to reduce speckle

of the commonly used complex motion estimation and compensation technique [8]. The two filters use novel fast temporal estimation methods based on the Kalman filter [4] and the running average filter, respectively. The final output of the proposed video filters is obtained by an adaptive combination of the spatial and spatiotemporal estimates of the original signal. Quantitative and qualitative performance of the proposed filters to reduce AWGN in videos is studied and compared with that of a few existing ones.

In Chapter 5, a fast unbiased homomorphic system to reduce speckle in videos is proposed. A detailed description of the algorithm, which uses the MM-filter proposed in Chapter 3 for spatial estimation and the technique based on the running average filter proposed in Chapter 4 for temporal estimation, is given. Quantitative and qualitative results of the proposed system to reduce speckle in a video are studied and compared with those of the two existing filters.

The thesis concludes with Chapter 6 by providing an overview of the contributions made along with a few suggestion for future research.

Chapter 2

An Unbiased Homomorphic System to Reduce a Multiplicative Noise

2.1 Introduction

Signal corrupted by noise of a multiplicative nature is often encountered in many applications such as coherent imaging systems and nonlinear communication channels. Filters to reduce speckle, which is a specific type of multiplicative noise, have been proposed by many authors [6][9]-[14]. However, the reduction of a multiplicative noise of a general nature, has seldom been considered. As in most applications, the PDF of the noise is known or can easily be determined; it would be desirable to have a system, for the reduction of multiplicative noise, whose design is based on the PDF of the noise.

The design of such a filter is proposed in this chapter [15, 16]. The design of the filter assumes the multiplicative noise to be stationary, white and uncorrelated to the uncorrupted original signal. The proposed filter belongs to the special class of nonlinear filters, namely, the homomorphic filter/system introduced in Chapter 1. As explained in Chapter 1, to reduce the multiplicative noise, a homomorphic system uses the natural logarithm to transform the multiplicative nature of corruption into an additive one and then processes the

resulting corrupted signal using a filter to reduce the additive white noise. An exponential function is then applied to the output of the filter. If a linear filter is used to reduce the additive white noise, it would not be effective when the additive noise has a non-Gaussian distribution, that is, the original multiplicative noise has a non-lognormal distribution. In such a case, a nonlinear filter might prove to be useful. The SFWO filter proposed in [5], which is a nonlinear filter and is easy to design, could be used as the filter to reduce the additive white noise provided the PDF of the noise is symmetric. Unfortunately, the additive noise obtained after the natural logarithm operation within the homomorphic system might not have a symmetric distribution.

A generalization of the SFWO filter is proposed in this chapter relaxing the symmetric PDF condition of the additive noise. The GSFWO filter is then used between the natural logarithm and the exponential functions to obtain a homomorphic system to reduce noise of a multiplicative nature. It is shown that the output after the exponentiation would be biased and hence, a bias compensation technique is applied to the output to get the unbiased estimate.

The organisation of this chapter is as follows. In Section 2.2, a brief description of a few order statistic-based nonlinear filters is given. Section 2.3 presents the derivation of the GSFWO filter. Section 2.4 describes the classical homomorphic system. The spatial domain unbiased homomorphic system to reduce multiplicative noise is presented in Section 2.5. In Section 2.6, the performance of the proposed unbiased homomorphic system to reduce multiplicative noise is studied and compared to the performance of a few known filters.

2.2 Order Statistic-Based Nonlinear Filters

In this section, a description of a few order statistic filters is given. Order statistics have been found useful in the statistical data analysis, particularly in the robust analysis of

data corrupted by outlying observations. Let X be a random variable, and its samples X_1,X_2,.....,X_N be arranged in an ascending order of magnitude, say,

$$X_{(1)} \leq X_{(2)} \leq \cdots \leq X_{(N)} \tag{2.1}$$

In the above, $X_{(i)}$is called the ith order statistics; X_i, $i = 1, \cdots, N$ are generally assumed to be independent identically distributed (i.i.d) random variables.

Order statistic-based nonlinear filters are popular in reducing additive noise with a non-Gaussian distribution. Ranked-order filters, L-filters, alpha trimmed mean filters are a few examples of order statistic filters. A brief description of each of these filters is given in the following subsections.

2.2.1 Ranked-Order Filters

An rth ranked-order filter [2] is given by

$$\text{RO}(X_1, X_2, \cdots\cdots, X_N; r) = X_{(r)} \tag{2.2}$$

As can be seen, the rth ranked-order filter selects out the rth order statistic of the samples $X_1, X_2, \cdots\cdots X_N$ present within the filter window. A few special cases of this filter are the sample median filter ($r = \lceil \frac{N}{2} \rceil + 1$), the maximum operation ($r = N$) and the minimum operation ($r = 1$), where $\lceil M \rceil$ stands for the largest integer less than M. The sample median filter is known to have a good edge preservation property. But, some low-order ranked-order filters with $r < \lceil \frac{N}{2} \rceil$ have been found to have a better denoising capability for various noise distributions than the sample median filters. The ranked-order filters are also known as the percentile filters.

2.2.2 L-Filters

An L-filter is obtained by a linear combination of order statistics. Linear combinations of order statistics have been found to be robust and often have optimal properties for estimating population parameters for i.i.d. observations. The expression of a L-filter is given by

$$L(X_1, X_2 \cdots\cdots, X_N; \mathbf{a}) = \sum_{i=1}^{N} a_i X_{(i)} \tag{2.3}$$

where $\mathbf{a} = (a_1, a_2 \cdots\cdots, a_N)^T$ is the coefficient vector of the L-filter. By varying the coefficients, which are normalized ($\sum_{i=1}^{N} a_i = 1$), one can obtain many useful estimators. The optimal design of L-filters to reduce an additive white noise is presented in [2]. The design is based on the distribution of the noise and assumes that the original signal is constant within a filter window. The optimal coefficients of the L-filter are given by

$$\mathbf{a} = \frac{\mathbf{R}^{-1}\mathbf{e}}{\mathbf{e}^T\mathbf{R}^{-1}\mathbf{e}} \tag{2.4}$$

where $\mathbf{R}$ is the correlation matrix of the noise and $\mathbf{e}$ is the unity vector. As stated in [5], this optimal design of the L-filter is cumbersome and can be achieved only by using complex numerical methods.

2.2.3 Alpha-Trimmed Filter

The sample median filter removes impulses (outliers) and preserves edges, but its performance in reducing the MSE between the desired response and the actual output is inferior to that of a sample mean filter [17], when applied to reduce an additive noise. Therefore, a compromise between the sample mean and sample median filter that would reduce the MSE and also preserve edges satisfactorily is desired. Such a filter is the alpha-trimmed

filter. Alpha-trimmed filter is defined by:

$$\mathrm{ATr}(X_1, X_2 \cdots\cdots X_N; \alpha) = \frac{1}{N - 2\alpha N} \sum_{i=\alpha N+1}^{N-\alpha N} X_{(i)} \tag{2.5}$$

A few samples amongst those within the filter window arranged in an ascending order are discarded at each end, and the output obtained by taking the average of the rest. The number of samples trimmed at each end depends on the value of α.

2.2.4 SFWO Filters

A new class of order statistic filters called the sampled function weighted order (SFWO) filter was proposed in [5]. The coefficients of this filter are samples of a bounded real-valued function. This real-valued function is derived for any given noise distribution by examining the asymptotic behavior of the coefficients of the corresponding L-filter. A good compromise between the alpha-trimmed mean filters, which are easy to design, and the optimal L-filters, which are more flexible but difficult to design, is achieved using the SFWO filter. A SFWO filter is given by

$$\mathrm{SFWO}(X_1, X_2 \cdots\cdots, X_N; \mathbf{a}) = \frac{\sum_{j=1}^{N} a(t_j) X_{(j)}(i)}{\sum_{j=1}^{N} a(t_j)} \tag{2.6}$$

where **a** is the unnormalized coefficient vector, which can be obtained for any given noise distribution. The design of SFWO filters to reduce an additive white noise based on the distribution of the noise is presented in [5]. The design assumes that the original signal is constant within a filter window and the PDF of the noise is symmetric. This design of SFWO filter is much simpler compared to that of the L-filter.

2.3 Generalization of the Sampled Function Weighted Order (SFWO) Filter

In this section, a generalization of the SFWO filter to reduce an additive white noise is proposed by relaxing the symmetry condition of the noise PDF. This design extends the usability of the filter to applications where additive noise with asymmetric PDF is encountered, e.g., a homomorphic system. As in [5], the classical problem of estimating a constant amplitude signal Λ from the additively corrupted observed samples $\Upsilon(i)$ within a filter window is considered:

$$\Upsilon(i) = \Lambda + n(i) \tag{2.7}$$

where $n(i)$ is assumed to be a stationary, white, zero-mean noise. It is also assumed that the uncorrupted signal Λ and the noise n are uncorrelated to each other. However, no assumption about the shape of the noise PDF is made, unlike the design given in [5]. Equation (2.7) can be rewritten as

$$\Upsilon(i) = \Lambda + \sigma v(i) \tag{2.8}$$

where $\sigma > 0$ is the standard deviation of $n(i)$. Thus, with this normalization $v(i)$ becomes a zero-mean unit-variance noise. Let the filter window be of size R x R. All the elements within that window, when put in an array in an ascending order of magnitude, can be expressed as

$$\Upsilon_{(1)}(i) \leq \Upsilon_{(2)}(i) \leq \Upsilon_{(3)}(i) ..... \leq \Upsilon_{(r)}(i),\ r = R^2 \tag{2.9}$$

The output of the GSFWO filter is given as

$$\Omega(i) = \frac{\sum_{j=1}^{r} h_j \Upsilon_{(j)}(i)}{\sum_{j=1}^{r} h_j} \tag{2.10}$$

where h_j stands for the unnormalized coefficients of the GSFWO filter, which will be determined using this design. All the noise elements within the filter window are assumed

to be i.i.d random values and thus, the observed corrupted samples will also be i.i.d samples. Dropping the index i for simplicity, each element of the array can be represented as

$$\Upsilon_{(j)} = \Lambda + \sigma v_{(j)}, j = 1, 2, 3....r \tag{2.11}$$

Let

$$C_{jk} = E[v_{(j)} - v_{(k)}] - E[v_{(j)}]E[v_{(k)}] \tag{2.12}$$

be the elements of the covariance matrix of v and $j, k = 1, 2, 3 \ldots\ldots r$, and $E[\cdot]$ stands for the expected value. From (2.11), it is clear that the order in Υ is the same as that in v. The MMSE criterion [1] is considered here to determine the coefficients of the GSFWO filter. The MSE between the corrupted signal Υ and the recovered signal Ω can be expressed as

$$E[(\Omega - \Lambda)^2] = E[\Omega^2] - 2E[\Omega\Lambda] + E[|\Lambda^2] \tag{2.13}$$

Substituting the expression for Ω from (2.10), we obtain

$$E[(\Omega - \Lambda)^2] = \frac{\sum_{j=1}^{r}\sum_{k=1}^{r} h_j h_k(\widetilde{E}[\Upsilon_{(j,k)}, \Lambda])}{\sum_{j=1}^{r}\sum_{k=1}^{r} h_j h_k} \tag{2.14}$$

where

$$\widetilde{E}[\Upsilon_{(j,k)}, \Lambda] = E[\Upsilon_{(j)}\Upsilon_{(k)}] - 2E[\Lambda\Upsilon_{(j)}]E[\Lambda\Upsilon_{(k)}] + E[\Lambda^2]$$

By simple algebraic manipulation, it can be shown that the result of minimization of the MSE given by (2.14) will yield the solution:

$$\sum_{j=1}^{r} h_j C_{jk} = 1 \tag{2.15}$$

and hence, the coefficients of the GSFWO filter are given by

$$h_j = \sum_{k=1}^{r} \bar{C}_{jk} \tag{2.16}$$

Here $\bar{C}_{jk}$ represents the elements of the inverse covariance matrix of v. Let the standard PDF of the additive noise v be $f_v(v)$ and the cumulative distributive function (CDF) of v be represented by $F_v(v)$.

Now, to obtain the values of the coefficients given by (2.16) their asymptotic behaviour ($r \rightarrow \infty$) shall be examined. As presented in [18], the samples of v, $v_{(j)}$ and $v_{(k)}$, given in (2.11) and (2.12) are asymptotically distributed (as $r \rightarrow \infty$) according to the normal bivariate distribution with the covariance:

$$C_{jk} = \frac{\lambda_j(1-\lambda_k)}{r f_v(v_j) f_v(v_k)}, \; 1 \leq i \leq j \leq r \tag{2.17}$$

where

$$\lambda_j = \frac{j}{r+1} \text{ and } v_j = F_v^{-1}(\lambda_j)$$

It is assumed in (2.17) that $f_v(v)$ is nonzero. It is also assumed that f_v' and f_v'' exist for $F_v^{-1}(0) < v < F_v^{-1}(1)$. As the covariance matrix is singular in nature, the well known Moore Penrose equations [19, 20] are used to find the elements of its pseudo-inverse and the matrix thus obtained is considered as the inverse covariance matrix. Thus, the elements of the inverse covariance matrix are derived as

$$\begin{aligned}
\bar{C}_{jj} &= \frac{2r f_v^2(v_j)}{\Delta\lambda(1-j\Delta\lambda)}, \; 1 \leq j \leq r-1 \\
\bar{C}_{jk} &= \frac{-r f_v(v_j) f_v(v_k)}{\Delta\lambda(1-j\Delta\lambda)}, \; j,k = 1,2,3...r-1, \mid j-k \mid = 1 \\
\bar{C}_{rr} &= \frac{r f_v^2(v_r)}{\Delta\lambda(1-r\Delta\lambda)} \\
\bar{C}_{jk} &\approx 0, \quad \text{for } \mid j-k \mid > 1
\end{aligned} \tag{2.18}$$

where

$$\Delta\lambda = \frac{1}{r+1}$$

Now, substituting the expressions for inverse covariance matrix elements given by (2.18) into the expression for the coefficients of the GSFWO filter given by (2.16), we get

$$\begin{aligned} h_j &= \frac{2rf_v^2(v_j)}{\Delta\lambda(1-j\Delta\lambda)} - \frac{rf_v(v_j)f_v(v_{j-1})}{\Delta\lambda(1-j\Delta\lambda)} - \frac{rf_v(v_j)f_v(v_{j+1})}{\Delta\lambda(1-j\Delta\lambda)} \\ &= -rf_v(v_j)\frac{1}{\Delta\lambda}\left[\frac{f_v(v_{j-1}) - 2f_v(v_j) + f_v(v_{j+1})}{1-j\Delta\lambda}\right] \\ &= -rf_v(v_j)\frac{1}{\Delta\lambda}\left[\frac{\delta^2 f_v(v_j)}{1-j\Delta\lambda}\right] \end{aligned}$$

or

$$h_j = -rf_v(v_j)\frac{1}{1-j\Delta\lambda}\left[\frac{\delta^2 f_v(v_j)}{(\Delta\lambda)^2}\right]\Delta\lambda \tag{2.19}$$

where $\delta^2(\cdot)$ is the second central difference. As can be seen, when $r \to \infty$ (asymptotic behavior), $\Delta\lambda \to 0$ and $(1 - j\Delta\lambda) \to 1$. Applying the limit $\Delta\lambda \to 0$ in (2.19), we get

$$H(\lambda) = \lim_{\Delta\lambda\to 0} h_j = -rf_v(v)\frac{d^2 f_v(v)}{d\lambda^2}d\lambda \tag{2.20}$$

Now, let $\phi_v(v) = \ln(f_v(v))$. Since $\dot{\lambda} = F_v(v)$, we get $d\lambda = f_v(v)dv$. Thus, (2.20) reduces to,

$$H(\lambda) = -r\phi_v''(v)d\lambda,\ 0 < \lambda < 1 \tag{2.21}$$

The multiplying term $-r$, which is independent of λ, will eventually be cancelled when the coefficients are normalized by putting them in the form of (2.10). Hence, omitting this term, we get

$$H(\lambda) = \phi_v''(v)d\lambda,\ 0 < \lambda < 1 \tag{2.22}$$

Similar to the one proposed in [5], to obtain the coefficients, we consider a special form $h(\cdot)$ of $H(\cdot)$:

$$h(\lambda) = \phi_v''(v),\ 0 < \lambda < 1 \tag{2.23}$$

It should be noted that h_j could be obtained from the expression of $h(\lambda)$ by sampling at intervals of $\frac{1}{n+1}$, for $0 < \lambda < 1$. Now, substituting the value of v from (2.17), we can write (2.23) as

$$h_j = \phi_v''\left(F_v^{-1}\left(\frac{j}{r+1}\right)\right), j = 1, 2, 3...r \tag{2.24}$$

Equation (2.24) gives the expression for the coefficients of the GSFWO filter, during whose design the symmetry condition of the noise PDF assumed for the design of the SFWO filter has been relaxed. Similar to the SFWO filter, the GSFWO filter has the following properties:

1. It is asymptotically efficient (that is, it satisfies the Cramer Rao lower bound [21]).

2. It can be designed with a simple methodology that does not require excessive computation as is the case with the design of L-filters.

3. It does not require redesigning when the data size changes, unlike in the classical L-filter design.

2.4 The Classical Homomorphic System

In many digital signal processing applications, both the desired and undesired components of the signals mixed in a nonlinear way are encountered. Linear processing techniques are not effective in such cases. Therefore, a special class of filters has been developed for processing signals that have nonlinearly related components. They are called homomorphic

filters/systems. The block diagram of the classical homomorphic system is shown in Figure 2.1 [1].

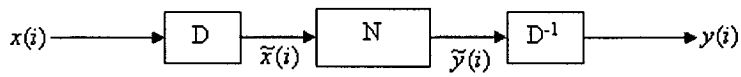

Figure 2.1: The block diagram of the classical homomorphic system.

In Figure 2.1, D stands for the forward homomorphic transform and D^{-1} for the inverse transform. The function D is chosen such that it transforms the input signal $x(i)$ to another signal $\tilde{x}(i)$, where all the components are additively mixed. N stands for a linear filter which is applied after the forward transformation.

Let two signals $x_1(i)$ and $x_2(i)$ be combined by the nonlinear operation $\star$:

$$x(i) = x_1(i) \star x_2(i) \tag{2.25}$$

When $x(i)$ passes through the homomorphic system H, we have:

$$\tilde{x}(i) = D[x(i)] = D[x_1(i)] + D[x_2(i)] = \tilde{x}_1(i) + \tilde{x}_2(i) \tag{2.26}$$

$$\tilde{y}(i) = N[\tilde{x}(i)] = N[\tilde{x}_1(i) + \tilde{x}_2(i)] = \tilde{y}_1(i) + \tilde{y}_2(i) \tag{2.27}$$

The output $y(i)$ of the homomorphic system H is given by

$$y(i) = D^{-1}[\tilde{y}_1(i) + \tilde{y}_2(i)] = y_1(i) \star y_2(i) \tag{2.28}$$

Thus, the basic idea is to use nonlinear functions to transform nonlinearly-related components to additively-related ones, and then to process them using a linear filter. The output from the linear filter is then transformed by using the inverse of the nonlinear function. Two examples of the nonlinear function used as the forward transform in a homomorphic

system are $\ln(x)$ and x^{γ} [1].

2.5 Unbiased Homomorphic System to Reduce Multiplicative Noise

2.5.1 System Description

The structure of the homomorphic system shown in Figure 2.1 can be used to reduce multiplicative noise corruption. Since linear filters are known to be ineffective in reducing additive noise with non-Gaussian distribution, we will replace the linear filter by the GSFWO filter, a nonlinear filter. The GSFWO filter is employed, since it can be designed based on the nature of the PDF of the corrupting noise. Such a system is shown in Figure 2.2.

Figure 2.2: A homomorphic system using the GSFWO filter to reduce multiplicative noise.

The forward and backward homomorphic transforms are respectively the natural logarithm and exponential functions. The natural logarithm transforms the multiplicative nature of corruption at the input to the system into one of an additive nature. A suitable GSFWO filter is designed to reduce this additive noise. The GSFWO filter is employed, as it can be used in applications where the PDF of the noise could be asymmetric. Let $x(i)$ and $y(i)$ be respectively the input to and output of the system. The input signal corrupted by a multiplicative noise may be written as

$$x(i) = x_1(i) \cdot x_2(i) \tag{2.29}$$

where $\cdot$ defines the multiplication operation and $x_2(i)$ is the noise component. Then, ap-

plying the natural logarithm, we get

$$\widetilde{x}(i) = \ln[x(i)] = \ln[x_1(i) \cdot x_2(i)] = \ln[x_1(i)] + \ln[x_2(i)] = \widetilde{x}_1(i) + \widetilde{x}_2(i) \tag{2.30}$$

where + stands for addition. Now, applying the GSFWO filter to remove the noise, ideally, we get

$$\widetilde{y}(i) = \text{GSFWO}[\widetilde{x}(i)] = \text{GSFWO}[\widetilde{x}_1(i) + \widetilde{x}_2(i)] = \widetilde{x}_1(i) \tag{2.31}$$

Then, the output from the homomorphic system is obtained by applying the exponential function and is given as

$$y(i) = \exp[\widetilde{y}(i)] = \exp[\widetilde{x}_1(i)] = x_1(i) \tag{2.32}$$

Thus, by using a homomorphic system, the removal of the multiplicative noise x_2 is achieved.

2.5.2 Coefficients of the GSFWO Filter Within the Homomorphic System

Noise corruption of a multiplicative nature in an image can be interpreted as each pixel of the uncorrupted original signal being multiplied by a random noise element. This noise corruption of a multiplicative nature is modelled either as

$$\Psi(i) = \Theta + \Theta \text{ x } \tau(i)$$

or

$$\Psi(i) = \Theta \text{ x } \tau(i) \tag{2.33}$$

where $\tau(i)$ is a stationary white multiplicative noise having a zero mean in the first expression and unit mean in the second expression of (2.33), Θ is the original signal that is

assumed to be constant within a filter window, and $\Psi(i)$ the observed corrupted signal. It is also assumed that the uncorrupted signal Θ and the noise τ are uncorrelated to each other. Both the expressions in (2.33) can be rewritten as

$$\Psi(i) = \Theta \text{ x } \Phi(i) \tag{2.34}$$

where $\Phi(i)$ is a unit mean multiplicative white noise. The corrupted signal is passed through the homomorphic system described in Section 2.5.1 to reduce the multiplicative noise. The first step in the homomorphic system is to take the natural logarithmic transform of the observed corrupted signal. Applying natural logarithm to both sides of (2.34), we get

$$\ln \Psi(i) = \ln \Theta + \ln \Phi(i) \tag{2.35}$$

Equation (2.35) can be written as:

$$\Upsilon(i) = \Lambda + n(i) \tag{2.36}$$

where $n(i)$ is a random zero-mean stationary white noise and $\Lambda = \ln \Theta + m$, m being the mean of $\ln \Phi(i)$. As the multiplicative noise is white, the additive noise obtained after the nonlinear transform will remain white [22]. Now, the (2.36) is the same as (2.7), which defines the problem of reduction of noise of an additive nature. To reduce the additive noise $n(i)$, the GSFWO filter is applied. Once the additive noise has been reduced, the original signal can be estimated by applying exponentiation followed by a bias compensation to nullify the shift m. The bias compensation technique will be explained in Section 2.5.3.

Now, the coefficients of the GSFWO filter within the homomorphic system for a given PDF of the multiplicative noise are derived. Now, let the standard PDF of the multiplicative noise Φ be $f_\Phi(\Phi)$ and the corresponding CDF be $F_\Phi(\Phi)$. The noise random variables v and Φ are related by $v = \ln(\Phi)$, where, $\Phi = F_\Phi^{-1}(\lambda)$, $0 \leq \lambda \leq 1$. The effect of the non-zero

mean m of $\ln(\Phi)$ is taken into account by appropriate bias compensation to be explained in Section 2.5.3. Now, from the relation of v and Φ, we can deduce the following relation:

$$F_v^{-1}(\lambda) = \ln\left(F_\Phi^{-1}(\lambda)\right),\ 0 \leq \lambda \leq 1 \tag{2.37}$$

The next task is to find the relation between ϕ_v and ϕ_Φ, where $\phi_\Phi = \ln(f_\Phi(\Phi))$. The relation between the PDFs is given by

$$f_v(v) = f_\Phi(\exp(v)) \mid J \mid \tag{2.38}$$

where $J = \frac{d\Phi}{dv}$ is the Jacobian of the transformation $v = \ln(\Phi)$ [23]. Therefore:

$$\begin{aligned} \phi_v(v) &= \ln f_v(v) \\ \phi_v(v) &= \ln(f_\Phi(\exp(v)) \cdot \exp(v)) \\ \phi_v(v) &= \phi_\Phi(\exp(v)) + v \end{aligned} \tag{2.39}$$

Further from (2.39),

$$\phi_v'(v) = 1 + \phi_\Phi'(\exp(v)) \cdot \exp(v) \tag{2.40}$$

$$\phi_v''(v) = \phi_\Phi'(\exp(v)) \cdot \exp(v) + \phi_\Phi''(\exp(v)) \cdot \exp(2v) \tag{2.41}$$

Hence, from (2.24), (2.37), (2.40) and (2.41), it is clear that the coefficients of the GSFWO filter within the homomorphic system can be obtained if $f_\Phi(\Phi)$ is known, which is the PDF of the multiplicative noise. At the end of the homomorphic system, exponentiation is applied to get the estimate of the original signal.

2.5.3 Bias Compensation

In this subsection, it is shown that the presence of m makes the output after the exponentiation biased and hence a corresponding bias compensation procedure is proposed. A method to compensate for the bias is explained in this subsection. Let the output from the GSFWO filter within the homomorphic system be denoted by $\hat{\Lambda}$, which is given by

$$\hat{\Lambda} = \ln(\hat{\Theta}) + \hat{m} \tag{2.42}$$

where $\hat{\Theta}$ is the unbiased estimate of the original uncorrupted signal and $\hat{m}$ is the estimate of the shift. Now, taking the exponential of the estimate $\hat{\Lambda}$, we get the biased estimate and is expressed as

$$\hat{\Theta}' = \exp\hat{\Lambda} = \exp\left(\ln(\hat{\Theta}) + \hat{m}\right) = \hat{\Theta} \cdot \exp(\hat{m}) \tag{2.43}$$

As can be seen, the output is biased by a factor $\exp(\hat{m})$. This bias can be compensated as follows. Taking the expected value on both sides of (2.43), we get

$$E[\hat{\Theta}'] = E[\hat{\Theta}] \cdot \exp(\hat{m}) \tag{2.44}$$

Now, by consistency theory of estimates [21], we have

$$E[\Theta] = E[\hat{\Theta}] \tag{2.45}$$

and since Φ was assumed to have unit mean, we get

$$E[\Theta] = E[\Psi] \tag{2.46}$$

Using (2.44), (2.45) and (2.46), a bias compensation constant ξ is defined and the compensation is achieved as follows.

$$\xi = \exp(\hat{m}) = \frac{E[\hat{\Theta}']}{E[\Psi]} \tag{2.47}$$

$$\hat{\Theta} = \frac{\hat{\Theta}'}{\xi} \tag{2.48}$$

Thus, as both the biased recovered signal ($\hat{\Theta}'$) and the observed signal (Ψ) are available, the unbiased estimate of the original signal ($\hat{\Theta}$) can readily be obtained using (2.48).

The overall block diagram of the proposed unbiased homomorphic system to reduce multiplicative noise is shown in 2.3.

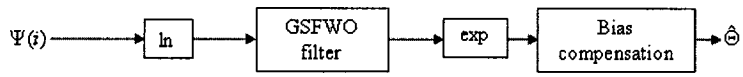

Figure 2.3: Proposed GSFWO filter based-unbiased homomorphic system to reduce noise of a multiplicative nature

2.6 Performance of the Proposed and Some Known Filters in Reducing Multiplicative Noise

In this section, the performance of the proposed unbiased homomorphic system to reduce a multiplicative noise is compared to that of a few known filters. The filter considered for comparison are as follows.

(1) Filter proposed by Kuan et al. [24]

(2) Sample mean filter [17] being used as the linear filter in the homomorphic system shown in Figure 2.1

(3) Sample median filter [25] being used in place of the linear filter in Figure 2.1

(4) Edge-adaptive Wiener filter [24, 7] being used in place of the linear filter in Figure

2.1

Now, let us consider the proposed unbiased homomorphic system to reduce noise of a multiplicative nature. The coefficients of the GSFWO filter are derived based on the nature of the PDF of the multiplicative noise. Hence, different GSFWO filters are obtained depending on the type of noise. Three different noise distributions are considered, and the corresponding expressions for $\phi_\Phi(\Phi)$ are given below.

1. Gaussian Distribution:

$$\phi_\Phi(\Phi) = \ln f_\Phi(\Phi) = K - \Phi^2 \tag{2.49}$$

2. Uniform Distribution:

$$\begin{aligned} \phi_\Phi(\Phi) &= \ln f_\Phi(\Phi) &&= \ln K - \Phi^\alpha \\ \text{and} \quad F_\Phi^{-1}(\lambda) &= &&2\lambda - 1 \end{aligned} \tag{2.50}$$

3. Lognormal Distribution:

$$\phi_\Phi(\Phi) = \ln f_\Phi(\Phi) = K - (\ln(\Phi))^2 \tag{2.51}$$

where K represents a constant and α is a very large integer [5]. For all the three cases, the corresponding coefficients of the GSFWO filter can be obtained using (2.24) and (2.41). Figure 2.4 shows the coefficients of the GSFWO filter obtained using the method proposed in Section 2.5 for the above three PDFs of the multiplicative noise. It is seen from Figure 2.4(c) that the GSFWO filter reduces to a mean filter when the multiplicative noise has a lognormal distribution.

Figure 2.5 shows the two original images (without corruption), namely, the 'Pepper' and 'Goldhill'. Figure 2.6 shows the 'Pepper' image corrupted by a multiplicative Gaussian noise of variance 0.25 (normalized with respect to maximum greyscale value, i.e, 255)

and the images filtered by the proposed system as well as the four filters mentioned in the previous paragraph. Figure 2.7 shows the corresponding images for the 'Goldhill' image corrupted again by a Gaussian noise. Figures 2.8 and 2.9 give similar results when the images are corrupted by a noise with uniform distribution. Finally, Figures 2.10 and 2.11 correspond to case when the noise has a lognormal distribution.

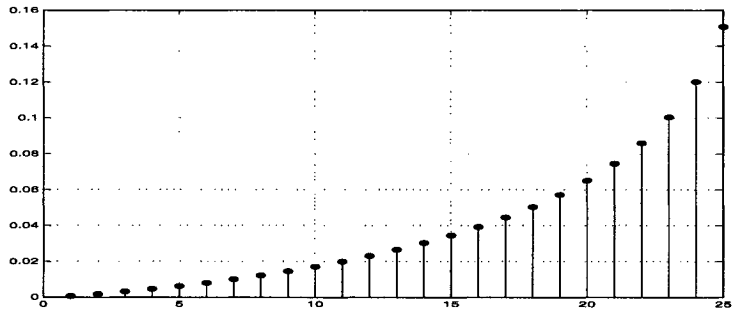

(a) Filter coefficients when noise PDF is Gaussian

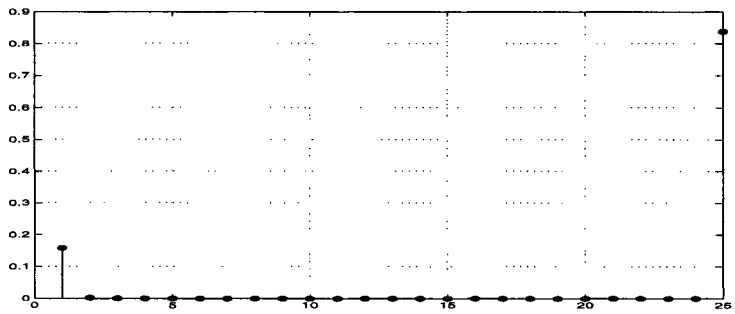

(b) Filter coefficients when noise PDF is uniform

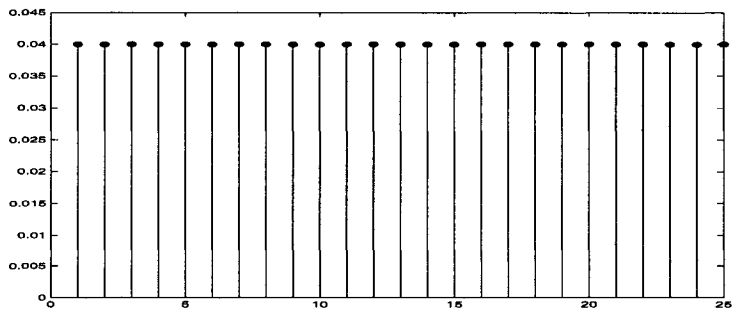

(c) Filter coefficients when noise PDF is lognormal

Figure 2.4: Coefficients of the GSFWO filter within the homomorphic system for multiplicative noise with different distributions

From these figures, it can be seen that the proposed spatial domain unbiased homomorphic system using the GSFWO filter effectively reduces the multiplicative noise for all the different distributions considered. The filter proposed by Kuan et al., which will henceforth be referred to as the Kuan filter, leaves behind a significant amount of noise and hence, has an inferior noise reduction capacity when compared to the proposed system. Even though the performance of the homomorphic system employing the sample mean or sample median filter is quite good when the noise has a lognormal distribution, the proposed filter has a even better performance. However, when the noise has a Gaussian or a uniform distribution, the proposed system is clearly superior to the mean or median filter-based systems in removing the noise. The homomorphic system employing the edge-adaptive Wiener filter leaves a significant amount of noise at the edges when the noise has a lognormal distribution, whereas the noise left behind is quite considerable not only at the edges but also in the homogeneous regions as compared to that in the images filtered using the proposed system. Thus, on a qualitative basis, it may be concluded that the GSFWO filter-based unbiased homomorphic system gives the best results amongst all the filters considered for reducing multiplicative noise.

Tables 2.1 and 2.2 give quantitative results obtained by the various filters in reducing multiplicative noise. The MSE between each recovered image and the original uncorrupted image is listed for the different kinds of multiplicative noise considered. The MSE is calculated as

$$\text{MSE} = \frac{1}{M \cdot N} \sum_{i=1}^{M} \sum_{j=1}^{N} (B(i,j) - A(i,j))^2 \tag{2.52}$$

where B is the recovered image and A is the original uncorrupted image, and $M \times N$ is the size of the image. Note that the MSE value given in the tables corresponding to the noisy image is obtained between the noisy image and the uncorrupted original image.

It is evident from the tables that the proposed system outperforms the others in reducing multiplicative noise having different distributions. This better performance of the proposed unbiased homomorphic system using GSFWO filter can be attributed to the fact that the

(a) Original Pepper Image

(b) Original Goldhill Image

Figure 2.5: The two original images (without corruption) considered

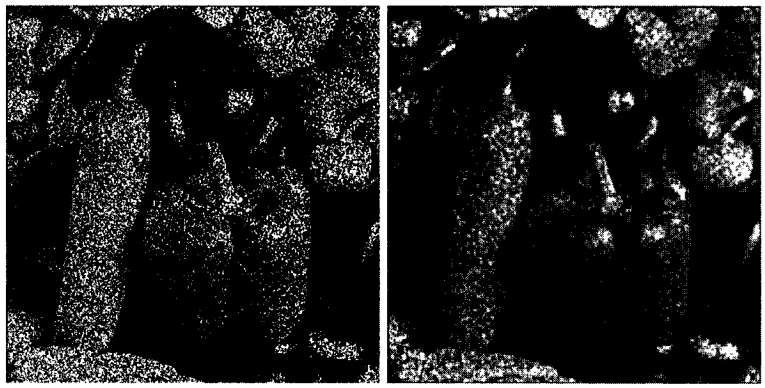

(a) Noisy image

(b) Image recovered by the proposed GSFWO filter-based unbiased homomorphic system

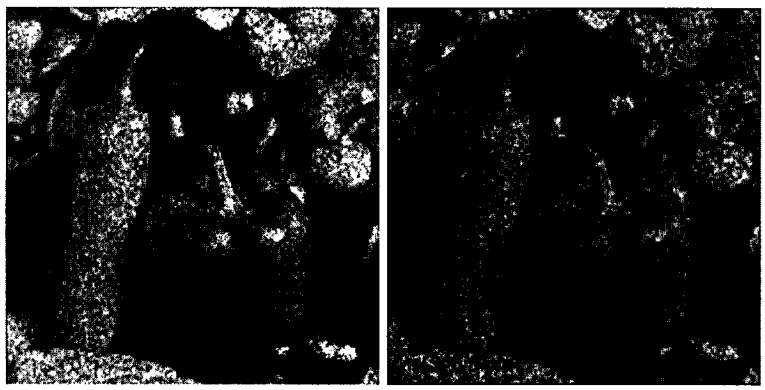

(c) Image recovered by the Kuan filter

(d) Image recovered by the sample mean filter-based homomorphic system

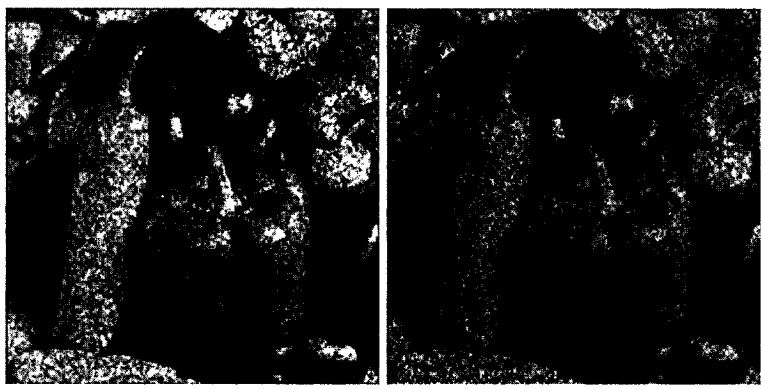

(e) Image recovered by the sample median filter-based homomorphic system

(f) Image recovered by the edge-adaptive Wiener filter-based homomorphic system

Figure 2.6: Qualitative results using the 'Pepper' image showing the performance of the various filters in reducing multiplicative noise having Gaussian distribution

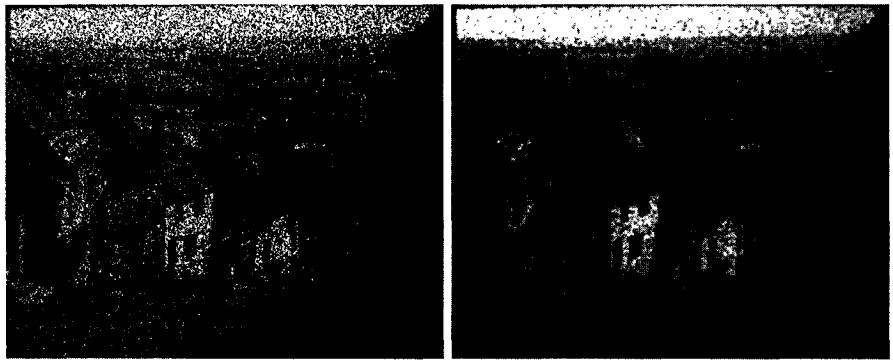

(a) Noisy image

(b) Image recovered by the proposed GS-FWO filter-based unbiased homomorphic system

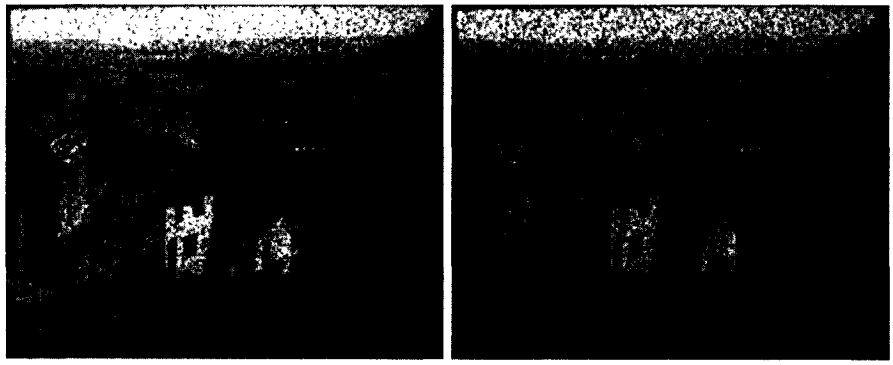

(c) Image recovered by the Kuan filter

(d) Image recovered by the sample mean filter-based homomorphic system

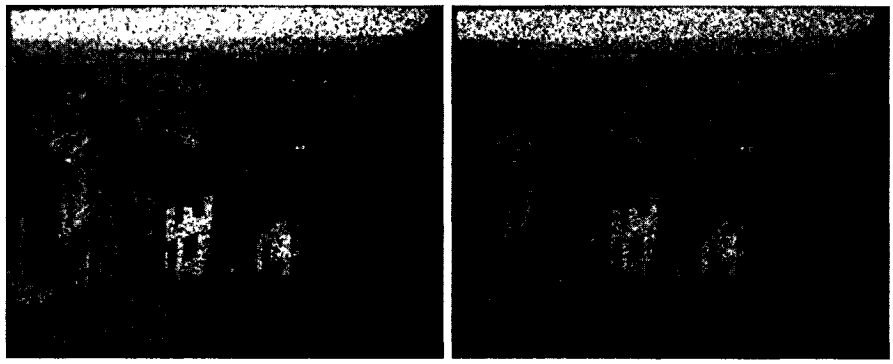

(e) Image recovered by the sample median filter-based homomorphic system

(f) Image recovered by the edge-adaptive Wiener filter-based homomorphic system

Figure 2.7: Qualitative results using the 'Goldhill' image showing the performance of the various filters in reducing multiplicative noise having Gaussian distribution

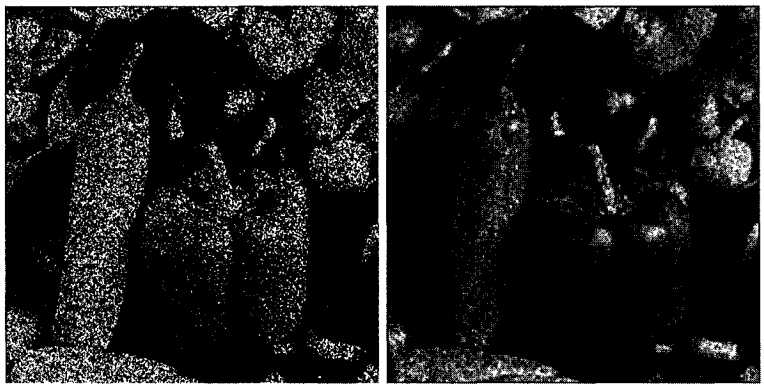

(a) Noisy image

(b) Image recovered by the proposed GSFWO filter-based unbiased homomorphic system

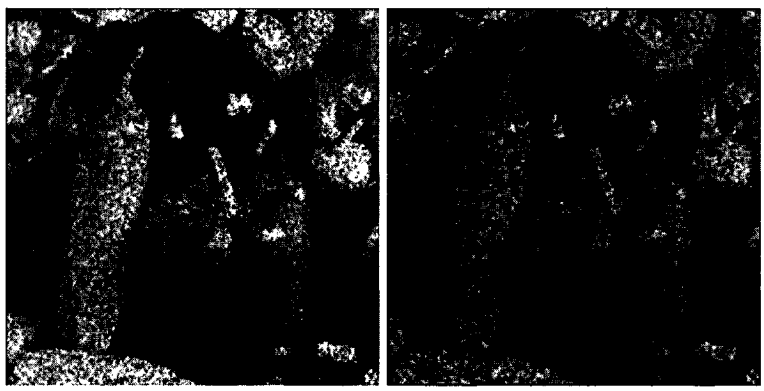

(c) Image recovered by the Kuan filter

(d) Image recovered by the sample mean filter-based homomorphic system

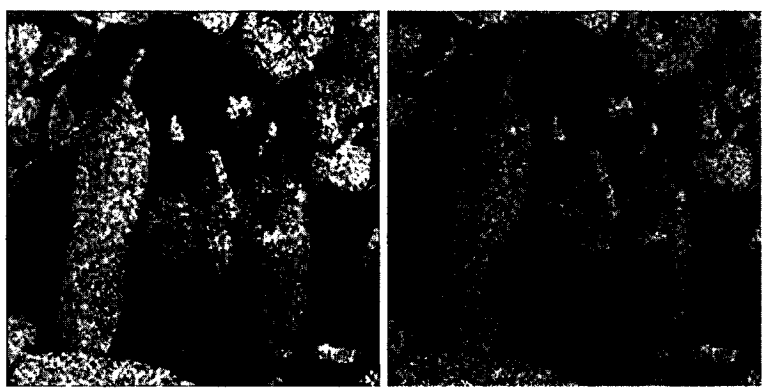

(e) Image recovered by the sample median filter-based homomorphic system

(f) Image recovered by the edge-adaptive Wiener filter-based homomorphic system

Figure 2.8: Qualitative results using the 'Pepper' image showing the performance of the various filters in reducing multiplicative noise having uniform distribution

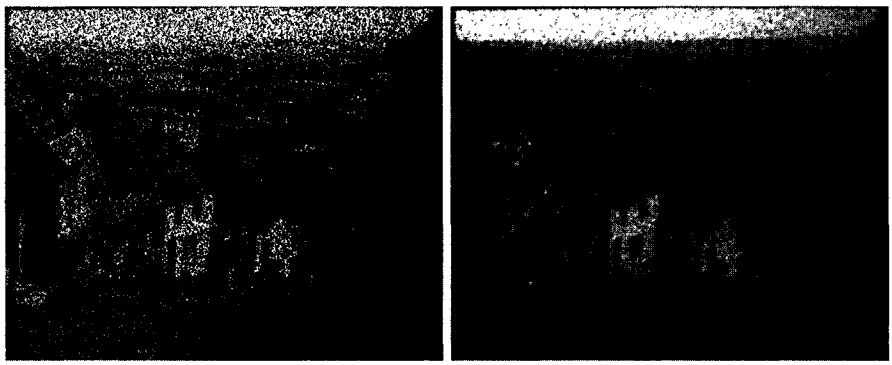

(a) Noisy image

(b) Image recovered by the proposed GS-FWO filter-based unbiased homomorphic system

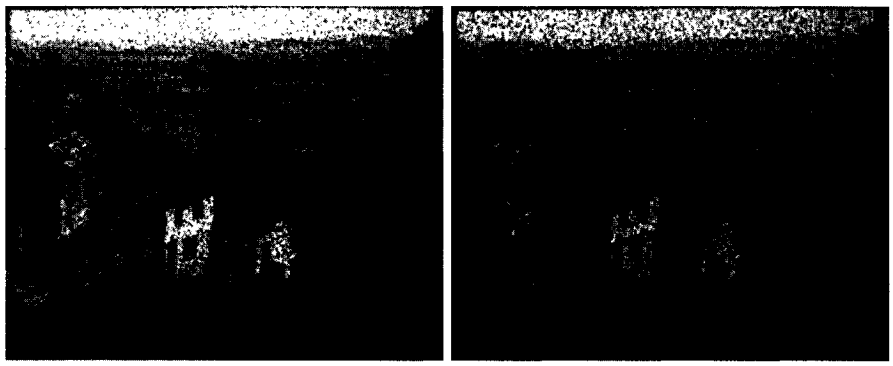

(c) Image recovered by the Kuan filter

(d) Image recovered by the sample mean filter-based homomorphic system

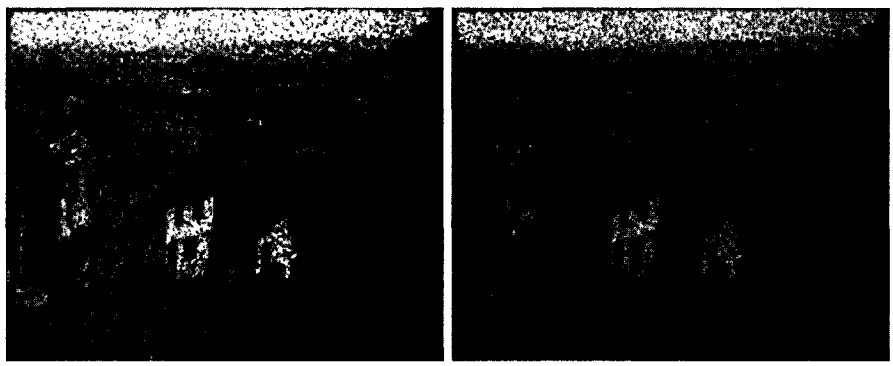

(e) Image recovered by the sample median filter-based homomorphic system

(f) Image recovered by the edge-adaptive Wiener filter-based homomorphic system

Figure 2.9: Qualitative results using the 'Goldhill' image showing the performance of the various filters in reducing multiplicative noise having uniform distribution

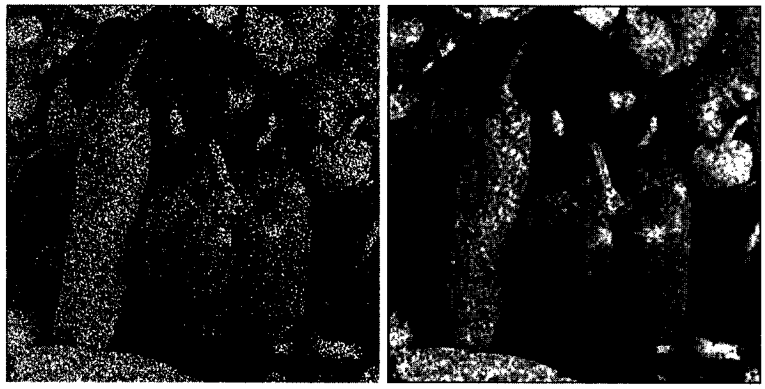

(a) Noisy image

(b) Image recovered by the proposed GSFWO filter-based unbiased homomorphic system

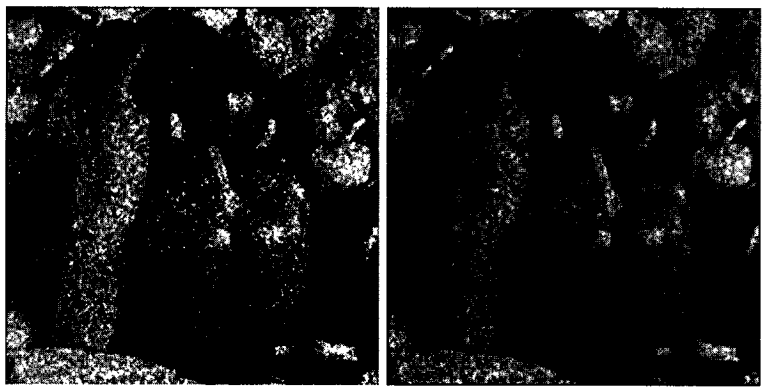

(c) Image recovered by the Kuan filter

(d) Image recovered by the sample mean filter-based homomorphic system

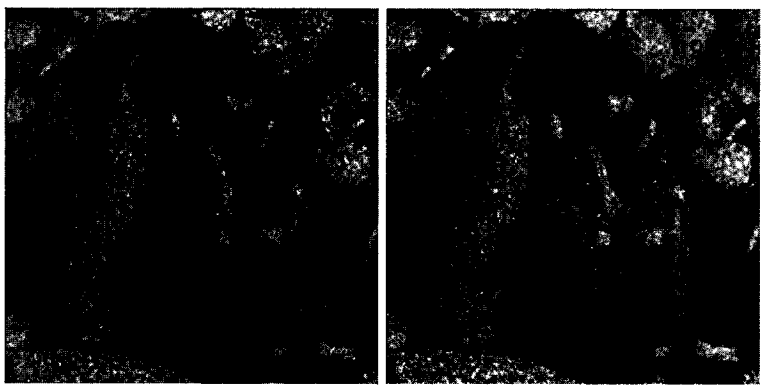

(e) Image recovered by the sample median filter-based homomorphic system

(f) Image recovered by the edge-adaptive Wiener filter-based homomorphic system

Figure 2.10: Qualitative results using the 'Pepper' image showing the performance of the various filters in reducing multiplicative noise having lognormal distribution

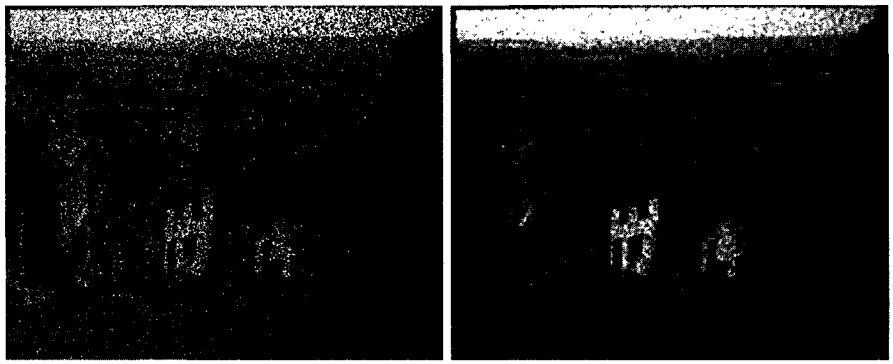

(a) Noisy image

(b) Image recovered by the proposed GS-FWO filter-based unbiased homomorphic system

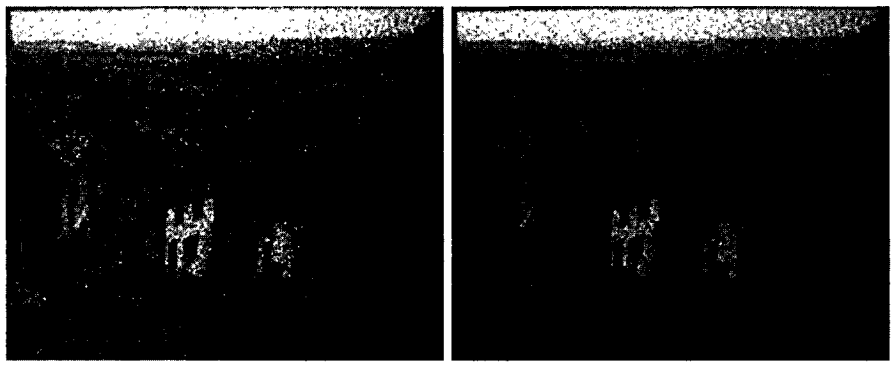

(c) Image recovered by the Kuan filter

(d) Image recovered by the sample mean filter-based homomorphic system

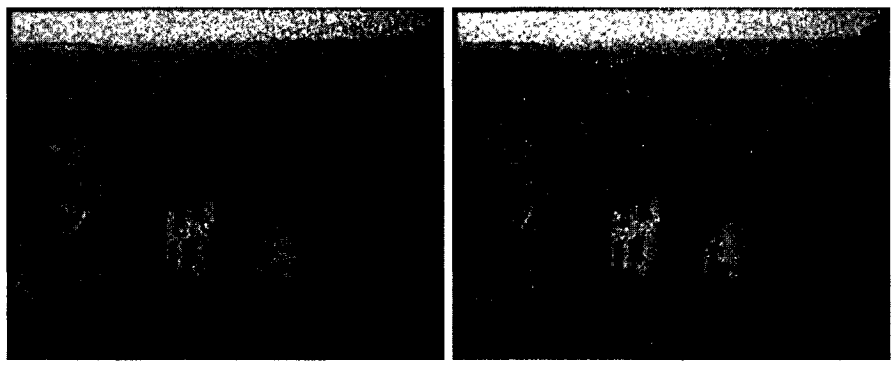

(e) Image recovered by the sample median filter-based homomorphic system

(f) Image recovered by the edge-adaptive Wiener filter-based homomorphic system

Figure 2.11: Qualitative results using the 'Goldhill' image showing the performance of the various filters in reducing multiplicative noise having lognormal distribution

TABLE 2.1

MSE FOR THE VARIOUS FILTERS IN REDUCING MULTIPLICATIVE NOISE USING THE 'PEPPER' IMAGE

Mean Square Error (MSE)	Gaussian Noise PDF	Uniform Noise PDF	Lognormal Noise PDF
Noisy Image	3159.8	3604.8	1917.1
Image recovered by the proposed GSFWO filter-based unbiased homomorphic system	226.54	289.4	326.67
Image recovered by the Kuan Filter	295.7	329.17	762.4
Image recovered by the sample mean filter-based homomorphic system	859.52	848.71	431.29
Image recovered by the sample median filter-based homomorphic system	371.37	596.43	526.61
Image recovered by the edge-adaptive Wiener filter-based homomorphic system	790.72	724.76	328.03

TABLE 2.2

MSE FOR THE VARIOUS FILTERS IN REDUCING MULTIPLICATIVE NOISE USING THE 'GOLDHILL' IMAGE

Mean Square Error (MSE)	Gaussian Noise PDF	Uniform Noise PDF	Lognormal Noise PDF
Noisy Image	2432.8	2739.3	1595.1
Image recovered by the proposed GSFWO filter-based unbiased homomorphic system	188.97	217.57	193.87
Image recovered by the Kuan Filter	248.01	267.09	607.95
Image recovered by the sample mean filter-based homomorphic system	598.13	591.28	275.07
Image recovered by the sample median filter-based homomorphic system	295.37	443.7	424.21
Image recovered by the edge-adaptive Wiener filter-based homomorphic system	634.67	576.82	284.27

TABLE 2.3

MSE FOR THE VARIOUS FILTERS IN REDUCING MULTIPLICATIVE NOISE USING THE 'PEPPER' IMAGE

Mean Square Error (MSE)	Gaussian Noise PDF	Uniform Noise PDF	Lognormal Noise PDF
Image recovered by the sample mean filter-based unbiased homomorphic system	582.81	524.91	326.67
Image recovered by the sample median filter-based unbiased homomorphic system	371.75	578.49	342.18
Image recovered by the edge-adaptive Wiener filter-based unbiased homomorphic system	605.47	465.39	213.6

coefficients of the filter are derived based on the type of distribution of the noise.

Next, we use the bias compensation proposed in this chapter in other homomorphic systems that have been considered to reduce multiplicative noise, and Figures 2.12 - 2.17 give the corresponding qualitative results. Tables 2.3 and 2.4 give the quantitative results for these unbiased homomorphic systems in reducing the multiplicative noise. It can be observed from the tables that the sample mean filter based-unbiased homomorphic system gives the same result as that of the proposed system when the noise is lognormally distributed. This should be the case since the GSFWO filter in the proposed system reduces to a sample mean filter for a multiplicative noise with lognormal distribution. However, for other types of noise considered, the proposed system gives a better performance. It can also be observed from Tables 2.3 and 2.4 that the edge-adaptive Wiener filter-based unbiased homomorphic system gives equally good or better results than the proposed system when the noise has a lognormal distribution, whereas the later outperforms the former in other cases. This is due to the fact that the Wiener filter used is adapted to the edges, and hence does not blur the edges. It is also evident from the tables that the systems with the bias compensation give better results compared to the those without the bias compensation. This endorses the presence of the proposed bias compensation block.

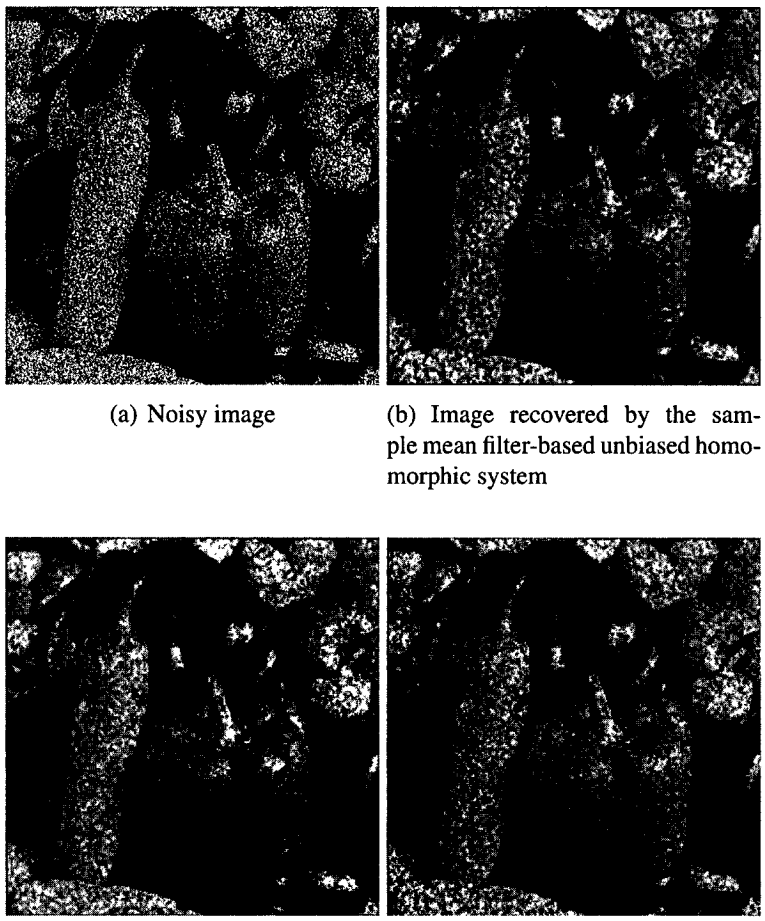

(a) Noisy image

(b) Image recovered by the sample mean filter-based unbiased homomorphic system

(c) Image recovered by the sample median filter-based unbiased homomorphic system

(d) Image recovered by the edge-adaptive Wiener filter-based unbiased homomorphic system

Figure 2.12: Qualitative results using the 'Pepper' image showing the performance of the various filters in reducing multiplicative noise having Gaussian distribution

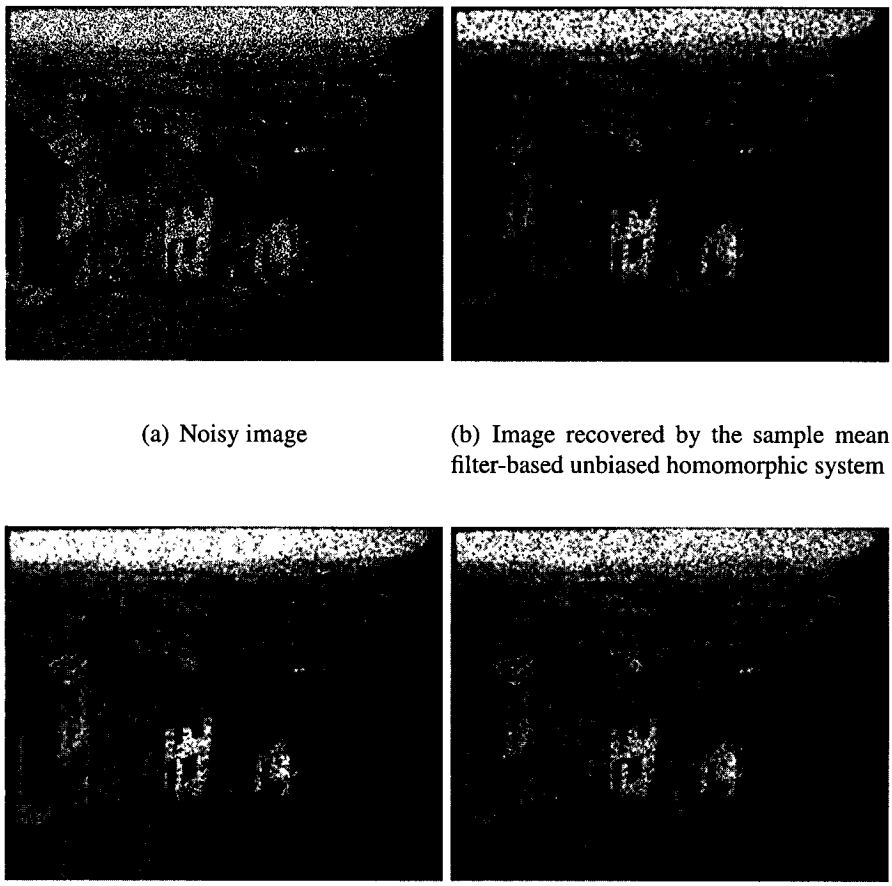

(a) Noisy image

(b) Image recovered by the sample mean filter-based unbiased homomorphic system

(c) Image recovered by the sample median filter-based unbiased homomorphic system

(d) Image recovered by the edge-adaptive Wiener filter-based unbiased homomorphic system

Figure 2.13: Qualitative results using the 'Goldhill' image showing the performance of the various filters in reducing multiplicative noise having Gaussian distribution

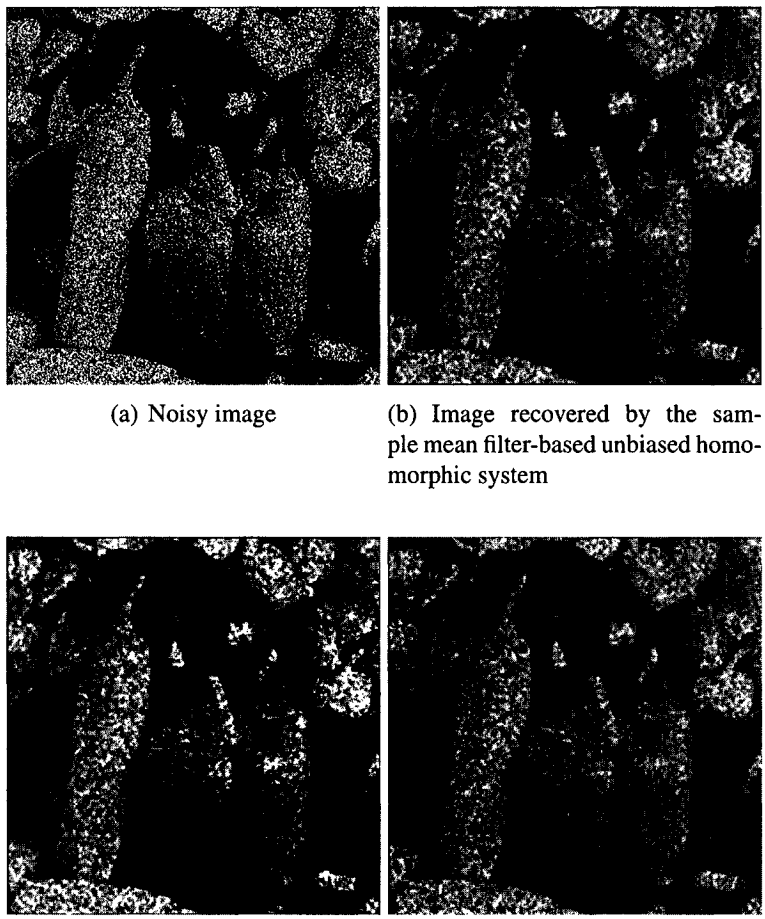

(a) Noisy image

(b) Image recovered by the sample mean filter-based unbiased homomorphic system

(c) Image recovered by the sample median filter-based unbiased homomorphic system

(d) Image recovered by the edge-adaptive Wiener filter-based unbiased homomorphic system

Figure 2.14: Qualitative results using the 'Pepper' image showing the performance of the various filters in reducing multiplicative noise having uniform distribution

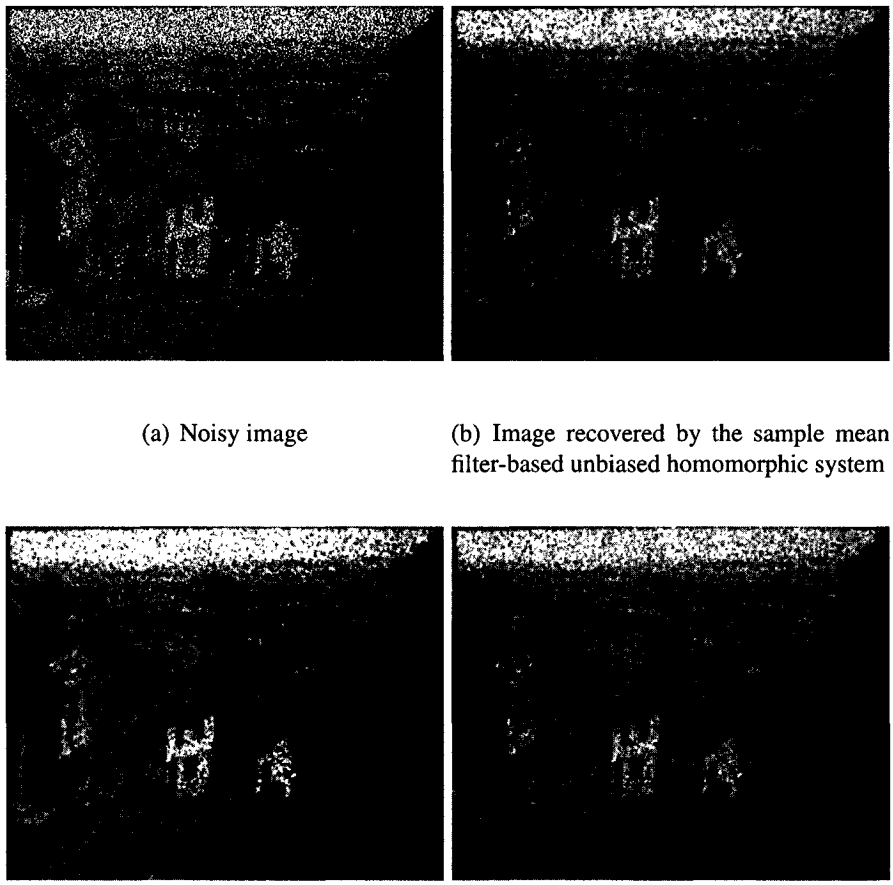

(a) Noisy image

(b) Image recovered by the sample mean filter-based unbiased homomorphic system

(c) Image recovered by the sample median filter-based unbiased homomorphic system

(d) Image recovered by the edge-adaptive Wiener filter-based unbiased homomorphic system

Figure 2.15: Qualitative results using the 'Goldhill' image showing the performance of the various filters in reducing multiplicative noise having uniform distribution

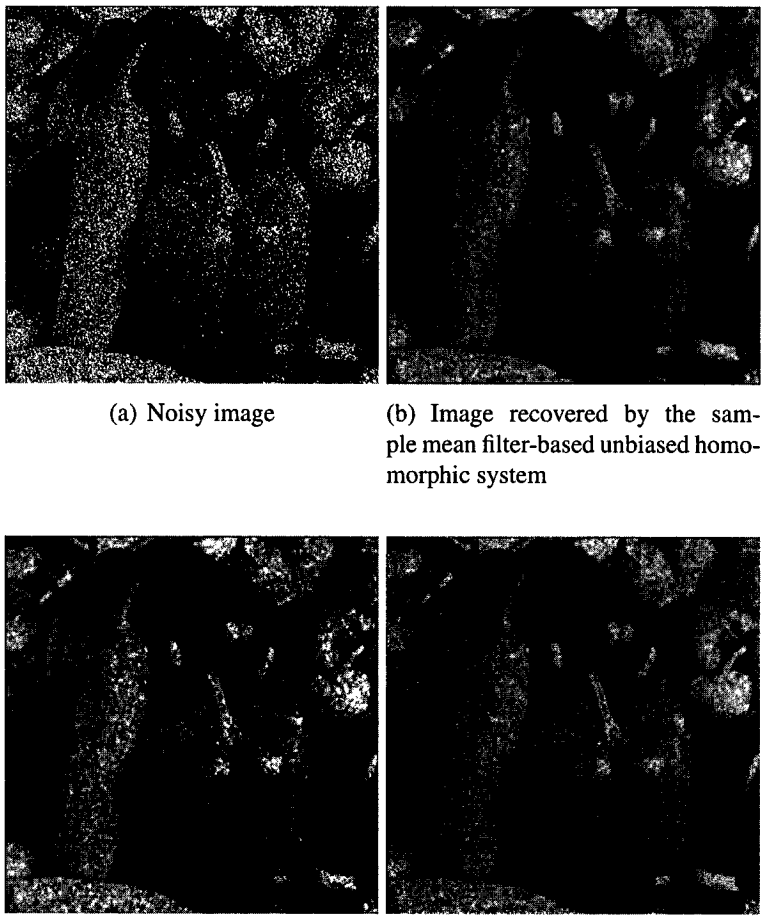

(a) Noisy image

(b) Image recovered by the sample mean filter-based unbiased homomorphic system

(c) Image recovered by the sample median filter-based unbiased homomorphic system

(d) Image recovered by the edge-adaptive Wiener filter-based unbiased homomorphic system

Figure 2.16: Qualitative results using the 'Pepper' image showing the performance of the various filters in reducing multiplicative noise having lognormal distribution

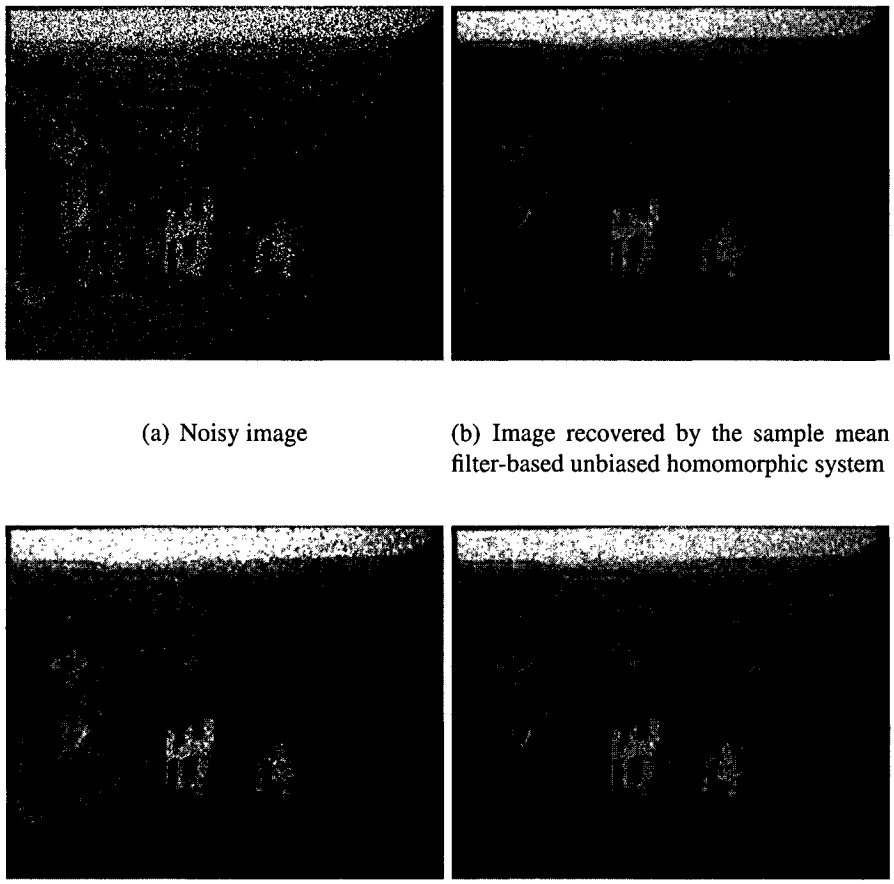

(a) Noisy image

(b) Image recovered by the sample mean filter-based unbiased homomorphic system

(c) Image recovered by the sample median filter-based unbiased homomorphic system

(d) Image recovered by the edge-adaptive Wiener filter-based unbiased homomorphic system

Figure 2.17: Qualitative results using the 'Goldhill' image showing the performance of the various filters in reducing multiplicative noise having lognormal distribution

TABLE 2.4

MSE FOR THE VARIOUS FILTERS IN REDUCING MULTIPLICATIVE NOISE USING THE 'GOLDHILL' IMAGE

Mean Square Error (MSE)	Gaussian Noise PDF	Uniform Noise PDF	Lognormal Noise PDF
Image recovered by the sample mean filter-based unbiased homomorphic system	406.15	367.1	193.87
Image recovered by the sample median filter-based unbiased homomorphic system	280.25	407.62	209.04
Image recovered by the edge-adaptive Wiener filter-based unbiased homomorphic system	512.89	410.35	199.18

2.7 Summary

In this chapter, we have generalized the SFWO filter introduced by Remzi Öten and Rui Figueiredo in [5] to the case when the additive noise corrupting the signal is not symmetric. This generalized SFWO filter is then used in an unbiased homomorphic system instead of a linear filter to reduce multiplicative noise corrupting a signal. A study of the qualitative and quantitative performance of the proposed GSFWO filter-based unbiased homomorphic system in reducing multiplicative noise has been carried out using two standard images, namely, the 'Pepper' and 'Goldhill', and compared to that of some of the existing ones. It has been found that the proposed GSFWO filter-based system consistently outperforms the others, irrespective of the type of distribution of the multiplicative noise.

Chapter 3

Reduction of Speckle in Images using an Unbiased Homomorphic System

3.1 Introduction

Images and videos captured using coherent imaging systems are corrupted by noise of a multiplicative nature called the speckle. Synthetic aperture radar (SAR) imaging systems, ultrasound imaging systems and LASER imaging systems are a few prominent examples of coherent imaging systems. SAR and LASER imaging systems are generally used in satellite and airborne vehicles to capture image and videos for various military and commercial applications [26, 27]. LASER imaging systems also find applications in modern day medical surgery. Ultrasound imaging systems for years, have had its applications in the field of medicine and health care. Moreover, many optical and infrared coherent imaging systems are used in various military, medical and commercial field [27].

The speckle present in such images and videos hinder the process of understanding and classification done by either a human interpreter or an automatic recognition system. Thus, despeckling (reduction of speckle) of these images and videos captured by various coherent imaging systems is of utmost importance. There have been different image restoration

approaches proposed in the literature to reduce speckle in images. One of the earliest filters to reduce speckle was suggested by Lee [13], wherein a linear approximation of the multiplicative noise model was used to obtain the filter. This filter was later found to be a particular case of the filter proposed by Kuan et al. [11], which is based on the MMSE criterion and obtained by modelling the multiplicative noise in the additive form. Frost et al. [12] have suggested a filter to reduce the speckle based on an adaptive estimation of the noise variance. An exponential weighting function, based on the sample noise variance, was applied to the samples within the filter window. Gamma filter, presented in [6] is a maximum aposteriori (MAP) estimator to reduce the speckle. It assumes that both the uncorrupted signal and the speckle noise have a gamma distribution. The PDF of the intensity of the speckle noise depends on the image formation process within the coherent imaging system. However, it can be shown that in most cases the intensity of the speckle approximately has a gamma distribution [28]. The lognormal distribution can also be assumed to be the PDF of the intensity of the speckle [6].

In this chapter, we consider the problem of reducing speckle using an unbiased homomorphic system wherein the speckle is assumed to be white, stationary and uncorrelated to the uncorrupted signal, and has a lognormal distribution [29, 16]. If the GSFWO filter-based unbiased homomorphic system is used to reduce the speckle, it reduces to the sample mean filter-based homomorphic system followed by the bias compensation, as noted in Chapter 2. The sample mean filter, is optimal in both the MMSE sense and the MLE sense, when used to reduce an AWGN. However, this design assumes that the uncorrupted signal to the filter is of constant amplitude within a filter window, which may not always be true. For this reason, we propose a nonlinear filter, which is referred to as the *mean median* (MM) filter, to reduce the AWGN corrupting the signal to the filter. The output of the MM-filter is obtained by a combination of the sample mean and the sample median estimates. It is shown that a combination of the sample mean and the sample median estimates would perform better than the sample mean filter in reducing AWGN, when the constant ampli-

tude condition of the uncorrupted signal within a filter window is not met. The proposed MM-filter is then used within the unbiased homomorphic system instead of the mean filter in order to reduce the speckle.

The organization of this chapter is as follows. Section 3.2 gives a brief overview of the characteristics of the speckle noise. Section 3.3 presents the MM-filter. A comparison of the performance of the MM-filter to that of a few other filters in reducing AWGN is given in this section. In Section 3.4, the unbiased homomorphic system to reduce speckle is introduced. In Section 3.5, the performance of the proposed filter to reduce speckle is studied and compared to the performance of a few other existing filters.

3.2 Speckle Corruption in Coherent Imaging Systems

Coherent imaging system receives signals as a coherent sum of various reflected waves. Speckle is generated due to the random interference between the returning coherent waves reflected from an irregular surface, and appears as strong dark and bright granulations in the image. This hinders both the manual and automatic image understanding capability and thus, speckle reduction systems are required. Computationally simple speckle reduction methods would be preferred, as reduced complexity is a boon for on-board and real-time imaging using coherent systems. A fully developed speckle has the characteristics of a random multiplicative noise [28].

Speckle reduction can be done in two ways, namely, multilook integration process and image restoration process. In the multilook integration process, incoherent averaging of signal frames, obtained from different segments of the signal frequency spectrum, is performed [9]. Thus, if 'L' different segments of the signal spectrum are considered, an L-look image is said to be produced. In an L-look image the standard deviation of the noise would have decreased by a factor $\sqrt{L}$, but the spatial resolution would have degraded by a factor of L [9], which is also referred to as the equivalent number of looks (ENL).

For a single look image, the intensity of the speckle is observed to follow negative exponential distribution. But, as $L \rightarrow \infty$, the speckle intensity would tend to follow a Gaussian distribution [28]. This is because of the fact that the addition of a large number of independent random variables produces a Gaussian distributed random variable, irrespective of the individual distributions. However, it can be shown that the speckle intensity approximately follows a gamma distribution in a multi-look image, when $1 < L < \infty$ [9, 6]. The mean-to-standard deviation ratio of a such a distribution satisfies the relation

$$\left(\frac{\text{mean}}{\text{standard deviation}}\right) = \sqrt{L}, \text{ a constant} \tag{3.1}$$

It should be noted that the standard deviation used in (3.1) is normalized with respect to largest greyscale value, i.e., 255 and the ENL $L \geq 1$. It has been found that the lognormal distribution, which is easy to handle statistically, can also be used to approximate the shape of PDF of the intensity of the speckle. According to [6], using either of the two distributions would not produce a significant difference in the filter performance.

Multilook integration process in a coherent imaging system is done before the final image is formed. However, this process usually results in minimal reduction in the speckle. Hence, it is necessary to apply an image restoration process to the image signal after it is formed by the coherent imaging system. The methods to reduce speckle in images, discussed in this chapter, are all examples of the image restoration process.

As mentioned earlier, speckle corruption is modelled as a random white multiplicative noise whose PDF follows a lognormal distribution. The multiplicative corruption is obtained by multiplying each pixel of the original image by a unit-mean lognormally-distributed random noise sample.

Thus, the speckle noise is modelled as

$$A = N \cdot B \tag{3.2}$$

where A is the corrupted signal, B the uncorrupted original signal, and N a unit-mean lognormally distributed multiplicative noise. The variance of the noise is given by $\frac{1}{L}$, where L is the ENL.

The speckle corruption can be evaluated using the the signal to average mean square error ratio, denoted by $\frac{S}{MSE}$ and expressed as

$$\frac{S}{MSE} = 10 \log \left[\frac{sig_a^2}{MSE_a} \right] \tag{3.3}$$

where MSE_a is the average mean square error between the corrupted signal and the uncorrupted original signal and sig_a is the average signal intensity. Apart from this, the MSE between the corrupted signal and the uncorrupted original signal can also be used to evaluate the amount of corruption.

As mentioned earlier, noise N has a lognormal distribution. A lognormally distributed random variable can be synthetically generated using [6]

$$N = \exp \left(N_{Normal} \sqrt{2 \log_{10} \left(\frac{M_{LN}}{m_{LN}} \right)} + \ln \left(m_{LN} \right) \right) \tag{3.4}$$

where M_{LN} and m_{LN} are the mean and median values of the distribution, N_{Normal} is the zero mean Gaussian random variable and N is the lognormal random variable. Without loss of generality M_{LN} can be assumed to be unity.

3.3 MM-Filter to Reduce Additive White Gaussian Noise

As mentioned in Section 3.1 and in Chapter 1, when a homomorphic system is employed to reduce the speckle, it utilizes a filter to reduce the AWGN present after the natural logarithm operation is carried out. The sample mean filter, which is optimal in both the MMSE sense [4] and the MLE sense [1], can be used to reduce the AWGN. The GSFWO filter design introduced in Chapter 2, which is based on the MMSE criterion, yields the sample mean

filter when the additive noise is white Gaussian noise. This filter is designed with the assumption that the uncorrupted signal is of constant amplitude within a filter window. This assumption may not always be true and may result in blurring the edges when used on images.

Edge-adaptive Wiener filter [7] is a popular filter used to reduce AWGN in images and does filtering based on the local sample variance and the estimated variance of noise. It essentially does sample mean filtering at the homogeneous regions of the image and does not do any filtering at the heterogeneous regions. Hence, a significant amount of noise might remain at the edges in an image recovered using the edge-adaptive Wiener filter. As the information in a greyscale image is given by spatial variation of the intensity, edges are key to the understanding of an image. Thus, a filter which leaves noise at the edges in an image might not be desirable.

The additive noise corruption model, where the uncorrupted original signal x is assumed to be of constant amplitude within a filter window, is expressed as

$$y(i) = x + n(i) \tag{3.5}$$

where $y(i)$ is the i^{th} observed sample and $n(i)$ the corresponding white noise sample.

Both the sample mean filter and the edge-adaptive Wiener filter, which are the commonly used ones to reduce an additive noise with Gaussian distribution in images, have drawbacks dealing with the spatially changing values of the uncorrupted signal to the filter. The sample mean filter causes blurring at the edges, whereas the edge-adaptive Wiener filter leaves noise at the edges.

The sample median filter is known for its edge preserving property and is optimal in the MMSE sense when the additive noise has a Laplacian distribution [1]. It is also an unbiased, consistent estimator of a signal corrupted by an additive noise having Gaussian distribution, but is not the minimum variance unbiased (MVU) estimator [21]. The sample

mean filter is the MVU estimator when the noise has a Gaussian distribution and hence, has a better noise reduction capability. Thus, a judicious combination of sample mean and sample median estimates might provide a better noise reduction as well as a better preservation of the edges.

The observed corrupted signal y in (3.5) can be depicted as a random variable having the same distribution as that of n, but with a mean x. Consider an image signal and let the filter window be currently over a part of the image where an edge is present. Let the original signal have two different amplitudes within the filter window, say, x_1 and x_2. Then, we can express the corrupted signal within the filter window as

$$y(i) = [x_1 \oplus x_2] + n(i) \tag{3.6}$$

where $[x_1 \oplus x_2]$ stands for either x_1 or x_2 depending on the value of i. Therefore

$$PDF(y) = PDF([x_1 \oplus x_2]) * PDF(n) \tag{3.7}$$

In (3.7), the index i has been dropped for simplicity. $PDF(.)$ stands for the probability density function of the corresponding random variable and $*$ stands for convolution. The PDF of n is Gaussian with a zero mean, since n is assumed to be an AWGN.

The PDF of n is given by

$$f_n(n) = \frac{1}{\sqrt{2\pi}\sigma} \exp\left(\frac{-n^2}{2\sigma^2}\right) \tag{3.8}$$

After carrying out the convolution operation in (3.7), we get the PDF of y to be

$$f_y(y) = \frac{H}{\sqrt{2\pi}\sigma} \exp\left(\frac{-(y-x_1)^2}{2\sigma^2}\right) + \frac{1-H}{\sqrt{2\pi}\sigma} \exp\left(\frac{-(y-x_2)^2}{2\sigma^2}\right) \tag{3.9}$$

where H gives the weight of the impulse corresponding to x_1. Hence, $1 - H$ will be the weight of the impulse corresponding to x_2 as the total area under any PDF curve is unity.

As mentioned earlier, y in (3.5) can be depicted as a random variable having the same PDF as that of n, but with a mean x. As the process of noise reduction is nothing but estimating the value of x, the process can also be portrayed as the estimation of the location or the mean of the PDF of the random variable y.

The asymptotic relative efficiency $[ARE]$ [1], which is a tool to compare the efficiency of estimates in estimating the location of any distribution (say f) will be used to show that a combination of the sample mean and sample median estimates could be a better estimator of a signal corrupted by Gaussian noise than the sample mean filter, when the constant amplitude assumption of the uncorrupted signal within a filter window is not met.

The measure ARE is used to analytically compare the performance of two estimators in estimating a parameter θ of a distribution f. In our case, the parameter to be estimated is the location of f. But, to use ARE, the estimators should be asymptotically normal. An estimator T working on s observed samples is said to be asymptotically normal if for large samples ($s \rightarrow \infty$), the distribution of $\sqrt{s}(\theta_s - \theta)$ tends weakly to the normal distribution, having a zero mean and a variance $V(T, f)$ [1], where θ_s is the estimate of θ based on s samples. The variance $V(T, f)$ is called the asymptotic variance.

The asymptotic relative efficiency is given by [1]

$$ARE = \frac{V(E_1, f)}{V(E_2, f)} \tag{3.10}$$

where $V(\kappa, f)$ stands for the asymptotic variance corresponding to the estimator κ, f being the PDF, and E_1 and E_2 the estimators, whose performances are to be compared.

In our case, f is the PDF of the observed corrupted signal. E_1 and E_2 are respectively the sample mean and sample median estimates, since our goal is to take advantage of the noise reduction property of the sample mean filter and the edge preservation property of the sample median filter. Fortunately, both the sample mean and the sample median estimates are asymptotically normal [1] and thus, ARE can be used for the analysis. The ARE corresponding to sample mean and median estimates, will henceforth be denoted by

ARE_{MM}.

The value of ARE_{MM} is 0.6367, when the PDF f is Gaussian and has zero mean and unit variance [1], whereas ARE_{MM} is calculated to be equal to 2 [31], when the distribution f is Laplacian and has a zero mean and unit variance. The sample mean (sample median) estimate corresponds to the MLE or the MVU estimate, if the observed signal has a Gaussian (Laplacian) distribution [1, 21].

A value of ARE_{MM} less than unity indicates that the sample mean filtering would provide a better estimate of the location of the PDF of the observed corrupted signal than the sample median one, whereas a value greater than unity implies that the sample median filter would give a better estimate. Thus, if it is shown that ARE_{MM} corresponding to the distribution in (3.9) can have any value above or below unity, it would essentially indicate that a combination of the sample mean and sample median estimates would perform better than a sample mean estimate in the AWGN reduction.

In (3.9), without loss of generality, we can shift the $f_y(y)$ by $-\frac{x_1+x_2}{2}$ to get

$$f_y(y) = \frac{H}{\sqrt{2\pi}\sigma} \exp\left(\frac{-(y-a)^2}{2\sigma^2}\right) + \frac{1-H}{\sqrt{2\pi}\sigma} \exp\left(\frac{-(y+a)^2}{2\sigma^2}\right)$$

where $a = \frac{x_1-x_2}{2}$. Again, without loss of generality we assume the standard deviation σ to be unity. Then, we have

$$f_y(y) = \frac{H}{\sqrt{2\pi}} \exp\left(\frac{-(y-a)^2}{2}\right) + \frac{1-H}{\sqrt{2\pi}} \exp\left(\frac{-(y+a)^2}{2}\right) \tag{3.11}$$

Now, we have to determine the ARE_{MM} for the PDF in (3.11), i.e., $f = f_y(y)$. Proceeding from (3.10), as given in [1], we have

$$ARE_{MM} = \frac{V(mean, f)}{V(median, f)} = \frac{\int IF(mean)^2 dF}{\int IF(median)^2 dF} \tag{3.12}$$

where IF stands for *influence function* defined for a particular estimate and for a given

distribution, and F is the CDF corresponding to f. Using the definitions of IF given in [1], the expressions of IF for the sample mean and the sample median estimates are derived as follows:

$$IF(mean) = y \tag{3.13}$$

$$IF(median) = \frac{sign(y-Q)}{2f(Q)} \tag{3.14}$$

where Q is a constant given by

$$Q = F^{-1}\left(\frac{1}{2}\right) \tag{3.15}$$

Using (3.13) and (3.14) and after some simple mathematical manipulations, we get

$$\int IF(mean)^2 dF = 1 + a^2 \tag{3.16}$$

$$\int IF(median)^2 dF = \frac{1}{4f^2(Q)} \tag{3.17}$$

Therefore, substituting (3.16) and (3.17) in (3.12), we get

$$ARE_{MM} = \frac{V(mean, f)}{V(median, f)} = (1 + a^2)4f^2(Q) \tag{3.18}$$

The quantities Q and a may range from $-\infty$ to ∞, whereas H has the range $0 < H < 1$, depending on the amplitude of the elements within the filter window. The value of CDF at $y = Q$ is given by integrating the PDF $f_y(y)$ in (3.11) as given below:

$$\begin{aligned} F(Q) &= H\int_{-\infty}^{Q} \frac{1}{\sqrt{2\pi}} \exp\left(\frac{-(y-a)^2}{2}\right)dy + (1-H)\int_{-\infty}^{Q} \frac{1}{\sqrt{2\pi}} \exp\left(\frac{-(y+a)^2}{2}\right)dy \\ &= H\int_{-\infty}^{Q-a} \frac{1}{\sqrt{2\pi}} \exp\left(\frac{-y_1^2}{2}\right)dy_1 + (1-H)\int_{-\infty}^{Q+a} \frac{1}{\sqrt{2\pi}} \exp\left(\frac{-y_2^2}{2}\right)dy_2 \\ &= H\left[\text{erf}(Q-a) + \frac{1}{2}\right] + (1-H)\left[\text{erf}(Q+a) + \frac{1}{2}\right] \end{aligned}$$

$$= \frac{1}{2} + H\Big[\text{erf}(Q-a)\Big] + (1-H)\Big[\text{erf}(Q+a)\Big] \tag{3.19}$$

Now, to find the value of Q, the expression $F(Q) = \frac{1}{2}$ from (3.15) is used in (3.19), which yields

$$H\Big[\text{erf}(Q-a)\Big] + (1-H)\Big[\text{erf}(Q+a)\Big] = 0 \tag{3.20}$$

When $a = 0$ the distribution is Gaussian and (3.20) reduces to

$$\begin{aligned} H\Big[\text{erf}(Q)\Big] + (1-H)\Big[\text{erf}(Q)\Big] &= 0 \\ \text{erf}(Q) &= 0 \end{aligned}$$

Thus, $Q = 0$ is obtained. Now, from (3.11), it is evident that when $a = 0$, $f_y(y)$ becomes a Gaussian distribution. Thus, when $Q = 0$ and $a = 0$ are substituted in (3.18), the value of ARE_{MM} obtained is 0.6367, as should be the case for a Gaussian PDF.

When there is an edge within the filter window, i.e., the concerned PDF is of the form given in (3.11), we show that the ARE_{MM} could have any value greater than or less than unity. Let the edge present be such that one-half the number of elements in the filter window have an amplitude x_1 and the rest an amplitude x_2. In this case, the value of $H = 0.5$. Using the fact that $\text{erf}(-g) = -\text{erf}(g)$, we obtain from (3.20) a value of $Q = 0$, when $H = 0.5$. Substituting the values $H = 0.5$ and $y = Q = 0$ in (3.11), we get

$$f_y(0) = \frac{1}{\sqrt{2\pi}} \exp\left(\frac{-a^2}{2}\right) = f(Q) \tag{3.21}$$

Thus, substituting (3.21) in (3.18), we get

$$ARE_{MM} = \frac{2}{\pi}(1+a^2)\exp\left(-a^2\right) \tag{3.22}$$

From (3.22), it can be easily shown that the value of ARE_{MM} is less than unity with the maximum value as 0.6367 for the case when $H = 0.5$ and for any value of a. Now, let us consider another possible case, when $a = 2$ and $H = 0.7$. By substituting these values of a and H in (3.20) we obtain $Q = 1.6$. Then, by substituting the value of $y = Q = 1.6$ in (3.11), we get

$$f_y(1.6) = \frac{0.64656}{\sqrt{2\pi}} = f(Q) \tag{3.23}$$

Thus, substituting (3.23) in (3.18), we get

$$ARE_{MM} = 1.33 \tag{3.24}$$

Thus, it is evident that ARE_{MM} can have values above or below unity, if an edge is present within the filter window, that is, when the signal within the filter window cannot be considered to be constant. Hence, an intelligent combination of the sample median and the sample mean estimates might give an asymptotic variance, whose value is less than that when either the sample mean or sample median estimate is used individually. Thus, this combination might give a better estimation of the location of the PDF of the random variable y.

Thus, we can conclude, that the sample mean estimate is the MLE or the MVU estimate of an image corrupted by AWGN, only when no edge or no spatial variation is present within the filter window. An intelligent combination of the sample mean and the sample median estimates could perform better in reducing the noise in image without blurring the edges. This combination filter will henceforth be referred to as the mean median (MM) filter. An attractive feature of this MM-filter, is that it is a smoothly trimmed filter [32], which applies a soft thresholding on the samples during the filtering process, and thus would not totally reject or accept any sample in the filter window.

3.3.1 Criteria to Combine the Mean and Median Estimates

In this subsection, three criteria are presented for combining the mean and median estimates to remove AWGN. The first two criteria are based on an unbiased weighting of the sample median and the sample mean estimates. The third criterion is based on some modifications to the edge-adaptive Wiener filter equations.

The first two criteria can be expressed as follows. Let γ represent the coefficients of the MM-filter. It can be expressed as

$$\gamma = \frac{\alpha\gamma_{mean} + \beta\gamma_{median}}{\alpha + \beta} \tag{3.25}$$

where γ_{mean} represents the coefficients of the sample mean estimator, γ_{median} those of the sample median estimator, and α and β are the weights used to obtain the coefficients of the MM-filter. Let σ be the standard deviation of the Gaussian noise. This standard deviation is estimated over the given image using the median of absolute deviations (MAD) formula, given by $\sigma^{'} = 1.483\text{MAD}$ [17]. Let $\sigma_I^{'}$ be the standard deviation of the observed corrupted image. The standard deviations $\sigma^{'}$ and $\sigma_I^{'}$ are normalized with respect to the maximum greyscale value (255) to obtain normalized variances σ and σ_I, respectively.

Criterion 1:

Let us recall that the sample mean filter has a better noise reduction capability, whereas the sample median filter is known for its edge preserving capability. Thus, intuitively, the weightage should be assigned such that when the noise content is high, the sample mean filtering dominates, whereas the sample median filtering would dominate if the noise is less. Hence, a possible choice for the weights is

$$\alpha = \sigma^2 \textbf{ and } \beta = \frac{1}{\sigma^2} - 1$$

It can be seen that as σ^2, the variance of the noise, increases, the weightage given to the

coefficients of the sample mean filter (sample median filter) increases (decreases). It can be shown that the sample mean filter dominates over the median filter as long as $\sigma^2 > 0.618$, otherwise the sample median filter takes over. As L, the ENL of a coherently generated image, cannot be less than unity, it can be shown that $\sigma^2 \leq 0.693$, from the relation between the variances of the lognormal distribution and the transformed Gaussian distribution. It is evident from the weights that this criterion does not take into account the amount of edge details present in the image. Thus, incorporating the edge content of the image by modifying the weights, a second criterion of combining the sample mean and sample median estimates is proposed below.

Criterion 2:

$$\alpha = \sigma^2 \cdot \frac{\sigma^2}{\sigma_I^2} \textbf{ and } \beta = \left(\frac{1}{\sigma^2} - 1\right) \cdot \frac{\sigma_I^2}{\sigma^2}$$

This criterion takes into account the amount of edge content in the original image which is represented by the standard deviation σ_I.

Criterion 3:

In this criterion, a minor modification is carried out in the edge-adaptive Wiener filter equations [7], such that the sample mean filter dominates in the smooth areas and the sample median filter in the edge areas of the image in contrast to the traditional edge-adaptive adaptive Wiener filter, wherein no filtering is performed in the edge areas.

Let a be the signal corrupted by noise and b be the original uncorrupted signal. The additive noise model is given by

$$a = b + \eta$$

where η is the zero mean AWGN noise. Let $\hat{b}$ be the recovered signal. The filter equation

of the traditional edge adaptive Wiener filter is given as [7]

$$\hat{b}(x,y) = \mu + \left(\frac{\sigma_{x,y}^2 - v^2}{\sigma_{x,y}^2}\right) \cdot (a(x,y) - \mu) \tag{3.26}$$

where

$$\mu = \frac{1}{M_w N_w} \sum_{n_1,n_2 \in \Lambda_{x,y}} a(n_1,n_2)$$

and

$$\sigma_{x,y}^2 = \frac{1}{M_w N_w} \sum_{n_1,n_2 \in \Lambda_{x,y}} a^2(n_1,n_2) - \mu^2$$

where $\Lambda_{x,y}$ represents all the pixel positions within the filter window of size $M_w \times N_w$ with the center at (x,y) and v is the variance of the corrupting noise η.

We add an extra term to (3.26) in order to find the estimate $\hat{b}$, such that noise reduction takes place at the edges without significant blurring effect. The MM-filter estimate obtained by modifying (3.26) is given as

$$\hat{b}(x,y) = (1 - \nabla_{x,y}) \left(\mu + \left(\frac{\sigma_{x,y}^2 - v^2}{\sigma_{x,y}^2}\right) \cdot (a(x,y) - \mu)\right) + \nabla_{x,y}\text{med}[R] \tag{3.27}$$

where med$[R]$ stands for the median value among the elements of an array R given by

$$R = [(a(n_1,n_2) - \mu)] \; \forall \; (n_1,n_2) \; \in \; \Lambda_{x,y}$$

In the above, $\nabla_{x,y} = \left[\widetilde{\frac{\sigma_{x,y}^2 - v^2}{\sigma_{x,y}^2}}\right]$, with the notation $\widetilde{[Z_{x,y}]}$ signifying normalization with respect to the maximum value amongst the values of Z_{n_1,n_2}, where (n_1,n_2) corresponds to the pixel positions within the filter window $\Lambda_{x,y}$.

3.3.2 Performance of the MM-Filter in Additive White Gaussian Noise Reduction

In this subsection, qualitative and quantitative results of the MM-filter in reducing AWGN from corrupted images are presented. The performance of the MM-filter is compared with that of the sample mean filter [17] and the edge-adaptive Wiener filter [7]. The complexity of the filters is given in terms of the time taken by the filters to process an image of size 512x512. The filters were implemented using MATLAB in windows operating system on a machine with a 2.5 GHz processor. The quantitative results are presented using a figure of merit (FOM) as given in [30] and the MSE between the the desired response and the actual output. The FOM is calculated as [30]

$$EP(\%) = \frac{1}{max(N_A, N_B)} \sum_{i=1}^{N_A} \frac{1}{1 + \nu d^2(i)} \times 100 \tag{3.28}$$

where A and B are two images representing the edge maps (binary images where '1' represents an edge pixel and '0' represents a non-edge pixel) of the desired response and the actual response, N_A and N_B are the number of edge pixels in the edge maps A and B, respectively, ν is an arbitrary penalty parameter for offset edge pixels, which is chosen equal to 10 as in [30], and d is given by

$$d(i) = I(i) - J(i)$$

In the above, I and J are one dimensional arrays obtained respectively from the two dimensional arrays A and B as follows

$$\begin{aligned} I &= [A(m', n')] \; \forall \; A(m', n') = 1 \\ J &= [B(m', n')] \; \forall \; A(m', n') = 1 \end{aligned}$$

where

$$m' = 0, 1, 2, \cdots\cdots, M$$
$$n' = 0, 1, 2, \cdots\cdots, N$$

In the above, $M \times N$ is the size of the images. The lengths of the arrays F and G will be equal to number of edge pixels $N_A$in edge map A. The FOM R assumes values $0\% - 100\%$, with $R = 100\%$ achieved when the desired image and the actual image are the same. The MSE is calculated as

$$\text{MSE} = \frac{1}{M \cdot N} \sum_{i=1}^{M} \sum_{j=1}^{N} (AR(i,j) - BR(i,j))^2 \tag{3.29}$$

where AR is the desired response and BR is the actual response. $M \times N$ is the size of the images AR and BR. Note that the MSE and the FOM values corresponding to a noise corrupted image are obtained using the uncorrupted original image and the noise corrupted image.

Smaller MSE signifies a better noise reduction property, whereas a larger FOM signifies a better edge preservation feature. The MM-filters obtained using all the three proposed criteria are considered. To show the qualitative results, the original 'Crowd' image is first synthetically corrupted by adding white Gaussian noise. Then, image recovery is carried out using the above mentioned filters to reduce AWGN.

In Figure 3.1, the 'Crowd' image is corrupted by a Gaussian noise of variance 0.01 (normalized with respect to maximum greyscale value, i.e, 255), which is considered to be a low level corruption. It is evident that the mean filter smooths out the edges, whereas the edge-adaptive Wiener filter does no filtering at the edges leaving behind noise. As can be seen from the qualitative results, the proposed MM-filter, using any one of the three criteria does a better balancing between the edge preservation and noise reduction. The MM-filter based on Criterion 3 is the best among the three proposed MM-filters when it comes to

(a) Original 'crowd' image

(b) Image corrupted by Gaussian noise of variance 0.01 (normalized)

(c) Image recovered using the sample mean filter

(d) Image recovered using the edge-adaptive Wiener filter

(e) Image recovered using the MM-filter (Criterion 1)

(f) Image recovered using the MM-filter (Criterion 2)

(g) Image recovered using the MM-filter (Criterion 3)

Figure 3.1: Qualitative performance of the various filters in reducing AWGN of variance 0.01 (normalized) in the 'Crowd' image

(a) Original 'crowd' image

(b) Image corrupted by Gaussian noise of variance 0.025 (normalized)

(c) Image recovered using the sample mean filter

(d) Image recovered using the edge-adaptive Wiener filter

(e) Image recovered using the MM-filter (Criterion 1)

(f) Image recovered using the MM-filter (Criterion 2)

(g) Image recovered using the MM-filter (Criterion 3)

Figure 3.2: Qualitative performance of the various filters in reducing AWGN of variance 0.025 (normalized) in the 'Crowd' image

TABLE 3.1

MSE, FOM AND THE TIME TAKEN TO PROCESS AN IMAGE OF SIZE 512X512 FOR THE VARIOUS FILTERS IN REDUCING AWGN IN THE 'CROWD' IMAGE

	For noise corrupted images		For images recovered by the sample mean filter		For images recovered by the edge-adaptive Wiener filter	
Time taken	-		≈ 5 seconds		≈ 8 seconds	
Noise variance	MSE	FOM %	MSE	FOM %	MSE	FOM %
0.01	650.51	11.339	151.46	20.198	111.59	51.517
0.025	1629.6	4.2043	191.6	16.295	192.85	36.953
0.075	4870.7	0.64044	321.99	8.5431	435.27	18.643

	For images recovered by MM - filter (Criterion 1)		For images recovered by MM - filter (Criterion 2)		For images recovered by MM - filter (Criterion 3)	
Time taken	≈ 6 seconds		≈ 6 seconds		≈ 13 seconds	
Noise variance	MSE	FOM %	MSE	FOM %	MSE	FOM %
0.01	144.77	39.037	144.79	39.073	116.07	45.227
0.025	219.48	24.696	219.56	24.726	176.85	33.77
0.075	435.51	11.698	435.84	11.694	365.25	17.146

edge preservation. Figure 3.2, where the 'Crowd' image is corrupted by a larger amount of Gaussian noise with variance 0.025 (normalized with respect to maximum greyscale value, i.e, 255), also shows similar results. Thus, it is evident that the MM-filters remove the noise satisfactorily both in the homogeneous regions and also in the edge areas of an image.This results in proper noise reduction while avoiding the blurring.

The quantitative results are shown in Table 3.1. Complexity of each filter is given in the table in terms of their processing time. It is assumed that, the processing time of the filters increases with the increase in the complexity. It is seen that sample mean filter is the least complex filter, whereas the proposed MM-filter based on Criterion 3 is the most complex among the filters considered for comparison. As can be seen from the same table, the MM-filters obtained using Criteria 1 and 2 provide much better FOM values

than the sample mean filter, signifying that the MM-filter does a better edge preservation. The complexity of these filters are comparable to that of the sample mean filter. It can be observed that among the three criteria of MM-filter, Criterion 3 gives the best balance between the mean square error and the figure of merit values. Thus, the quantitative results of the proposed MM-filter suggests that it provides a balance between noise reduction and edge preservation. On the other hand, the sample mean filter is good at noise reduction, whereas the edge-adaptive Wiener filter is good at avoiding blurring.

3.4 MM-Filter-Based Unbiased Homomorphic System to Reduce Speckle

In this section, a homomorphic system using the MM-filter introduced in the previous section is presented in order to reduce speckle in images. As given in Section 3.2, the speckle noise corruption is modelled as

$$as = bs \cdot \eta s \tag{3.30}$$

where as is the observed corrupted signal, bs is the original uncorrupted signal and ηs is the multiplicative white noise with lognormal distribution (speckle). The problem is to get an estimate $\hat{bs}$ of bs from the observed signal as.

As explained in Chapter 2, when the unbiased homomorphic system employing the GSFWO filter shown in Figure 2.3 is employed to reduce the speckle, the system reduces to an unbiased homomorphic system employing the sample mean filter. However, as the design of the GSFWO filter assumes that the uncorrupted signal to the filter is of constant amplitude within the filter window, the proposed MM-filter is used in its place in the unbiased homomorphic system to reduce the speckle. The block diagram of the proposed unbiased MM-filter-based homomorphic system to reduce the speckle is shown in Figure 3.3.

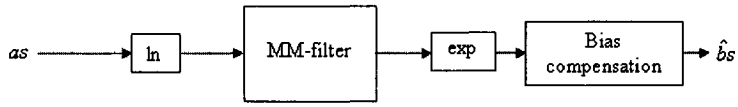

Figure 3.3: Unbiased homomorphic system to reduce speckle employing the MM-filter

The description of the proposed filter to reduce the speckle is as follows. The observed corrupted signal as is first subjected to the natural logarithm. As explained in Chapter 2, the multiplicative noise is change to an additive one by this transformation. As the multiplicative noise is assumed to be white, the additive noise will also be white [22].

The MM-filter is then applied to reduce this additive white noise, which is Gaussian distributed. As shown in Section 3.3, the MM-filter would work better when the signal is not constant within the filter window, which is generally true in most cases. The output from the MM-filter is then subjected to the exponentiation operation. Finally, the bias compensation as explained in Section 2.5.3 is applied to the signal resulting from the exponentiation operation. The unbiased estimate $\hat{bs}$ of the original uncorrupted signal bs is obtained at the output of this bias compensation.

3.5 Performance of the Proposed and Some Existing Filters in Reducing Speckle

In this section, a comparative study of the performance of some of the existing filters and the proposed system is carried out. Both the quantitative and qualitative results are considered. A comprehensive review of the speckle removal filters for images has been presented in [6] and [9]. The filters considered for comparison are as follows:

(1) Lee filter [13]

(2) Filter proposed by Kuan et al. [11]

(3) Filter proposed by Frost et al. [12]

(4) Gamma filter [14]

(5) Homomorphic system employing an edge-adaptive Wiener filter [7]

The 'Pepper' image, two nearly uncorrupted SAR images and two unprocessed images generated by a coherent imaging system are considered for the qualitative analysis. One of the two unprocessed images corrupted by speckle is a SAR image obtained from earth resource satellite (ERS). Figures 3.4-3.6 present a qualitative performance of the various filters for speckle reduction. In these cases the uncorrupted signal is combined with the speckle noise by doing pixel-wise multiplication. On the other hand, Figures 3.7 and 3.8 show the qualitative performance of the filters on images generated from coherent imaging systems having unknown amount of speckle already present. In Figures 3.5 and 3.6, SAR images, respectively, with low and high amount of edge details are considered.

The mean square error and the figure of merit described in Section 3.3.2, are used to present the quantitative results. These values of MSE and FOM are presented for the 'Pepper' image and the two nearly uncorrupted SAR images. As mentioned earlier, a low MSE signifies a good noise reduction property, whereas a higher percentage of the FOM signifies a good edge preservation property. Tables 3.2-3.4 give the values of the quantitative results when the three uncorrupted or nearly uncorrupted images are used. Note that the MSE and the FOM values given in the tables corresponding to the noise corrupted images are obtained using the uncorrupted original images and the corresponding noise corrupted images.

Analysis of the complexity of speckle reduction filters is of crucial importance, as most of these filters are required to operate in an on-board or a real-time system [33]. A study of the complexity of the filters is provided in Table 3.5. Each of the existing filters discussed above and the proposed filter are implemented using MATLAB in windows operating system on a machine with 2.5GHz processor. The time taken to process an image of size 512x512 is obtained. The number of addition, multiplication, comparison and other operations is used as a criterion to measure the complexity. The operation of the square root is

implemented using the well known Newton iterative method, and that of the exponentiation and natural logarithm is implemented using the Taylor series expansion.

As mentioned earlier, the Lee filter (LF) [13] is one of the earliest filters used for the reduction of the speckle. It is evident from Figures 3.4-3.6, that even though the filter does not result in blurring the image, it tends to leave a significant amount of noise behind. The filter applied on the unprocessed images containing speckle, as shown in Figures 3.5 and 3.6, provide the same result. The quantitative results given in Tables 3.2-3.4 support the qualitative results and hence one would not be encouraged to use Lee filter as a reliable tool for reducing the speckle. As seen from Table 3.5, the complexity of the Lee filter is moderate, with the most time consuming process being the square root operation.

The filter proposed by Kuan et al. (KF) [11], which will henceforth be referred to as the Kuan filter, is nothing but a generalized Lee filter. Although there is not much difference between the qualitative performance of the two filters, the quantitative results given in Tables 3.2-3.4 show clearly that the former outperforms the later. However, the Kuan filter still leaves significant amount of noise in the recovered image. As seen from Table 3.5 the complexity of the Kuan filter is slightly greater than that of the Lee filter, and can be considered as moderately complex.

The filter proposed by Frost et al. (FF) [12], which will henceforth be referred to as the Frost filter, has been stated to be the best spatial domain state-of-the-art filter to reduce speckle in an image [6]. This is evident from the reduction in the MSE obtained by various filters given in Tables 3.2-3.4. However , when FOM is compared, the existing Gamma filter and the edge-adaptive Wiener filter-based homomorphic system are found to perform better than the Frost filter. It is evident from the qualitative results presented in Figures 3.4-3.8, that the edge-adaptive Wiener filter-based homomorphic system and the Gamma filter perform better than the Frost filter, which results in a considerable amount of blurring of the edges. However the Frost filter performs better than the Lee filter and the Kuan filter. One very important drawback of the Frost filter, which can be seen from Table 3.5, is that it

has large complexity. It has very slow processing speed, and hence, might not be prefered in applications where speed is crucial.

(a) Original 'pepper' image

(b) Image corrupted by speckle (ENL=20)

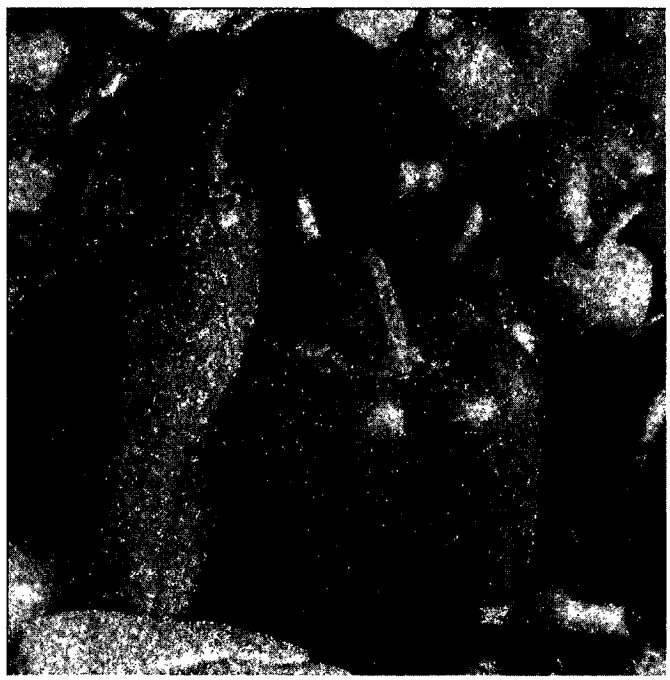

(c) Image recovered by the Lee filter

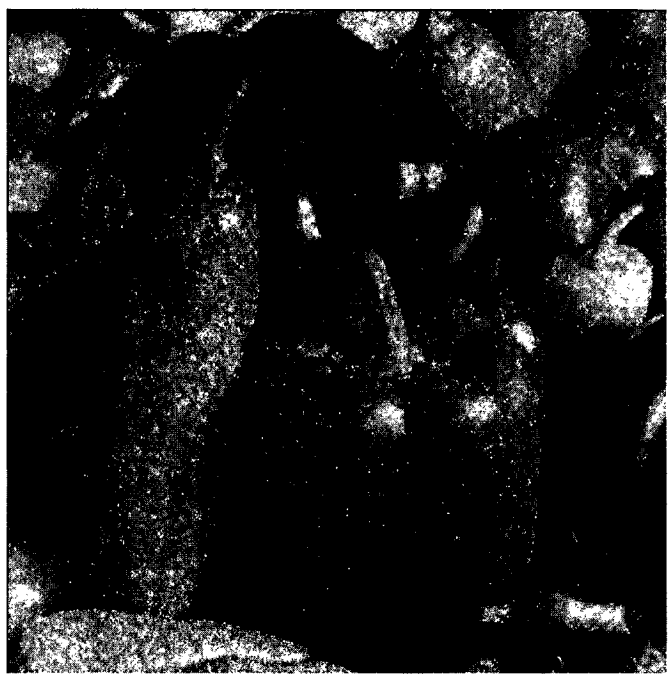

(d) Image recovered by the Kuan filter

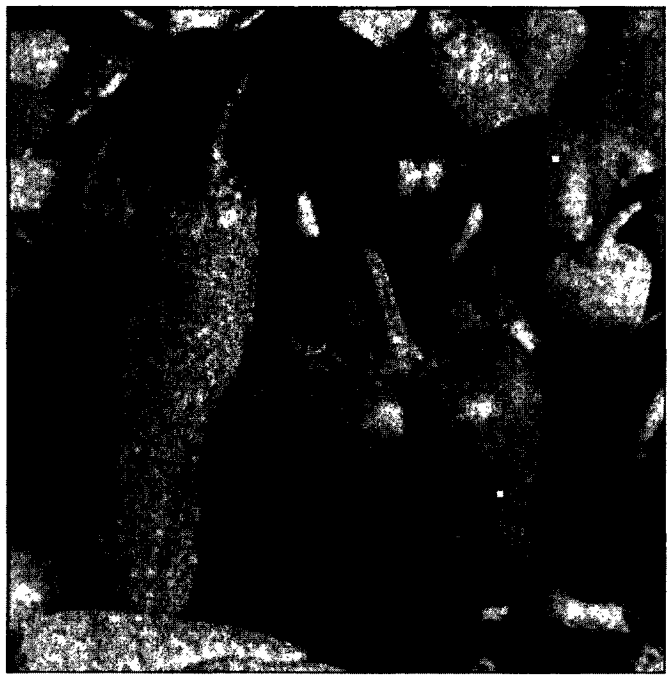

(e) Image recovered by the Frost filter

(f) Image recovered by the Gamma filter

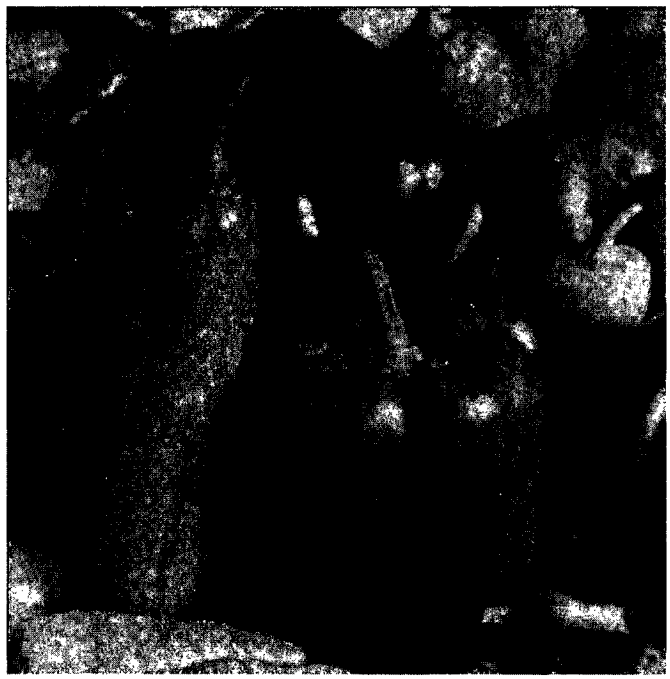

(g) Image recovered by the edge-adaptive Wiener filter-based homomorphic system

(h) Image recovered by the MM-filter (Criterion 1) based unbiased homomorphic system

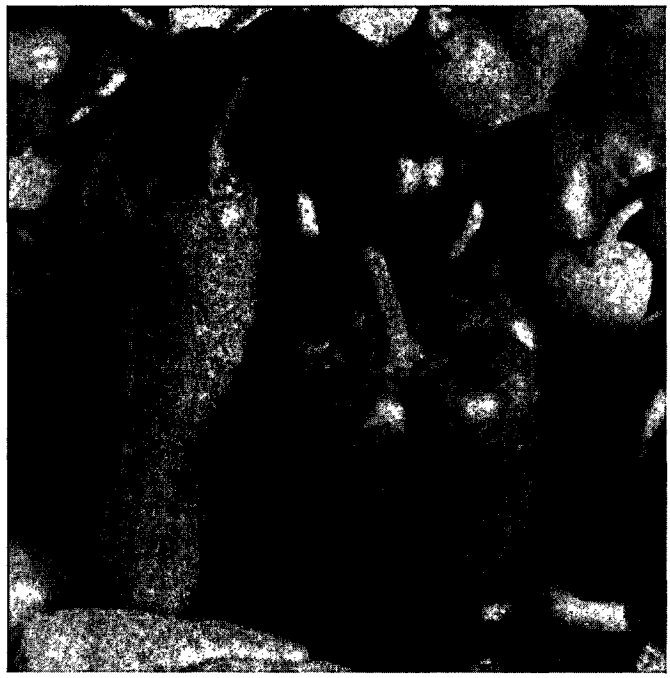

(i) Image recovered by the MM-filter (Criterion 2) based unbiased homomorphic system

(j) Image recovered by the MM-filter (Criterion 3) based unbiased homomorphic system

Figure 3.4: Qualitative performance of the various filters in reducing speckle in the 'Pepper' image

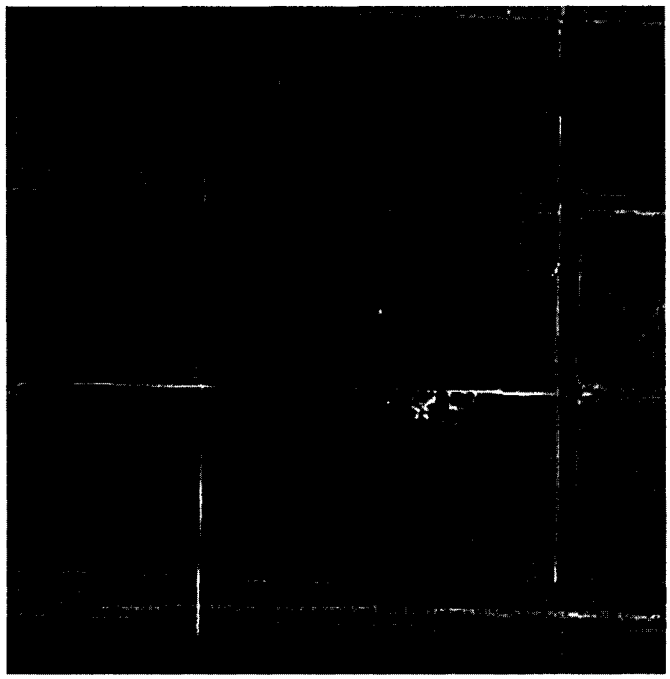

(a) Nearly uncorrupted SAR image

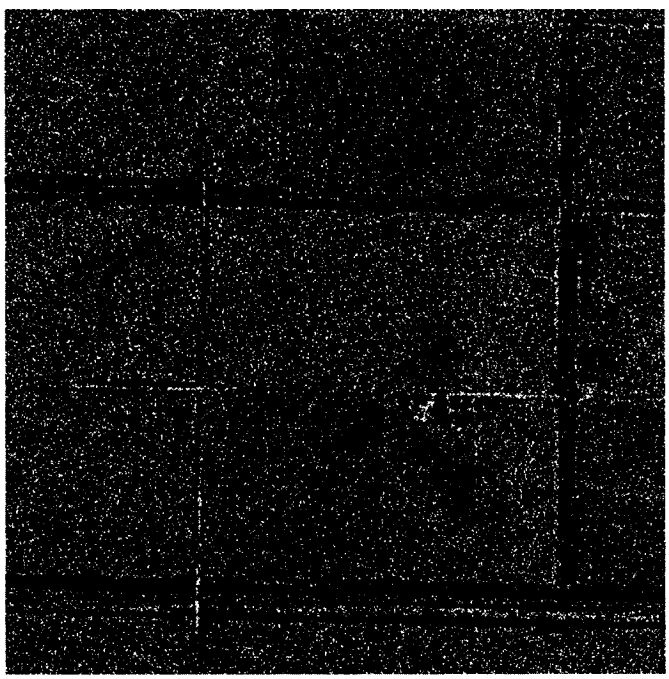

(b) Image corrupted by speckle (ENL=3.333)

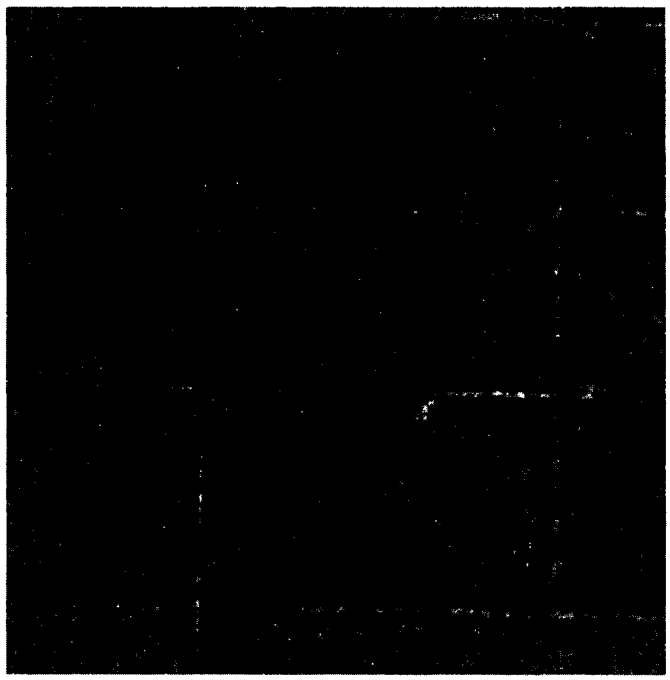

(c) Image recovered by the Lee filter

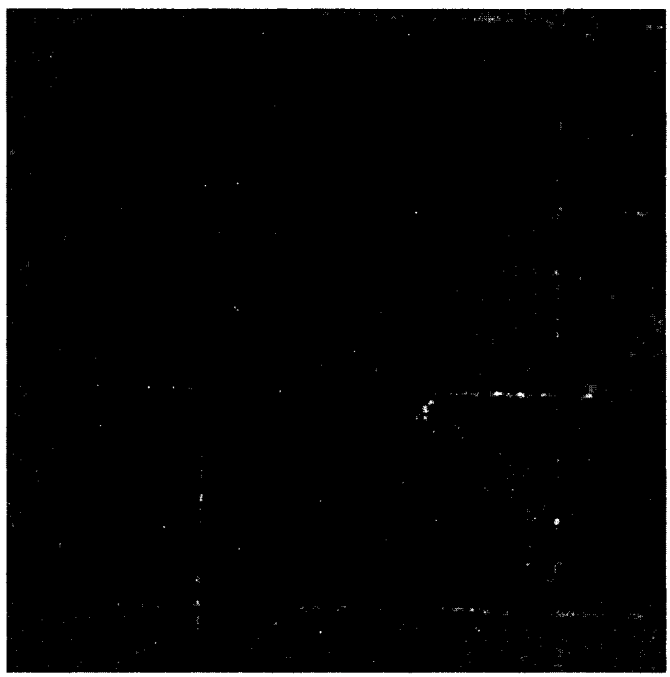

(d) Image recovered by the Kuan filter

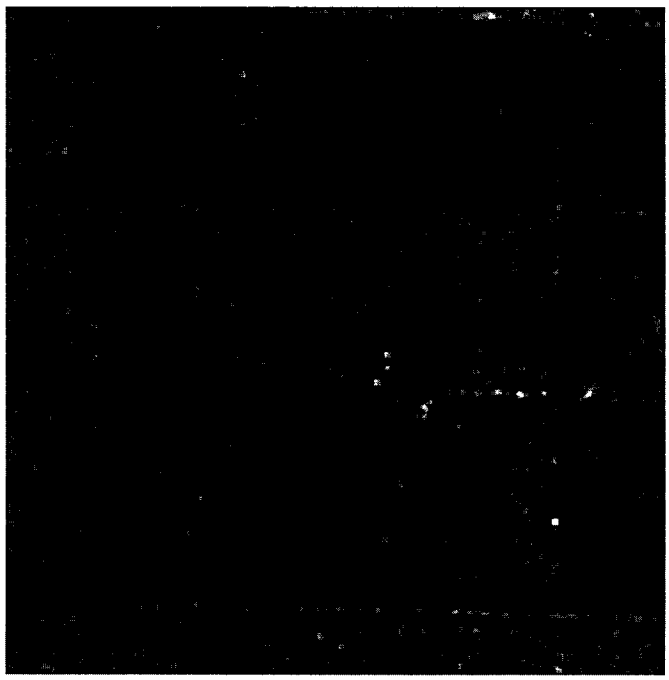

(e) Image recovered by the Frost filter

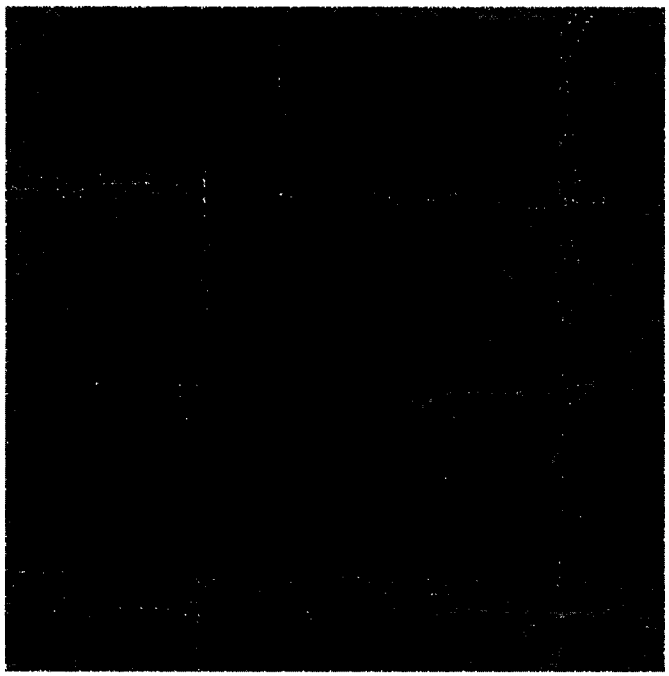

(f) Image recovered by the Gamma filter

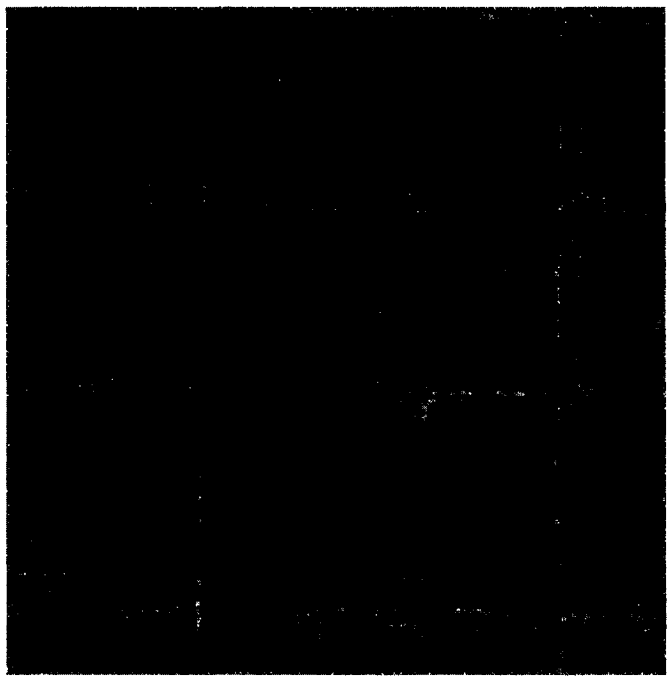

(g) Image recovered by the edge-adaptive Wiener filter-based homomorphic system

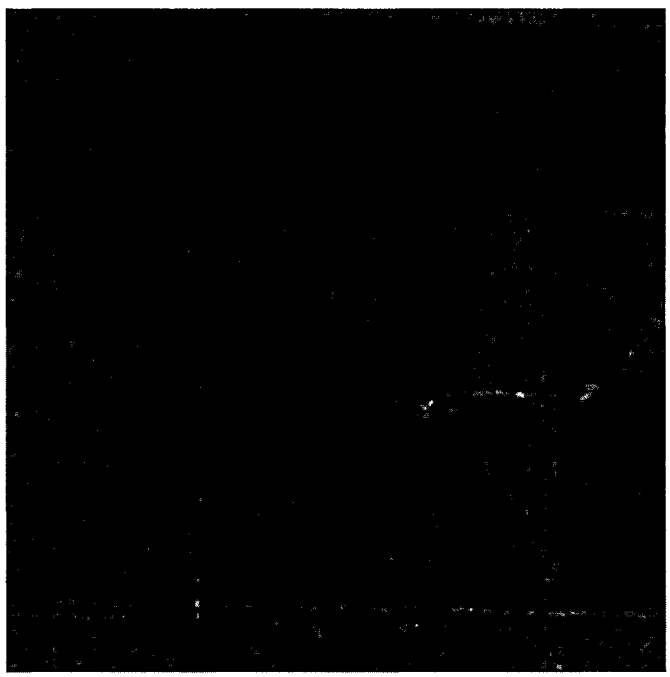

(h) Image recovered by the MM-filter (Criterion 1) based unbiased homomorphic system

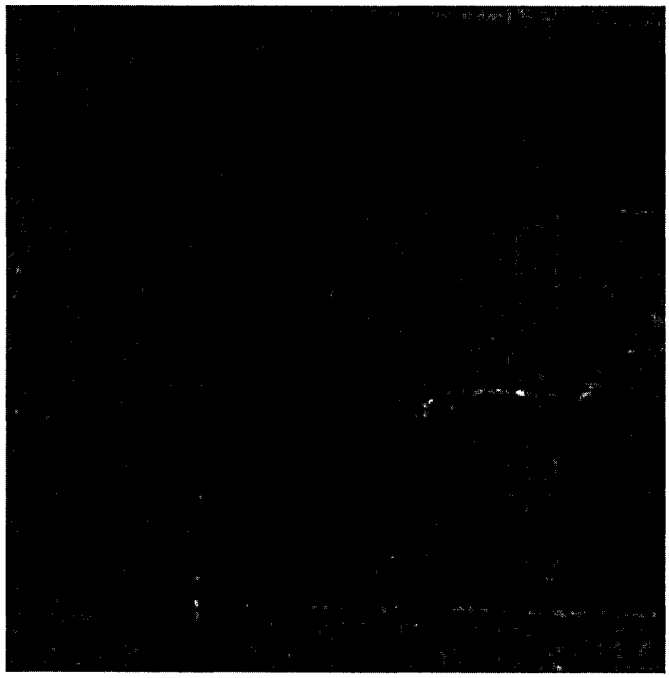

(i) Image recovered by the MM-filter (Criterion 2) based unbiased homomorphic system

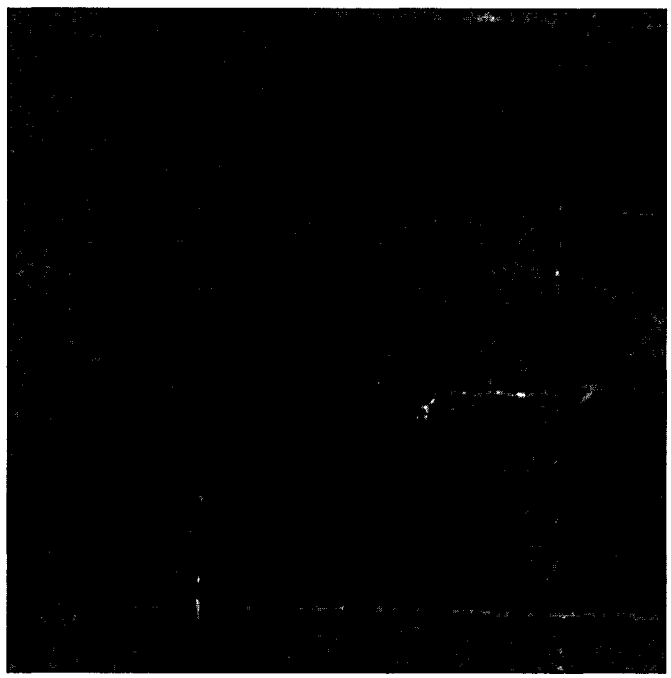

(j) Image recovered by the MM-filter (Criterion 3) based unbiased homomorphic system

Figure 3.5: Qualitative performance of the various filters in reducing speckle in a nearly uncorrupted SAR image having small amount of edge detail

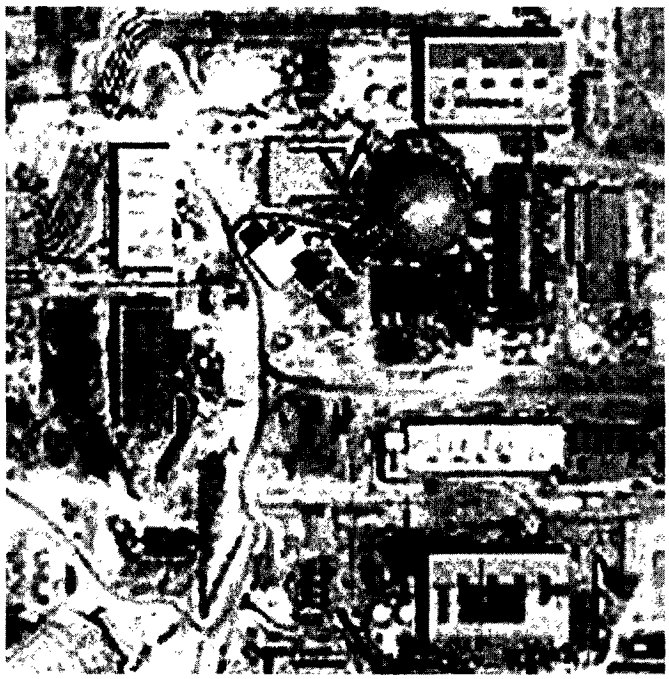

(a) Nearly uncorrupted SAR image

(b) Image corrupted by speckle (ENL=10)

(c) Image recovered by the Lee filter

(d) Image recovered by the Kuan filter

(e) Image recovered by the Frost filter

(f) Image recovered by the Gamma filter

(g) Image recovered by the edge-adaptive Wiener filter-based homomorphic system

(h) Image recovered by the MM-filter (Criterion 1) based unbiased homomorphic system

(i) Image recovered by the MM-filter (Criterion 2) based unbiased homomorphic system

(j) Image recovered by the MM-filter (Criterion 3) based unbiased homomorphic system

Figure 3.6: Qualitative performance of the various filters in reducing speckle in a nearly uncorrupted SAR image having large amount of edge detail

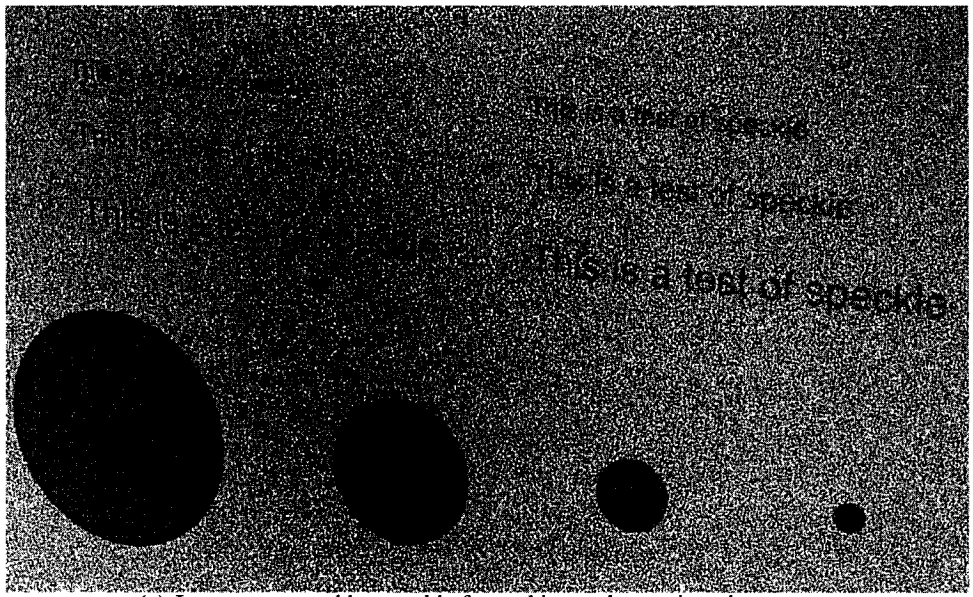

(a) Image corrupted by speckle formed in a coherent imaging system

Gamma filter (GF) is one of the better filters to reduce the speckle, and it especially works well when the scene is mostly homogeneous. This is evident from Figure 3.5, where the scene is mostly homogeneous, and also from Table 3.3. But as evident from all the other figures, Gamma filter tend to leave noise at the edges, which constitute significant details of an image. But, denoising performance of the Gamma filter in homogeneous region is better. The Gamma filter has a moderate to high complexity as can be seen from Table 3.5.

A homomorphic system employing an edge-adaptive Wiener filter (HAWF), is the only kind of homomorphic system which has been used for speckle reduction. As evident from Tables standard3.2-3.4, this filter performs well, when the noise is less. It also gives good a FOM result. Its complexity is less, and hence, its processing time is also less as shown in Table 3.5. But, as can be seen from the qualitative results presented in Figures 3.4-3.8, this homomorphic system like the Gamma filter leaves a significant amount of noise at the edges in an image. Thus, it might be preferable to use this filter when the noise content can be expected to be less.

First of the proposed filters used to reduce speckle is the unbiased homomorphic system, HMMFC1, employing the MM-filter based on Criterion 1 of Section 3.3.1. This filter has

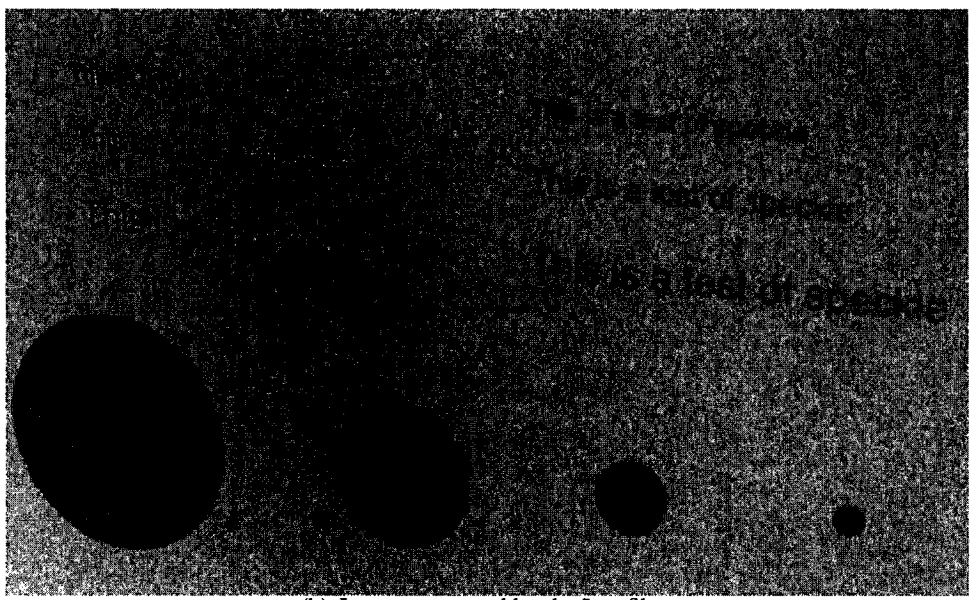

(b) Image recovered by the Lee filter

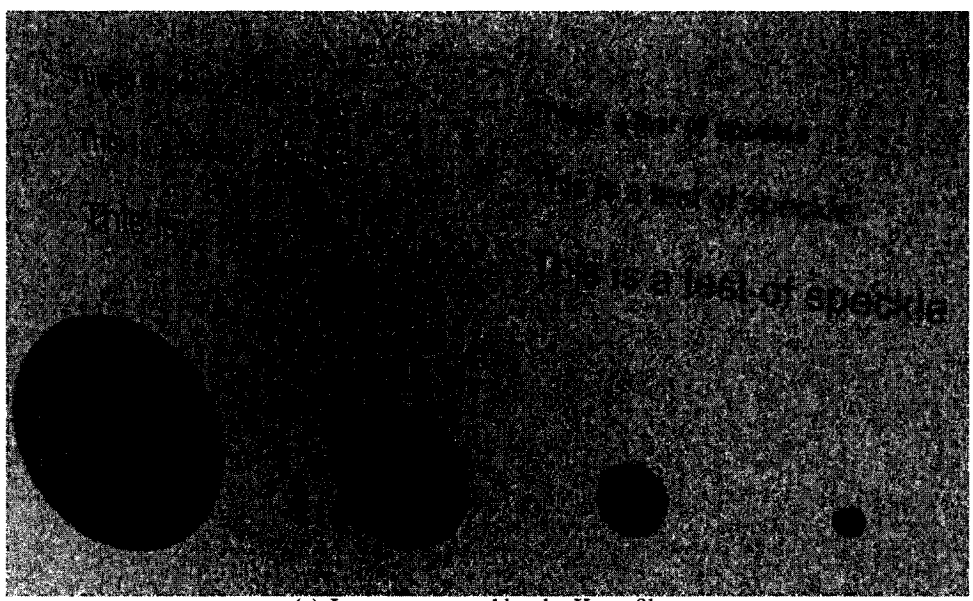

(c) Image recovered by the Kuan filter

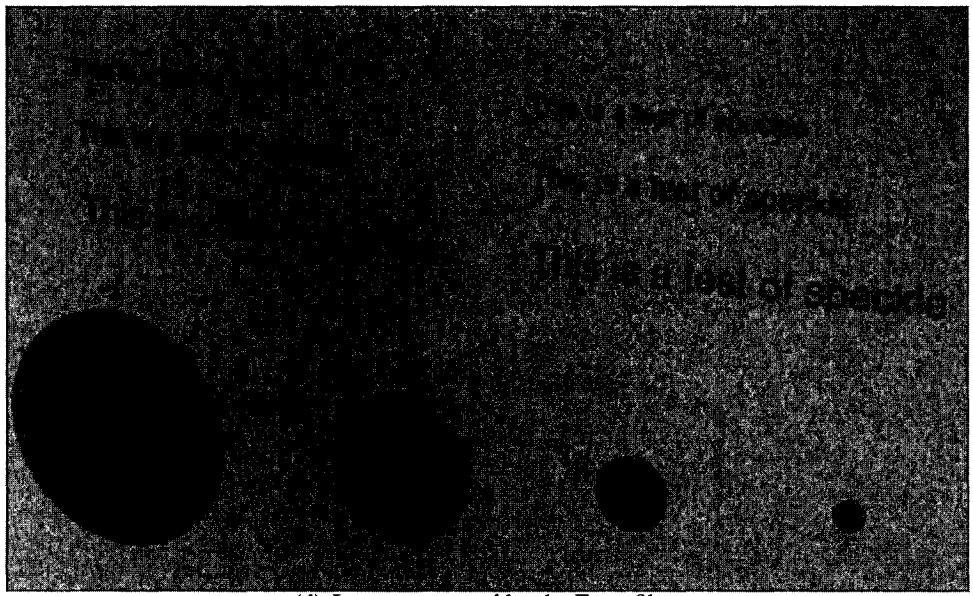

(d) Image recovered by the Frost filter

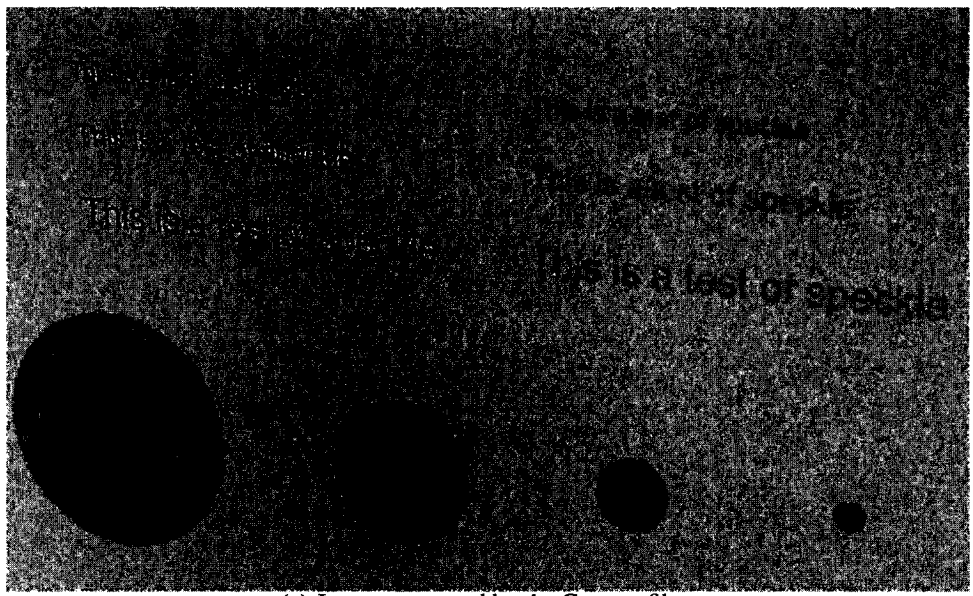

(e) Image recovered by the Gamma filter

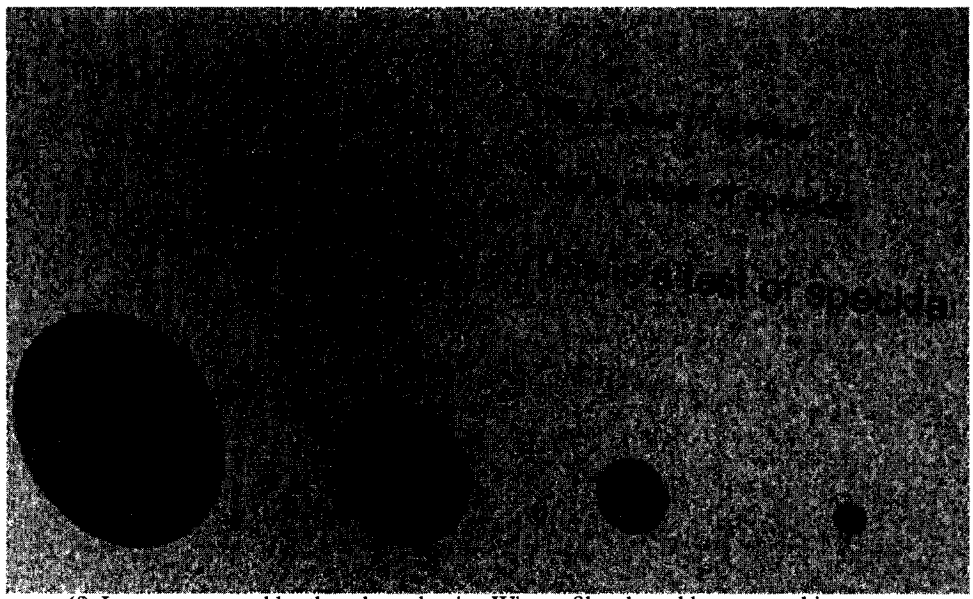

(f) Image recovered by the edge-adaptive Wiener filter-based homomorphic system

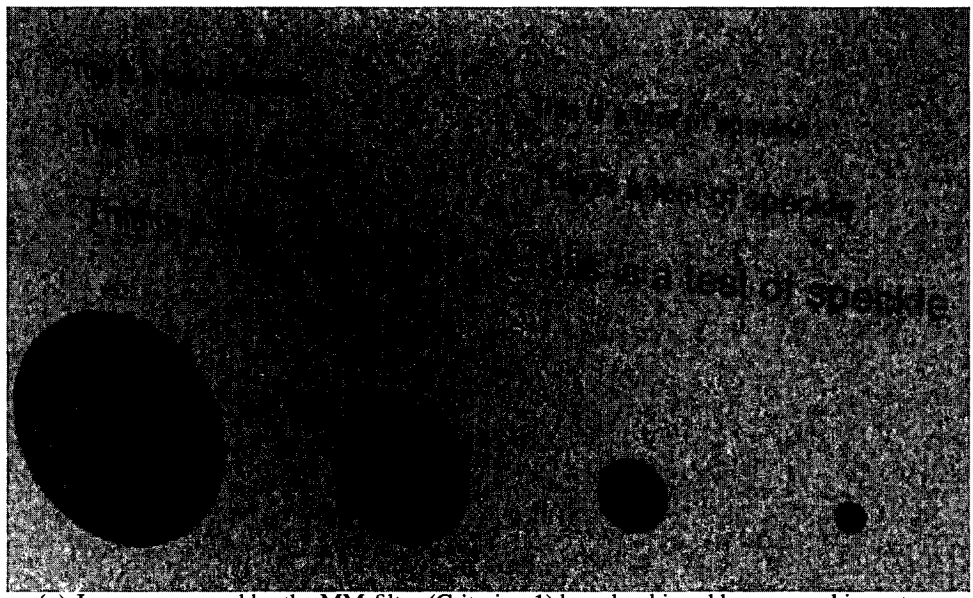

(g) Image recovered by the MM-filter (Criterion 1) based unbiased homomorphic system

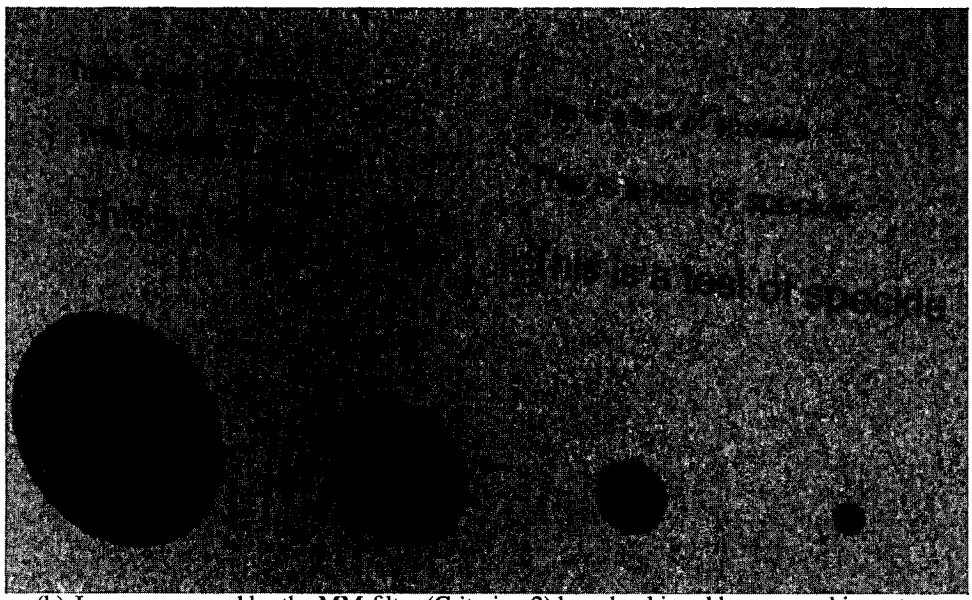

(h) Image recovered by the MM-filter (Criterion 2) based unbiased homomorphic system

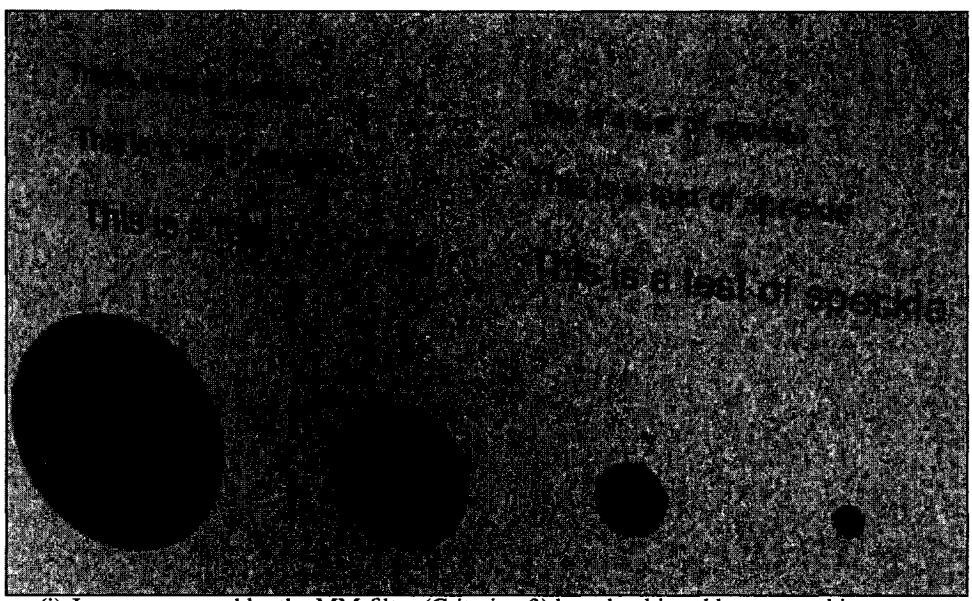

(i) Image recovered by the MM-filter (Criterion 3) based unbiased homomorphic system

Figure 3.7: Qualitative performance of the various filters in reducing speckle in an unprocessed image generated using a coherent imaging system

(a) Image taken by a SAR system corrupted by speckle

a very low complexity. The filter performs well, qualitatively in that it is good in removing the noise and satisfactorily preserving the edges. Thus, the filter does not have the problem of noise residual encountered in most of the filters discussed. The quantitative results of this filter, given in Tables 3.2-3.4, shows that it has good performance in reducing the MSE and also when the speckle content is less, a higher percentage of FOM.

The second proposed filter used is the unbiased homomorphic system, HMMFC2, employing the MM-filter based on Criterion 2. The performance of this filter is similar to that of the homomorphic system, HMMFC1. Qualitatively, they both show very similar characteristics. This filter also has a low complexity and performs well in reducing the MSE figure.

The third proposed filter used is the unbiased homomorphic system, HMMFC3, employing the MM-filter based on Criterion 3. This is a filter with low to moderate complexity. As seen from Figures 3.4-3.8, this filter gives the best qualitative performance for the images considered. Thus, among the three proposed unbiased homomorphic systems,

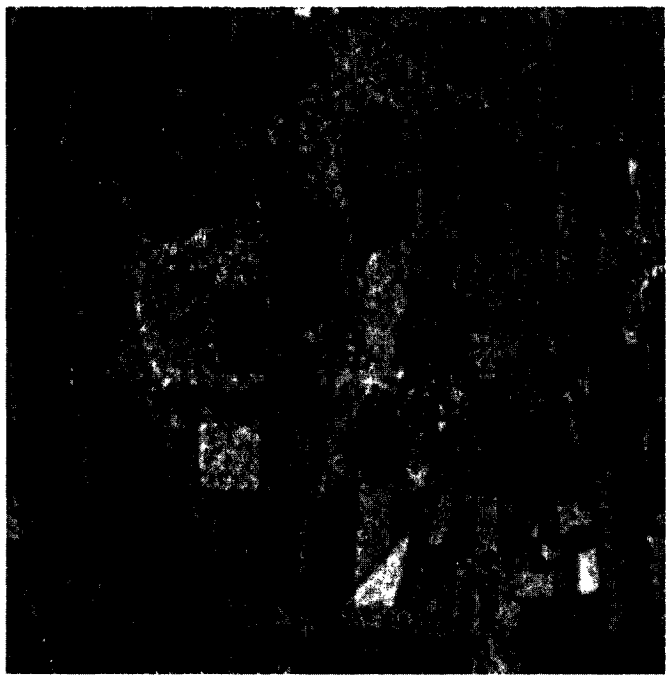

(b) Image recovered by the Lee filter

(c) Image recovered by the Kuan filter

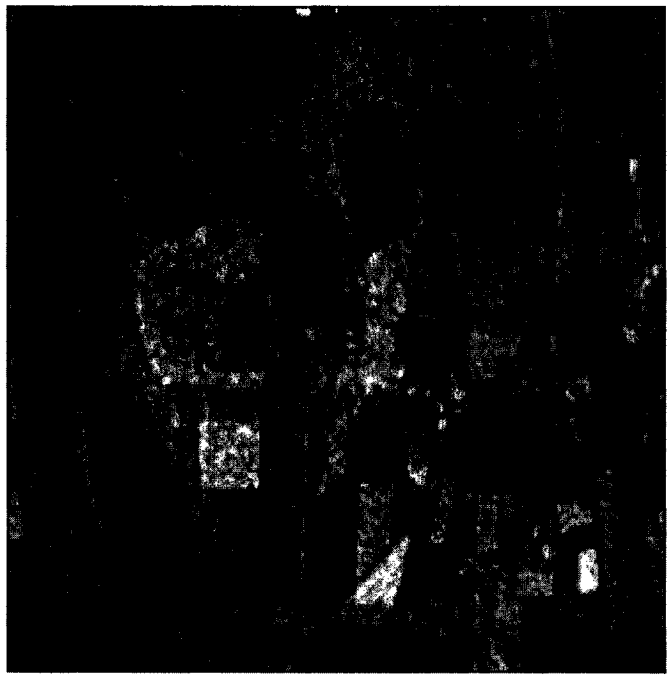

(d) Image recovered by the Frost filter

(e) Image recovered by the Gamma filter

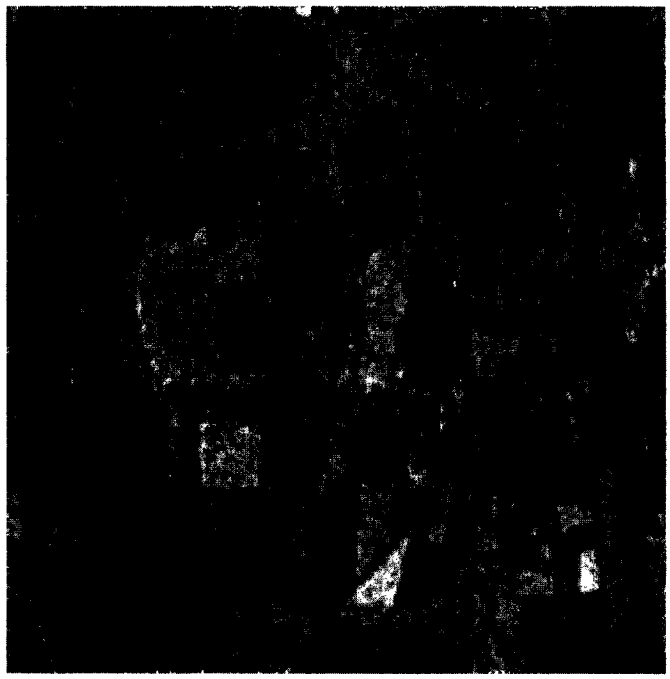

(f) Image recovered by the edge-adaptive Wiener filter-based homomorphic system

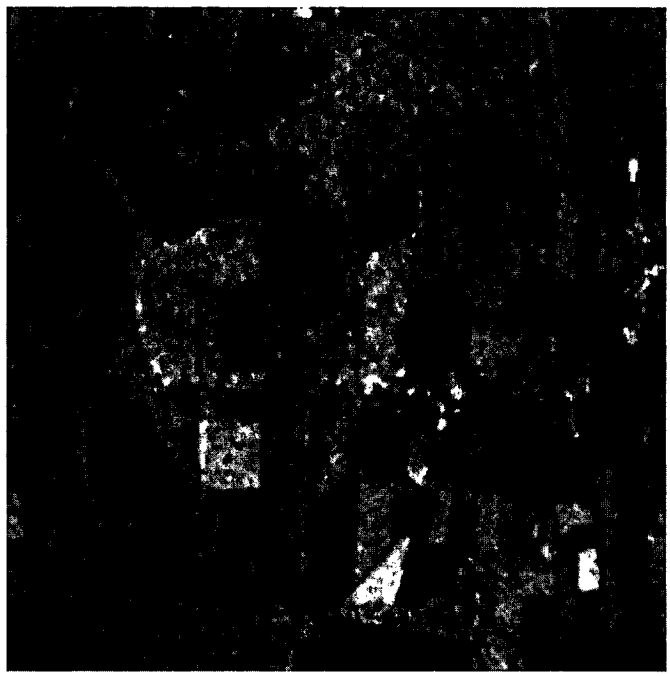

(g) Image recovered by the MM-filter (Criterion 1) based unbiased homomorphic system

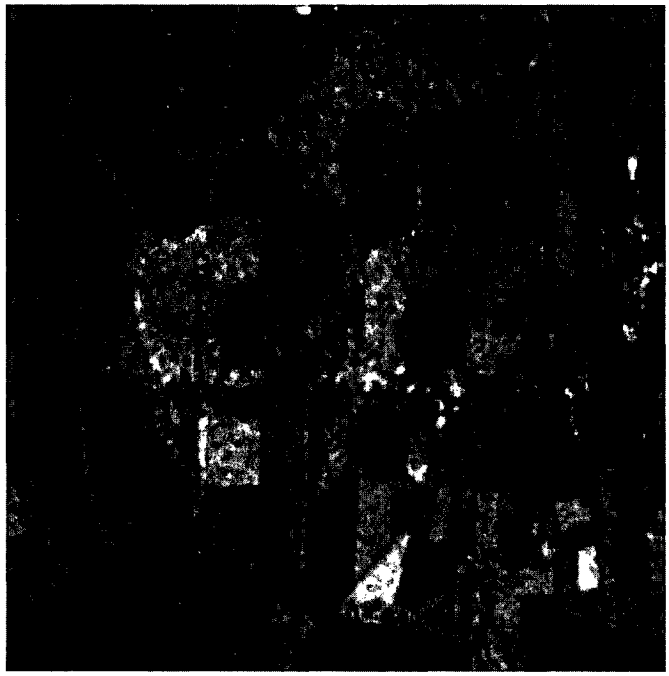

(h) Image recovered by the MM-filter (Criterion 2) based unbiased homomorphic system

(i) Image recovered by the MM-filter (Criterion 3) based unbiased homomorphic system

Figure 3.8: Qualitative performance of the various filters in reducing speckle in an unprocessed image obtained from earth resource satellite (ERS) SAR system

HMMFC3 seems to provide the best combination of the mean and median estimates from the point of view of reducing speckle. The quantitative results given in the tables are good especially when the noise content is high.

One important thing to note is that, most of the computation of the proposed unbiased homomorphic systems is taken up by the quick sorting function which on average uses 35 comparisons. The processing time can be considerably reduced by implementing the filter on a processor, using a parallel sorting scheme such as shear sorting [34].

TABLE 3.2

MSE AND FOM FOR THE VARIOUS FILTERS IN REDUCING SPECKLE IN THE 'PEPPER' IMAGE

		For noise corrupted images		For images recovered by LF		For images recovered by KF	
Noise var	ENL	MSE	FOM %	MSE	FOM %	MSE	FOM %
0.05	20	609.18	18.748	549.06	24.674	504.65	25.129
0.1	10	1006.3	11.412	1377.1	15.125	1164.2	14.99
0.2	5	1643.9	5.6628	1580.4	12.423	1178.5	12.327
0.3	3.33	2200.7	3.5021	1725.6	11.877	1169.7	11.254
0.4	2.5	2700.2	1.7966	1690.8	11.954	1077.5	10.836
0.5	2	3184.7	1.0199	2034	11.29	1201.7	10.055
0.6	1.67	3628.7	0.6994	2025.2	11.256	1165.5	9.5532
0.7	1.429	4071.2	0.4182	1924.8	10.384	1122.7	9.0027
0.8	1.25	4528.5	0.256	2060.7	10.365	1174.7	8.6144
0.9	1.11	4950.1	0.138	2174	9.9245	1225.1	8.6457
1	1	5359.7	0.0953	2167.1	9.6855	1244.8	8.4565

		For images recovered by FF		For images recovered by GF		For images recovered by HAWF	
Noise var	ENL	MSE	FOM %	MSE	FOM %	MSE	FOM %
0.05	20	128.45	26.347	141.97	50.012	94.269	45.474
0.1	10	163.67	23.368	181.45	41.302	143.16	41.102
0.2	5	239.76	16.718	245.03	30.604	267.82	32.054
0.3	3.33	308.55	13.792	322.86	25.482	402.94	27.177
0.4	2.5	376.26	13.357	399.23	23.36	551.74	25.109
0.5	2	447.18	12.203	497.56	22.419	720.95	21.554
0.6	1.67	518.53	12.59	582.02	22.845	912.78	20.667
0.7	1.429	607.85	11.543	674.28	21.176	1126.3	18.775
0.8	1.25	668.65	11.398	785.94	19.653	1375.5	16.984
0.9	1.11	744.41	11.29	872.21	16.405	1676.6	15.485
1	1	824.3	11.511	977.11	14.858	1934.7	14.227

		For images recovered by					
		HMMFC1		HMMFC2		HMMFC3	
Noise var	ENL	MSE	FOM %	MSE	FOM %	MSE	FOM %
0.05	20	64.73	58.53	65.9	58.56	209.28	29.543
0.1	10	95.032	52.722	96.139	52.545	228.24	28.631
0.2	5	158.33	40.659	158.35	40.584	265.05	24.049
0.3	3.33	229.16	31.258	227.95	31.392	304.03	21.562
0.4	2.5	298.43	23.364	297.99	24.408	345.18	20.274
0.5	2	370.44	17.69	373.07	19.232	400.79	18.162
0.6	1.67	425.63	13.821	430.11	15.917	454.69	17.981
0.7	1.429	494.74	9.8391	500.02	11.482	525.66	16.318
0.8	1.25	556.44	8.3086	559.05	9.1905	601.02	15.387
0.9	1.11	628.53	7.448	628.3	7.4466	695.21	14.754
1	1	709.65	7.017	713.16	7.044	804.67	13.419

TABLE 3.3

MSE AND FOM FOR THE VARIOUS FILTERS IN REDUCING SPECKLE IN A NEARLY UNCORRUPTED SAR IMAGE HAVING SMALL AMOUNT OF EDGE DETAIL

		For noise corrupted images		For images recovered by			
				LF		KF	
Noise var	ENL	MSE	FOM %	MSE	FOM %	MSE	FOM %
0.05	20	632.8	12.916	426.13	21.317	394.92	21.373
0.1	10	1068.4	8.1561	1032.6	14.147	882.17	13.798
0.2	5	1729.4	3.9939	1291.2	10.776	981.29	10.238
0.3	3.33	2284.4	2.0435	1291.1	9.2149	911.29	8.7273
0.4	2.5	2791	1.0297	1390.4	8.2397	927.66	7.6083
0.5	2	3322.9	0.466	1494.4	7.3143	949.81	6.7073
0.6	1.67	3657.5	0.2612	1558.4	7.209	964.38	6.2479
0.7	1.429	4050.8	0.2302	1607	6.4502	982.22	5.8871
0.8	1.25	4413.2	0.1325	1722.7	5.8693	1020.1	5.438
0.9	1.11	4802	0.0808	1766.4	5.9942	1049	5.1684
1	1	5161.8	0.0291	1780.2	5.4615	1069.6	5.0481

		For images recovered by					
		FF		GF		HAWF	
Noise var	ENL	MSE	FOM %	MSE	FOM %	MSE	FOM %
0.05	20	224.46	20.511	196.17	46.11	140.88	54.456
0.1	10	252.78	16.479	204.34	46.372	185.07	47.634
0.2	5	307.02	12.014	266.19	36.899	303.79	38.417
0.3	3.33	368.24	9.4921	308.76	28.993	403.37	32.745
0.4	2.5	422.65	8.9763	355.02	25.715	523.4	29.9
0.5	2	468.46	8.1035	403.94	22.019	647.76	27.225
0.6	1.67	529.88	7.5087	428.02	24.689	796.71	24.437
0.7	1.429	586.45	6.9529	483.77	21.644	954.47	22.529
0.8	1.25	625.58	7.1198	535.61	19.566	1146.2	21.572
0.9	1.11	697.75	6.5081	591.76	15.674	1359.9	18.39
1	1	758.16	6.9732	641.65	14.156	1615.6	17.017

		For images recovered by					
		HMMFC1		HMMFC2		HMMFC3	
Noise var	ENL	MSE	FOM %	MSE	FOM %	MSE	FOM %
0.05	20	162.9	52.829	161.94	52.801	278.97	32.181
0.1	10	185.17	48.05	184.78	48.222	291.67	30.702
0.2	5	234.67	37.809	232.7	38.749	322.41	27.935
0.3	3.33	292.37	28.194	288.89	29.461	349.25	25.507
0.4	2.5	355.56	19.463	351.27	21.744	386.47	23.452
0.5	2	416.16	13.283	415.52	16.126	417.03	21.48
0.6	1.67	472.44	10.319	477.58	12.335	456.54	19.706
0.7	1.429	525.54	8.1326	535.39	9.723	501.18	19.953
0.8	1.25	574.69	6.5795	584.68	7.2917	546.81	16.745
0.9	1.11	638.86	6.2864	642.15	6.3879	616.03	14.491
1	1	708.76	5.6616	696.19	5.9623	694.74	13.027

TABLE 3.4

MSE AND FOM FOR THE VARIOUS FILTERS IN REDUCING SPECKLE IN A NEARLY UNCORRUPTED SAR IMAGE HAVING LARGE AMOUNT OF EDGE DETAIL

		For noise corrupted images		For images recov ered by			
				LF		KF	
Noise var	ENL	MSE	FOM %	MSE	FOM %	MSE	FOM %
0.05	20	774.26	9.59	974.52	16.832	898.62	17.2
0.1	10	1276.4	6.032	2457.52	10.251	2083.8	10.22
0.2	5	2129.4	2.376	2893.6	9.578	2167.4	9.629
0.3	3.33	2921	0.836	3093.5	9.263	2115.1	9.266
0.4	2.5	3696	0.3158	3420.4	9.356	2176.9	9.453
0.5	2	4445.9	0.1528	3591.7	9.338	2183.2	9.423
0.6	1.67	5183	0.0124	3779	9.36	2221.3	9.476
0.7	1.429	5954.9	0.00206	3926.2	9.255	2250.5	9.432
0.8	1.25	6649.2	0.00248	4008.7	9.378	2277.7	9.735
0.9	1.11	7364.8	0	4105.7	9.216	2340.7	9.576
1	1	8034	0	4266.1	9.332	2401.7	9.282

		For images recovered by					
		FF		GF		HAWF	
Noise var	ENL	MSE	FOM %	MSE	FOM %	MSE	FOM %
0.05	20	236.99	31.76	242.62	37.492	198.3	45.102
0.1	10	306.92	25.966	350.43	40.224	296.09	39.761
0.2	5	453.14	19.156	585.53	39.537	518.34	32.667
0.3	3.33	573.53	15.319	828.66	35.548	769.56	29.122
0.4	2.5	737.46	13.847	1084.3	32.043	1071.5	26.54
0.5	2	868.47	14.491	1379.7	30.889	1368.2	25.634
0.6	1.67	1019.9	12.218	1653.7	29.653	1795.5	23.914
0.7	1.429	1137.7	11.981	1959.3	23.72	2231.4	21.392
0.8	1.25	1266.3	12.41	2223.3	22.894	2680.4	19.771
0.9	1.11	1428.3	12.094	2500.1	20.422	3214.2	18.638
1	1	1533.2	11.415	2760.6	17.752	3822.7	17.876

		For images recovered by					
		HMMFC1		HMMFC2		HMMFC3	
Noise var	ENL	MSE	FOM %	MSE	FOM %	MSE	FOM %
0.05	20	141.72	49.181	141.5	49.065	475.24	33.907
0.1	10	199.1	49.2	198.11	49.005	509.46	32.698
0.2	5	320.5	38.492	315.97	38.888	575.57	30.745
0.3	3.333	450.48	32.173	442.61	33.389	637.85	29.923
0.4	2.5	395.43	25.237	589.3	26.742	719.42	27.448
0.5	2	730.56	19.912	734.44	21.708	803.07	27.977
0.6	1.6667	871.12	17.686	900.61	17.139	909.26	25.495
0.7	1.42857	987.76	15.389	1036.8	15.007	1010.2	23.842
0.8	1.25	1112.6	14.483	1159.4	13.816	1146.8	21.443
0.9	1.111	1257.8	14.361	1277.8	13.88	1325.8	20.933
1	1	1425.2	13.021	1405.7	12.551	1516.2	18.774

3.6 Summary

In this chapter, we have introduced a new filter referred to as the MM-filter in order to reduce the additive white Gaussian noise (AWGN). The estimation of the uncorrupted signal by the MM-filter has been achieved by using a combination of the mean and the median estimates of the uncorrupted signal. Three criteria have been given to perform the combination judiciously. A study of the qualitative and quantitative performance of the proposed MM-filter in reducing the AWGN has been carried out and compared with the sample mean filter and the edge-adaptive Wiener filter. The MM-filter has been found to perform better noise reduction and edge preservation than the others. This MM-filter has then been used within the unbiased homomorphic system, presented in Chapter 2, to reduce the speckle. The qualitative and quantitative performance of the proposed MM-filter-based unbiased homomorphic system in reducing the speckle has been analyzed and compared with that of a few other known filters. The proposed system has been found to perform considerably better than the others.

TABLE 3.5

COMPLEXITY OF THE VARIOUS FILTERS IN REDUCING SPECKLE IN TERMS OF THE TIME TAKEN TO PROCESS AN IMAGE OF SIZE 512X512 AND THE NUMBER OF COMPUTATIONS PER INPUT SAMPLE

Filter	Time taken to process a 512x512 image	Number of multiplication (m)	Number of addition (a)	Number of comparisons (c)
LF	$\approx$ 46 seconds	16	78	1
KF	$\approx$ 47 seconds	19	79	1
FF	$\approx$ 1150 seconds	708	148	0
HAWF	$\approx$ 10 seconds	7	100	2
GF	$\approx$ 60 seconds	21	79	4
HMMFC1	$\approx$ 7 seconds	30	26	35
HMMFC2	$\approx$ 7seconds	30	28	35
HMMFC3	$\approx$ 17seconds	11	101	35

...

Filter	other operations (o)	complexity (m+a+c+o)
LF	1 square root	96
KF	1 square root	100
FF	25 square roots & 25 exponential	906
HAWF	1 exponential & 1 logarithm	111
GF	3 square roots	107
HMMFC1	1 exponential & 1 logarithm	93
HMMFC2	1 exponential & 1 logarithm	95
HMMFC3	1 exponential & 1 logarithm	145

Chapter 4

Additive White Gaussian Noise Reduction in Videos

4.1 Introduction

Videos are generated using coherent imaging systems mounted on air-borne vehicles, which are used for applications such as terrain monitoring, surveillance and soil analysis [26]. Coherent systems are also used to generate videos for the purpose of various commercial, military and medicinal applications. As discussed in Chapter 2, images generated by coherent imaging systems are corrupted by speckle. Hence, the frames of a video captured using a coherent imaging system gets corrupted by speckle. The MM-filter-based homomorphic system, presented in Chapter 3, can readily be applied to each frame of the video to reduce the speckle. But, in such a filtering process the presence of correlation between the frames of the video is not exploited.

The process of filtering a video exploiting the interframe (intraframe) correlation is called temporal (spatial) filtering. To reduce the speckle in videos, a homomorphic system, which involves both spatial and temporal filtering, is considered in this thesis. As discussed in Chapter 3, a homomorphic system used to reduce speckle employs a filter that minimizes

the AWGN after the natural logarithmic operation.

In this chapter [36, 37], the problem of reducing the AWGN from videos is considered. One major aspect of temporal filtering to reduce the AWGN in videos is the way in which it tackles the interframe motion. Many researchers have proposed spatiotemporal filters for the AWGN reduction in videos [35]-[41]. One obvious way of designing a filter is to consider the video as a 3D signal and extend the techniques of designing 2D filters to the design of 3D filters. The authors in [35] have extended the 2D alpha trimmed filter and the 2D K-nearest neighborhood filter to the corresponding 3D filters and have presented a comparison of their performance.

In [39], the authors have not only presented a 3D linear minimum mean square error (LMMSE) filter but also proposed a 3D adaptive weighted average (AWA) filter. The performance of these two filters have also been compared. In [40], to reduce noise in videos, a method incorporating temporal Kalman estimates and spatial Wiener estimates has been proposed. In [41], to obtain the estimate of the uncorrupted signal, Hadamard transform is first applied in the temporal direction to the corrupted signal to remove the correlation between the successive frames, followed by the use of the edge-adaptive Wiener filter to smooth the frames.

All the filters mentioned above are motion compensated filters, i.e., these filters use motion estimation and compensation techniques to deal with the interframe motion. As motion estimation and compensation are computationally very expensive [8, 42], one would be interested in avoiding such a process, when noise reduction is of prime concern. A fast denoising scheme is needed, since in many cases the receiver might have to work under real-time conditions. In [38], a 3D rational filter, which does not require motion estimation and compensation, has been proposed and its real-time implementation shown.

In this chapter, two low-complexity filters that do not use motion estimation and compensation techniques are proposed to reduce AWGN in videos. These filters consist of a temporal estimation part and a spatial estimation part; both the spatiotemporal and spatial

estimates are used to get the final estimate of the uncorrupted signal.

The organization of the chapter is as follows. An overview of the temporal filtering in videos using the sample mean filter and the scalar Kalman filter [43, 44] is given in Section 4.2. In Section 4.3, the algorithms of the proposed filters are presented. In Section 4.4, the performance of the proposed filters to reduce AWGN in videos is studied and compared to the performance of a few other existing filters.

4.2 Temporal Filtering in Videos

In general, there are two approaches that are used for video filtering. In the first method, a 3D window consisting of elements from the current frame and the previous and succeeding frames is considered. These elements are then used to get an estimate of the uncorrupted current frame. The second method involves a 2D spatial filtering in the current frame and 1D filtering in the temporal direction. These spatial and temporal estimates are then combined to get the estimate of the uncorrupted current frame.

In this section, a brief study of the temporal filtering is presented. As discussed in Chapter 3, when a signal is corrupted by an AWGN, the sample mean filter gives an optimal estimate under the assumption of the signal being constant within the filter window. Motion in videos is represented by the change in intensity along the temporal direction. Hence, the presence of the motion would make the constant amplitude assumption invalid. In general, techniques to compensate the motion are used prior to the filtering. Ideally, once the interframe motion is dealt with, the change of intensity along the temporal direction should be zero and hence, the constant amplitude assumption within a window can be made. Such a case is considered in this section for the analysis of temporal filtering. We shall now show that the 1D scalar Kalman filter when used as the temporal filter is an optimal estimator like the sample mean filter, but has a much less storage requirement.

A signal corrupted by an AWGN can be modeled as

$$x = I + N \tag{4.1}$$

where I is the uncorrupted original signal, N is a zero mean AWGN and x is the observed corrupted signal. The model in (4.1) can be written as

$$x = I + \sigma v \tag{4.2}$$

where σ is the standard deviation of the noise N, and v a zero mean unit-variance Gaussian noise. The squared error between the corrupted and the uncorrupted signals is given by

$$(x - I)^2 = \sigma^2 v^2 \tag{4.3}$$

It can be inferred from (4.3) that for a signal corrupted by an additive noise, the squared error between the noisy and uncorrupted signals is directly proportional to the variance of the noise.

Now, let x_0 and x_1 represent the first and second noisy frames. Let (i, j) represent the position of a pixel in a frame. Writing the expressions for x_0 and x_1 in the form given by (4.2), we get

$$\begin{aligned} x_0(i,j) &= I_0(i,j) + \sigma v_0(i,j) \\ x_1(i,j) &= I_1(i,j) + \sigma v_1(i,j) \end{aligned} \tag{4.4}$$

where it is assumed that the AWGN corresponding to x_0 is independent of that corrupting x_0, but having the same standard deviation σ. Ideally, when the interframe motion has been compensated for, we have $I_0(i,j) = I_1(i,j) = I(i,j)$. Let us consider the use of the sample mean filter as the temporal filter to reduce the AWGN in x_1. The application of the

filter in the temporal direction results in the estimate of x_1 as

$$\frac{x_0(i,j) + x_1(i,j)}{2} = I(i,j) + \frac{\sigma}{2}(v_0(i,j) + v_1(i,j)) \tag{4.5}$$

Let $v_0 + v_1 = \sqrt{2}V_1$. It is known that the sum of independent Gaussian processes produces another Gaussian process [23]. Thus, V_1 is a unit-variance zero-mean white Gaussian noise. Therefore, (4.5) can be rewritten as

$$X_1(i,j) = I(i,j) + \sigma' V_1(i,j) \tag{4.6}$$

where $\sigma' = \frac{\sigma}{\sqrt{2}}$, and $X_1(i,j) = \frac{x_0(i,j)+x_1(i,j)}{2}$ is the estimated value at the pixel position (i,j) of the second frame. As can be seen, the standard deviation of the noise is decreased by a factor $\sqrt{2}$.

Next, let us consider the reduction of noise in x_2, the third frame. Ideally, when the interframe motion has been compensated for, we have $I_0(i,j) = I_1(i,j) = I_2(i,j) = I(i,j)$. The application of the sample mean filter in the temporal direction (using all the previous frames) results in the estimate of x_2 as

$$\frac{x_0(i,j) + x_1(i,j) + x_2(i,j)}{3} = I(i,j) + \frac{\sigma}{3}(v_0(i,j) + v_1(i,j) + v_2(i,j)) \tag{4.7}$$

Let, $v_0 + v_1 + v_2 = \sqrt{3}V_2$. Then, as mentioned before, sum of independent Gaussian processes produces another Gaussian process. Hence, V_2 is a unit-variance zero-mean white Gaussian noise, and (4.7) can be rewritten as

$$X_2(i,j) = I(i,j) + \sigma'' V_2(i,j) \tag{4.8}$$

where $\sigma'' = \frac{\sigma}{\sqrt{3}}$, and $X_2(i,j) = \frac{x_0(i,j)+x_1(i,j)+x_2(i,j)}{3}$ is the estimated value at the pixel position (i,j) of the third frame. Proceeding in a similar manner, it can be easily shown that, if the first r frames are considered for the reduction of noise in the r^{th}frame x_{r-1} using

the sample mean filter, the estimated r^{th} frame can be expressed as

$$X_{r-1}(i,j) = I(i,j) + \frac{\sigma}{\sqrt{r}} V_{r-1}(i,j) \tag{4.9}$$

showing that the standard deviation of the noise is decreased by a factor $\sqrt{r}$. Hence, it is desirable to include as many previous frames as possible for the temporal estimation. It is evident from (4.9) that the reduction in the noise variance is proportional to the number of frames considered. But, this involves the storage of all the previous frames being considered and a heavy computation needed for the motion compensation required among the different frames.

We now consider the temporal scalar Kalman filter used in [40], given by the following equations:

Initialization:

$$\begin{aligned} \hat{I}_{0|-1}(i,j) &= x_0(i,j) \\ \xi_{0|-1}(i,j) &= \text{VAR}[x_0 - I_0] \approx \text{VAR}(n_0) \end{aligned} \tag{4.10}$$

Measurement updates:

$$\begin{aligned} K_n(i,j) &= \frac{\xi_{n|n-1}(i,j)}{\xi_{n|n-1}(i,j) + R_n} \\ \hat{I}_{n|n}(i,j) &= \hat{I}_{n|n-1}(i,j) + K_n(i,j)\Big(x_n(i,j) - \hat{I}_{n|n-1}(i,j)\Big) \\ \xi_{n|n}(i,j) &= \xi_{n|n-1}(i,j) - K_n(i.j)\xi_{n|n-1}(i,j) \end{aligned} \tag{4.11}$$

Time updates:

$$\hat{I}_{n+1|n}(i,j) = \hat{I}_{n|n}(i,j)$$

$$\xi_{n+1|n}(i,j) = \xi_{n|n}(i,j) + Q_n(i,j) \tag{4.12}$$

In the above equation, R_n is the variance of the noise in the $(n+1)^{th}$ frame, and $Q_n(i,j)$ the variance of the difference between the n^{th} frame and the $(n+1)^{th}$ frames calculated within a neighborhood window centered at (i,j) after the interframe motion has been compensated, $\hat{I}_{n|n}$ is the required estimate of I_n, the $(n+1)^{th}$ frame of the uncorrupted video, and $\xi_{n|n}(i,j)$ is the corresponding variance of the error of the estimate calculated within the neighborhood window centered at (i,j).

Since we have assumed ideal motion compensation, the value of $Q_n(i,j)$ will be zero at every update. Thus, the measurement and time updates given respectively by (4.11) and (4.12), reduce to the following simplified form:

$$\begin{aligned} K_n(i,j) &= \frac{\xi_{n-1}(i,j)}{\xi_{n-1}(i,j) + R_n} \\ \hat{I}_n(i,j) &= \hat{I}_{n-1}(i,j) + K_n(i,j)\Big(x_n(i,j) - \hat{I}_{n-1}(i,j)\Big) \\ \xi_n(i,j) &= \xi_{n-1}(i,j) - K_n(i,j)\xi_{n-1}(i,j) \end{aligned} \tag{4.13}$$

where $\hat{I}_n$ is the required estimate of I_n, and $\xi_n(i,j)$ the variance of error of the estimate within the filter window. Let us consider the first two frames, i.e., when $n = 1$. Then $\hat{I}_{n-1} = x_0$. Also, $\xi_{n-1}(i,j)$ $(\xi_0(i,j))$ is assumed to be equal to σ^2, the variance of the noise. It can be easily seen that the value of $K_1(i,j)$ equals $\frac{1}{2}$. Thus, when the first two frames are considered, using (4.13), we get

$$\hat{I}_1(i,j) = x_0(i,j) + \frac{1}{2}(x_1(i,j) - x_0(i,j)) = \frac{x_0(i,j) + x_1(i,j)}{2} = X_1(i,j) \tag{4.14}$$

and

$$\xi_1(i,j) = \xi_0(i,j) - \frac{1}{2}\xi_0(i,j) = \frac{1}{2}\xi_0(i,j) = \frac{1}{2}\sigma^2$$

Thus, $\xi_1(i,j)$ becomes half the original noise variance. Since we have assumed that the

AWGN corrupting all the frames have the same variance, R_2 will be equal to σ^2, the noise variance. Thus, by substituting the value of $\xi_1(i,j)$ and R_2 in the expression for $K_n(i,j)$ in (4.13), we get $K_2(i,j) = \frac{1}{3}$. Thus, using (4.13), we get

$$\begin{aligned}
\hat{I}_2(i,j) &= \hat{I}_1(i,j) + \frac{1}{3}(x_2(i,j) - \hat{I}_1(i,j)) \\
&= \frac{x_0(i,j) + x_1(i,j)}{2} + \frac{1}{3}\Big(x_2(i,j) - \frac{x_0(i,j) + x_1(i,j)}{2}\Big) \\
&= \frac{x_0(i,j) + x_1(i,j) + x_2(i,j)}{3} = X_2(i,j) \qquad (4.15)
\end{aligned}$$

It can be observed that (4.14) and (4.15) are equivalent to (4.5) and (4.7), respectively. If the temporal 1D scalar Kalman filter is further extended to r frames; following the same procedure used as above it can be shown that $\hat{I}_{r-1}(i,j) = X_{r-1}(i,j)$, where $X_{r-1}(i,j)$ is given by (4.9). Hence, the Kalman filter gives the same reduction in the noise variance as that yielded by the sample mean filter. However, an attractive feature of the 1D Kalman filter is that at each update, it requires the storage of only two frames and the motion compensation between these two frames, thus reducing the complexity significantly. It should be noted that the performance of the Kalman filter in reducing the noise is heavily dependent on the accuracy of the motion estimation and compensation.

4.3 Fast Filters to Reduce Additive White Gaussian Noise in Videos

In the literature, most of the filters proposed to reduce the AWGN in videos are motion compensated filters. They have motion estimation and compensation as an integral part to tackle the interframe motion. But as mentioned earlier and analyzed in [45], motion estimation and compensation is a complex process that adds a great deal to the overall computational load. Thus, it is desirable to avoid this process, when the reduction in noise is a primary concern.

In this section, two new filters to reduce the AWGN in videos are proposed based on a structure, wherein both the spatial and the temporal estimations are first carried out and the resulting estimates then suitably combined to get the final filtered output. In the proposed filter structure, spatial filtering is first carried out followed by the temporal filtering. The motion estimation and compensation process is avoided; instead, a change detection technique [46, 47] is used to deal with the interframe motion. The temporal filtering done at each pixel of a frame are weighted depending on the amount of change that has occurred at that position between consecutive frames. The two proposed filters to reduce AWGN in videos basically have the same structure, but differ in the way the temporal estimation is done.

4.3.1 Proposed Filter Structure

Let the frames of a noisy video signal a be represented by

$$a_n = b_n + \eta_n \tag{4.16}$$

where n gives the frame number with $n \geq 0$, b is the uncorrupted original signal (frame) and η is the AWGN with zero mean. Figure 4.1 shows the proposed filter structure.

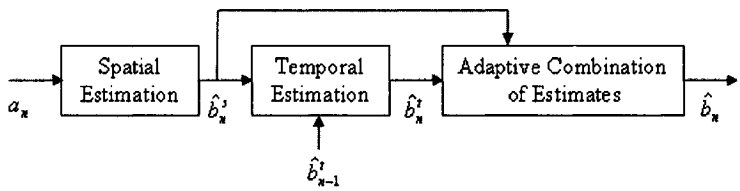

Figure 4.1: Basic structure of the proposed filters

In Figure 4.1, $\hat{b}_n^s$ signifies the spatial estimate of b_n, $\hat{b}_n^t$ the spatiotemporal estimate of b_n, and $\hat{b}_n$ the final estimate of b_n. An edge-adaptive Wiener filter is applied to the frame under consideration, to get the spatial estimate of the uncorrupted signal. This Wiener filter is a pixel-wise adaptive filter based on the statistics estimated from a local neighborhood

of each pixel. Once the noise reduction is achieved by exploiting the spatial correlation in the frame, temporal filtering is carried out on the spatial estimate to take advantage of the temporal correlation existing between successive frames. We now introduce two kinds of temporal filters:

1. Temporal weighted Kalman filter:

Here, a 1D scalar Kalman filter is applied along the temporal direction. The 1D Kalman filter is similar to that given in [40] and discussed in Section 4.2; however, the filter is applied on the frame as a whole and the update equations are weighted according to the motion at each pixel detected by employing a suitable change detection technique.

2. Temporal weighted running average filter:

In this case, a 1D running average filter is applied along the temporal direction. The update equations of the 1D running average filter are weighted according to the motion detected at each pixel using the change detection technique. While computing the running average, these update equations are designed so as to give a greater importance to the immediate previous frame than that given to the other previous frames.

An adaptive combination of spatial and the spatiotemporal estimates is done to make the final estimate of the uncorrupted video, as shown in Figure 4.1. The adaptive combination is based on the variance of the noise, the variance of the interframe motion and the size of the frame. A detailed explanation of the spatial estimation, spatiotemporal estimation and the their adaptive combination is given in the next few subsections.

4.3.2 Spatial Estimation

The spatial estimation is done using an adaptive filter, which uses a pixel-wise adaptive Wiener method based on the statistics estimated from a local neighborhood of each pixel. This filter is effective in preserving edges and does total smoothing when no edge is present. Consider the noise model given in (4.16). The spatial Wiener estimate ($\hat{b}^s$) for any frame is

given by [7]

$$\hat{b}^s(i,j) = \mu + \frac{\sigma^2 - v^2}{\sigma^2}\Big(a(i,j) - \mu\Big) \tag{4.17}$$

where

$$\begin{aligned} \mu &= \frac{1}{s_1 s_2} \sum_{n_1,n_2 \in \lambda} a(n_1,n_2) \\ \sigma^2 &= \frac{1}{s_1 s_2} \sum_{n_1,n_2 \in \lambda} a^2(n_1,n_2) - \mu^2 \\ i = 1,2,3,\ldots,S_1 & \quad j = 1,2,3,\ldots,S_2 \end{aligned}$$

In the above $S_1 \times S_2$ is the size of a frame, λ represents all the pixel positions within a filter window of size $s_1 \times s_2$ and v represents the standard deviation of the corrupting AWGN. The local statistics employed are estimated using the elements within the filter window and v is estimated over a frame using formula, $v = 1.483\text{MAD}$, where MAD is the median of the absolute deviations [17]. For convenience a variable $\beta(i,j)$ is sometimes denoted by β^{ij} henceforth in this chapter.

4.3.3 Spatiotemporal Estimation

In this subsection, we describe the two proposed temporal filters, namely, the 1D weighted scalar Kalman filter and the 1D weighted running average filter. As shown in Figure 4.1, frames that have passed through the spatial filter are considered for temporal filtering. It is to be noted that the temporal filters proposed are filters with low complexity and hence faster, as they do not use motion estimation and compensation. Instead, the filters use a change detection technique and work on the frame as a whole and not on its blocks. A normalized difference between the spatial estimate of the current frame and the spatiotemporal estimate of the previous frame is used as a measure of motion. We use the symbol nrm$[A]$ for the normalization of the elements of the array A with respect to the largest element and VAR$[B]$ for the variance (normalized with respect to the maximum greyscale value, i.e,

255) of B.

4.3.3.1 Temporal Weighted Kalman Filtering

The equations of the 1D scalar Kalman filter are modified by using weights that are based on the value of the measure of the interframe motion using the change detection technique mentioned earlier. This modified Kalman filter works on the frame as a whole rather than on its blocks. The resulting equations of the weighted Kalman filter are given as follows: Initialization:

$$\begin{aligned} \hat{b}^t_{0|-1}(i,j) &= \hat{b}^s_0(i,j) \\ \xi^{ij}_{0|-1} &= \text{VAR}[a_0 - b_0] \approx \text{VAR}[\eta_0] \end{aligned} \tag{4.18}$$

Measurement updates:

$$\begin{aligned} R_n &= \text{VAR}[\eta_n] \\ d^{ij}_n &= \text{nrm}[\hat{b}^s_n(i,j) - \hat{b}^t_{n|n-1}(i,j)] \\ W^{ij}_n &= (1 - d^{ij}_n) + \left(\frac{\xi^{ij}_{n|n-1} + R_n}{\xi^{ij}_{n|n-1} + \frac{1}{255}}\right) \cdot (d^{ij}_n) \\ K^{ij}_n &= \left(\frac{\xi^{ij}_{n|n-1}}{\xi^{ij}_{n|n-1} + R_n}\right) \cdot W^{ij}_n \\ \hat{b}^t_{n|n}(i,j) &= (1 - K^{ij}_n) \cdot (\hat{b}^t_{n|n-1}(i,j)) + (K^{ij}_n) \cdot (\hat{b}^s_n(i,j)) \\ \xi^{ij}_{n|n} &= \xi^{ij}_{n|n-1} - (K^{ij}_n) \cdot (\xi^{ij}_{n|n-1}) \end{aligned} \tag{4.19}$$

Time updates:

$$\begin{aligned} Q_n &= \text{VAR}[d_n] \\ \hat{b}^t_{n+1|n}(i,j) &= \hat{b}^t_{n|n}(i,j) \\ \xi^{ij}_{n+1|n} &= \xi^{ij}_{n|n} + Q_n \end{aligned} \tag{4.20}$$

In the above, $\hat{b}^t_{n|n}$ and $\xi_{n|n}$ are respectively the spatiotemporal estimate and the estimation error matrix corresponding to the $(n+1)^{th}$ frame of the uncorrupted video, R_n is the variance of the noise corrupting the $(n+1)^{th}$ frame. As given in (4.18), the initial value of the spatiotemporal estimate is set equal to the spatial estimate of the first frame. The initial value of all the elements of the estimation error matrix is set equal to the variance of the noise in the first frame. The elements of the matrix d_n has values in the range (0,1) with 0 signifying no motion at the pixel and 1 signifying maximum motion. These values are used to define the weight matrix W_n, which is used to carry out the spatiotemporal estimation. The term $\frac{1}{255}$, signifying the minimum greyscale value normalized with respect to the maximum value, is used in the expression for W_n to ensure the stability of the system represented by the expressions in (4.19). As a result, the elements of matrix K_n will always be less than unity, i.e., $K^{ij}_n < 1$.

Let the standard deviation of the noise corrupting the signal at the input of the temporal filter be v_t. Let us consider a factor Δ that gives the reduction in noise variance achieved by carrying out the temporal estimation. Let the video signal be time invariant, in which case we have $d_n = 0$. Now, when $d_n = 0$, (4.19) and (4.20) would be essentially same as the update equations given in (4.13). As shown in Section 4.2, the standard deviation of the noise reduces to $\Delta \cdot v_t$, where the value of Δ is given by

$$\Delta = \frac{1}{\sqrt{n+1}} \tag{4.21}$$

where $n \geq 0$ is the frame number. It is evident from (4.21) that for a time-invariant video signal, $\Delta \rightarrow 0$ as $n \rightarrow \infty$.

Next, a comparison of the proposed weighted 1D scalar Kalman filter represented by (4.18), (4.19) and (4.20) with the Kalman filter proposed in [40] given by equations (4.10), (4.11) and (4.12) is presented.

The first difference is that the proposed weighted 1D scalar Kalman filter work on

the whole frame once, whereas the Kalman filter proposed in [40] works on each pixel of the motion compensated frame considering a small neighbourhood window around it. Furthermore, in (4.12), the time updates are obtained using the value of Q_n calculated from all the elements in the filter window, which might not give an accurate measure of the motion corresponding to that particular pixel. In the proposed Kalman filter, Q_n is calculated using all the elements of the frame. Further, a weight matrix W_n, depend on the interframe motion corresponding to each pixel is introduced. The measurement and time update equations corresponding to the variance of the estimation error of the Kalman filter proposed in [40] are given in Section 4.2. They are

$$\begin{aligned} \xi^{ij}_{n|n} &= \xi^{ij}_{n|n-1} - K^{ij}_n \xi^{ij}_{n|n-1} \\ \xi^{ij}_{n+1|n} &= \xi^{ij}_{n|n} + Q^{ij}_n \end{aligned} \tag{4.22}$$

Combining the two expressions in (4.22), we get

$$\xi^{ij}_{n|n} = \xi^{ij}_{n-1|n-1} - K^{ij}_n \xi^{ij}_{n-1|n-1} + Q^{ij}_{n-1} - K^{ij}_n Q^{ij}_{n-1} \tag{4.23}$$

The corresponding expression for the proposed Kalman filter for each pixel can be obtained using (4.19) and (4.20) and is given by

$$\xi^{ij}_{n|n} = \xi^{ij}_{n-1|n-1} - K^{ij}_n W^{ij}_n \xi^{ij}_{n-1|n-1} + Q^{ij}_{n-1} - K^{ij}_n W^{ij}_n Q^{ij}_{n-1} \tag{4.24}$$

A comparison of (4.23) and (4.24) reveals the fact that the amount of temporal filtering applied is made adaptive to the motion at each pixel in the case of the proposed Kalman filter.

4.3.3.2 Temporal Weighted Running Average Filter

It is evident from (4.19) that the proposed 1D Kalman filter gives a weightage to all the previous frames depending on the corresponding values of $\xi_{n|n}^{ij}$ and d_n^{ij}. Intuitively, this might make the filter sensitive to large interframe motion. In this subsection, we present another temporal filter that gives a greater weightage to the immediate previous frame and successively less weights to the other previous frames. Intuitively, this might make the filter less sensitive to fast motion and avoid the accumulation of error. This proposed filter is a 1D running average filter, where the change detection technique used is the same as the one used for the proposed 1D Kalman filter. The corresponding update equations are as follows

Initialization:

$$\hat{b}_{-1}^{t}(i,j) = \hat{b}_{0}^{s}(i,j) \tag{4.25}$$

Updates:

$$\begin{aligned} d_n^{ij} &= \text{nrm}[\hat{b}_n^s(i,j) - \hat{b}_{n-1}^t(i,j)] \\ \hat{b}_n^t(i,j) &= \frac{(1-d_n^{ij}) \cdot (\hat{b}_{n-1}^t(i,j)) + \hat{b}_n^s(i,j)}{1+1-d_n^{ij}} \\ \hat{b}_{n+1}^t(i,j) &= \hat{b}_n^t(i,j) \end{aligned} \tag{4.26}$$

In the above equations, $\hat{b}_n^t$ is the spatiotemporal estimate of the $(n+1)^{th}$ frame of the uncorrupted video. The initial value of the spatiotemporal estimate is set equal to the spatial estimate of the first frame.

We now derive an expression for Δ introduced in the previous subsection for the 1D weighted running average filter. Again, we assume that the video is time invariant, i.e, $d_n = 0$. The signal corrupted by the AWGN at the input of the temporal filter is modelled as

$$\hat{b}^s = b + \kappa = b + v_t\omega \tag{4.27}$$

where v_t is the standard deviation of the noise κ, while ω is a zero-mean unit-variance noise. Now, let us consider the first three input frames $\hat{b}_0^s$, $\hat{b}_1^s$ and $\hat{b}_2^s$ to the temporal filter. Let (i, j) represent the position of a pixel in a frame. Writing the expressions for $\hat{b}_0^s$, $\hat{b}_1^s$ and $\hat{b}_2^s$ in the form given by (4.27), we get

$$\begin{aligned}
\hat{b}_0^s(i,j) &= b_0(i,j) + v_t\omega_0(i,j) \\
\hat{b}_1^s(i,j) &= b_1(i,j) + v_t\omega_1(i,j) \\
\hat{b}_2^s(i,j) &= b_2(i,j) + v_t\omega_2(i,j)
\end{aligned} \tag{4.28}$$

Since we have assumed the variance of the noise corrupting each frame of the video to be the same and the video to be time invariant, we get $b_0(i,j) = b_1(i,j) = b_2(i,j) = b(i,j)$ and $d_n = 0$. Hence, from (4.26) when only the first two frames are considered, we get the spatiotemporal estimate to be

$$b_1^t(i,j) = \frac{\hat{b}_0^s(i,j) + \hat{b}_1^s(i,j)}{2} = b(i,j) + \frac{v_t}{2}(\omega_0(i,j) + \omega_1(i,j))$$

or

$$\hat{b}_1^t(i,j) = b(i,j) + \frac{v_t}{\sqrt{2}}(\Lambda'(i,j)) \tag{4.29}$$

where Λ' is a unit variance noise and $\sqrt{2}\Lambda' = (\omega_0 + \omega_1)$. If we now consider $\hat{b}_1^t$ and the third frame $\hat{b}_2^s$, we get the running average to be

$$\hat{b}_2(i,j) = \frac{\hat{b}_1^t(i,j) + \hat{b}_2^s(i,j)}{2} = b(i,j) + \frac{v_t}{2}\left(\frac{1}{\sqrt{2}}\Lambda'(i,j) + \omega_2(i,j)\right)$$

which reduces to

$$\hat{b}_2^t(i,j) = b(i,j) + \left(\frac{1+\sqrt{2}}{4}\right) v_t \cdot \Lambda(i,j) = b(i,j) + \Delta \cdot v_t \cdot \Lambda(i,j) \tag{4.30}$$

where Λ is a unit variance noise and $\frac{1+\sqrt{2}}{2}\Lambda = (\frac{1}{\sqrt{2}}\Lambda' + \omega_3)$. From (4.30), $\Delta = \left(\frac{1+\sqrt{2}}{4}\right)$. As we keep augmenting frames in a similar manner the successive values of Δ from the first frame onwards is given by $1, \frac{1}{\sqrt{2}}, \left(\frac{1+\sqrt{2}}{4}\right), \left(\frac{5+\sqrt{2}}{8\sqrt{2}}\right), \left(\frac{5+9\sqrt{2}}{32}\right)$and so on. The value of Δ at the $(n+1)^{th}$ frame may be written as

$$\Delta = \begin{cases} 1 & n = 0 \\ \frac{1+\sum_{\rho=1}^{n-1}(\sqrt{2})^{3\rho-2}}{(\sqrt{2})^{3n-2}} & n = 1, 2, 3 \cdots\cdots \end{cases} \tag{4.31}$$

Let us now consider the second expression in (4.31), it can be rewritten as

$$\Delta = \frac{2}{q^n} + \frac{q^{n-1}-1}{(q-1)q^{n-1}}, \quad n = 1, 2, 3 \cdots\cdots \tag{4.32}$$

where $q = 2\sqrt{2}$. It is evident from (4.32) that as $n \to \infty$, $\Delta \to \frac{1}{q-1} = 0.5469$. Comparing this with that of the one obtained for Δ given by (4.21) corresponding to proposed 1D Kalman filter, it can be seen that as successive frames of a video are considered, the reduction in noise variance of the proposed 1D running average filter is not as much as that in the proposed 1D Kalman filter, under the assumption that the video is time invariant. In fact, there is no appreciable reduction in the noise variance after 5 or 6 frames have been used for the 1D running average filter.

4.3.4 The Final Estimate

An adaptive combination of the spatial and spatiotemporal estimates to get the final filtered output is presented in this subsection. A novel criterion is used to determine whether the spatiotemporal estimate should be weighted more than the spatial estimate or vice versa.

The following equation shows the proposed method of combining the estimates

$$\hat{b}_n^{ij} = \frac{K^2\text{VAR}[d_n]}{K^2\text{VAR}[d_n] + \text{VAR}[\eta_n]} \cdot \hat{b}_n^s(i,j) + \frac{\text{VAR}[\eta_n]}{K^2\text{VAR}[d_n] + \text{VAR}[\eta_n]} \cdot \hat{b}_n^t(i,j) \quad (4.33)$$

where $K = \frac{(352)(288)}{S_1 S_2}$, $\hat{b}_n$ the estimate of the $(n+1)^{th}$ frame of the uncorrupted video. In the combination of the spatial and spatiotemporal estimates, less weightage is given to the spatiotemporal estimate when the variance of the matrix d_n representing the interframe motion is high, since in this case the error to the spatiotemporal estimation would be large. Also, less weightage is given to the spatial estimate when the noise variance is high, since in this case the error to the spatial estimation would be large. The factor K associated with VAR$[d_n]$ has been introduced to take into account the size $S_1 \times S_2$ of the frames, which is also the size of the d_n matrix. The figure 352×288, which represents the size of a CIF format video frame, is used to determine the value of K.

4.4 Performance of the Various Filters in Reducing AWGN in Videos

In the previous section, we have proposed two filters based on the structure given in Figure 4.1 for reducing AWGN in videos. Both these filters use the edge-adaptive Wiener filter for the spatial estimation, while the temporal estimation is carried out using either the proposed 1D weighted scalar Kalman filter or the proposed 1D weighted running average filter. These two filters will henceforth, be referred to as Wiener-weighted Kalman filter and Wiener-weighted running average filter, respectively.

In this section, the performance of the proposed filters is studied and compared with that of a few other existing filters. The existing filters considered for comparison are as follows:

(1) 3D α-trimmed filter [35]

(2) 3D K-nearest neighborhood (Knn) filter [35]

(3) 3D linear minimum mean square error (LMMSE) filter [48]

(4) 3D adaptive weighted average (AWA) filter [39]

(5) Joint Wiener and Kalman estimation (Wiener-Kalman filter) [40]

(6) Joint Hadamard transform and Wiener estimation (Hadarmard-Wiener filter) [41]

(7) 3D rational filter [38]

Except for the last one, all the above filters are motion compensated filters. In the process of motion estimation and compensation the motion between the frames is first estimated, and the estimate is then used to carry out the compensation. The motion estimation technique used in this chapter for the motion compensated filtering is the exhaustive block matching algorithm (EBMA) [8].

We use the peak signal to noise ratio (PSNR) to quantify the amount of noise corrupting a video. The PSNR is given by

$$\text{PSNR} = 10 \log \frac{\psi_{max}^2}{\sigma_e^2} \text{ dB} \tag{4.34}$$

where ψ_{max} is the peak (maximum) intensity value of the video signal and σ_e^2 is the MSE between the original and the corrupted signals, given by

$$\sigma_e^2 = \frac{1}{J} \sum_k \sum_{m,n} (\psi(m,n,k) - \gamma(m,n,k))^2 \tag{4.35}$$

In 4.35, ψ and γ are respectively the intensity values of the corrupted and original videos, and J is the total number of pixels in either video.

Figures 4.2-4.5 show the qualitative performance of the various filters. Each figure shows an original frame (or field) of the video, the corresponding frame (or field) corrupted by the AWGN and the ones recovered using the various filters. The original videos considered are the 'Miss America', 'Flower Garden', 'Patrol Car' and 'Tennis' sequences. Two values of noise power are used to corrupt the original signal so that the input to the filters

have PSNR values of 20 dB and 25 dB.

From these figures, it can be seen that the motion compensated filters reduce the noise effectively, but tend to blur the edges present in the frames (or fields) of the video. This is due to the fact that perfect motion compensation estimation and compensation cannot be achieved. Although the 3D rational filter does not blur the edges, it leaves behind significant amount of noise at both the homogeneous and edge regions. As is evident from the figures, the two proposed filters perform equally well in reducing the noise effectively, and in not blurring the edges. Thus, on a qualitative basis, it may be concluded that the proposed filters give the best results in reducing AWGN when compared to the various filters considered.

Tables 4.1 and 4.2 give the quantitative results of the various filters in reducing AWGN in videos when the input has PSNRs of 20 dB and 25 dB, respectively. The original videos considered in the tables are the 'Miss America' (MA), 'Flower Garden' (FG), 'Patrol Car' (PC), 'Tennis' (T), 'Coast Gaurd' (CG) and 'Susie' (S) sequences. The improvement in PSNR (PSNRi), that is the difference between the PSNRs of the recovered and corrupted videos, obtained by applying the filters to the corrupted frames (or fields) is given in these tables. The PSNR of the recovered video is calculated using (4.34), where ψ is the recovered video.

The 3D LMMSE filter seems to give a slightly better performance than the proposed filters in videos such as 'Coast Gaurd' sequence and 'Flower Garden', wherein there are large high frequency components. On the other hand with the sequences like 'Miss America' and 'Susie' which have very little motion, the Hadamard-Wiener filter has a slight edge over the proposed filters. However, on an overall basis it is evident that the performance of the proposed filters consistently is about the same as or better than that of the other filters. It is found that in most of the cases the proposed Wiener-weighted running average filter has a better performance than the proposed Wiener-weighted Kalman filter. This could be due to the fact that the latter is more sensitive to motion between the frames.

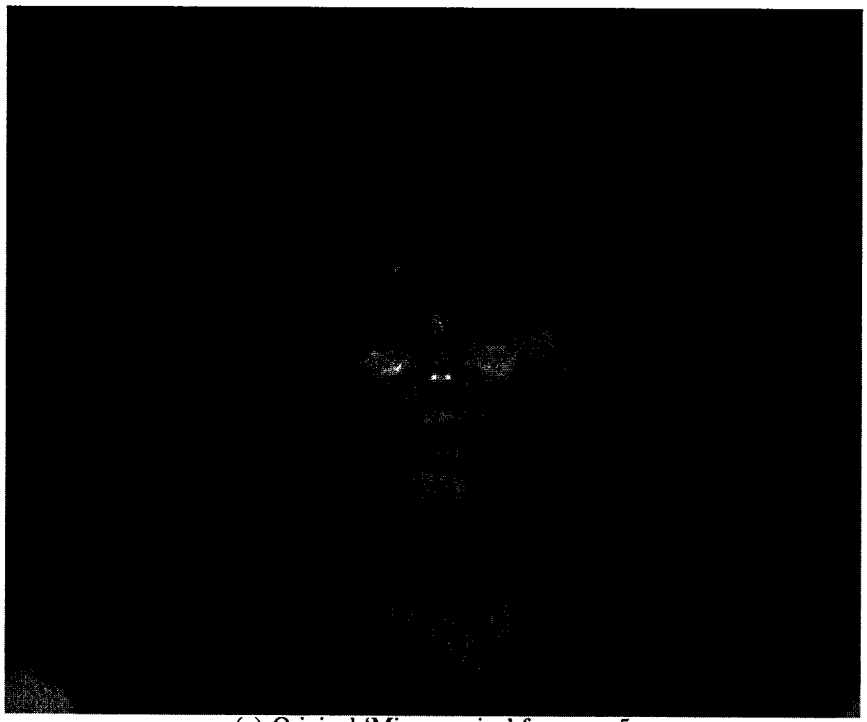

(a) Original 'Miss america' frame no.5

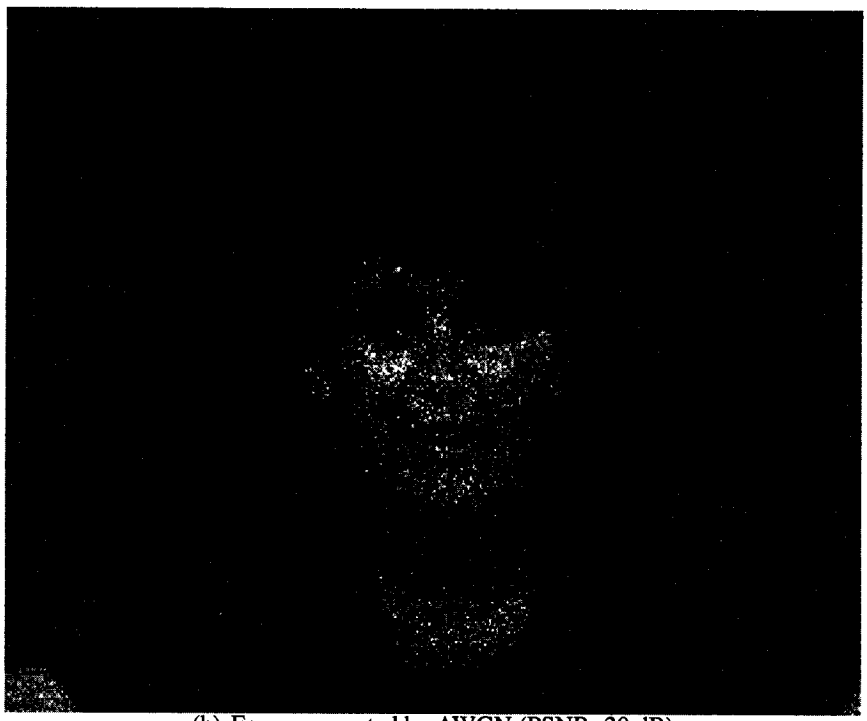

(b) Frame corrupted by AWGN (PSNR=20 dB)

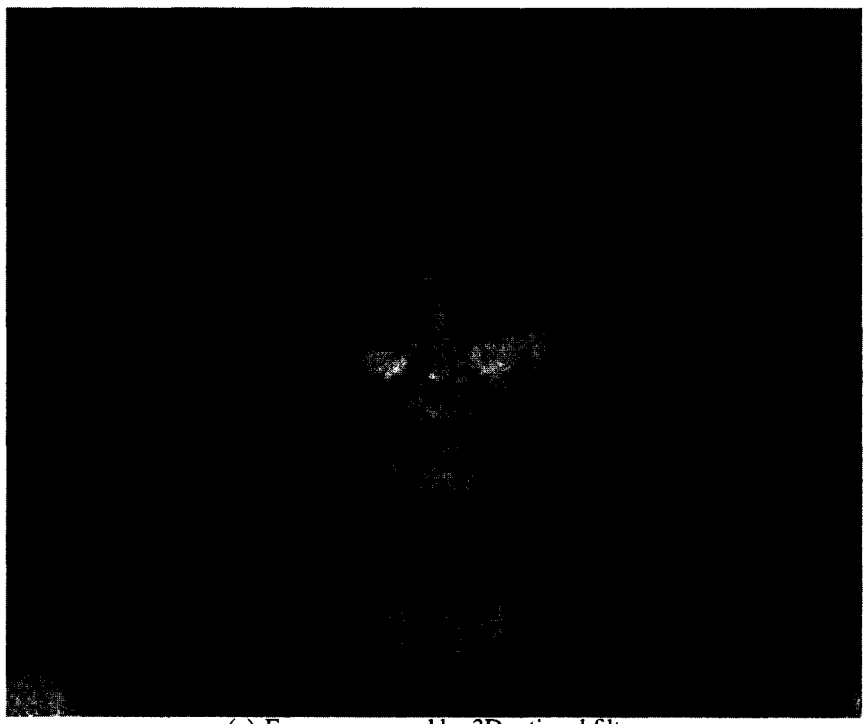

(c) Frame recovered by 3D rational filter

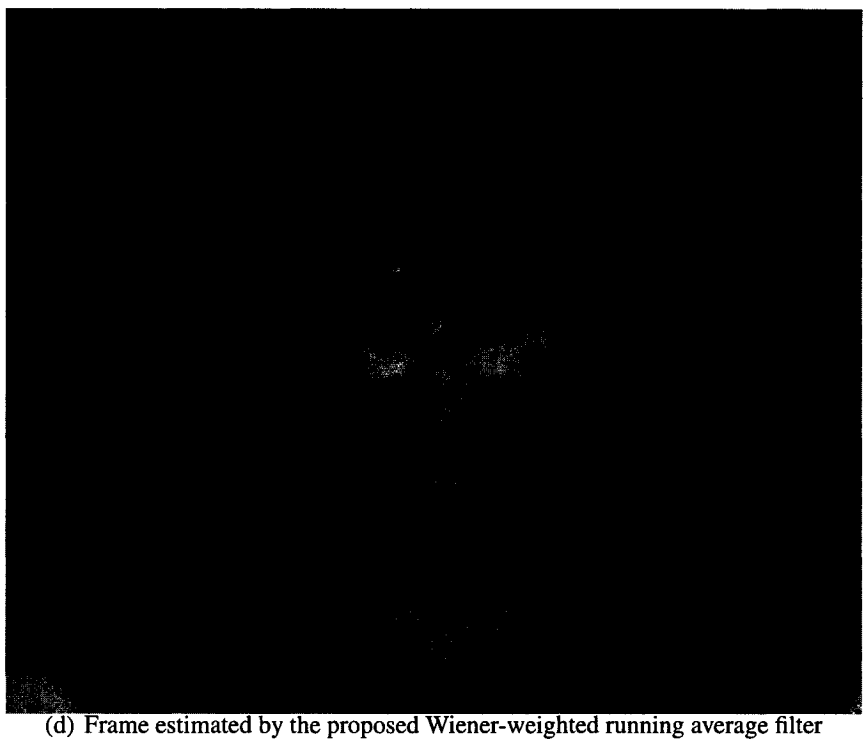

(d) Frame estimated by the proposed Wiener-weighted running average filter

(e) Frame recovered by the proposed Wiener-weighted Kalman filter

(f) Frame recovered by 3D alpha trimmed filter

(g) Frame recovered by 3D Knn filter

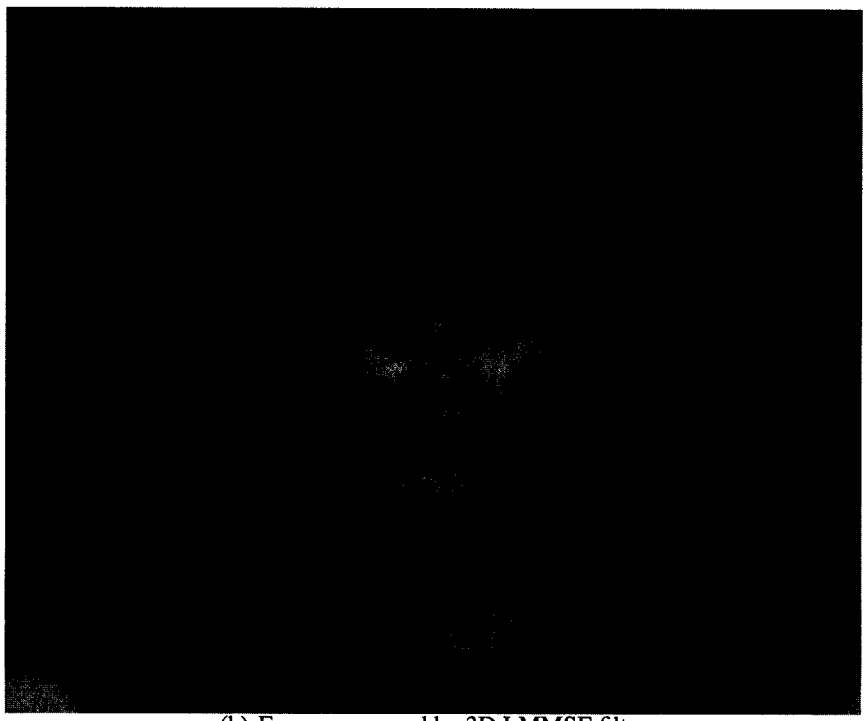

(h) Frame recovered by 3D LMMSE filter

(i) Frame recovered by 3D AWA filter

(j) Frame recovered by Wiener-Kalman filter

(k) Frame recovered by Hadamard-Wiener filter

Figure 4.2: Qualitative performance of the various filters using the 'Miss America' test sequence

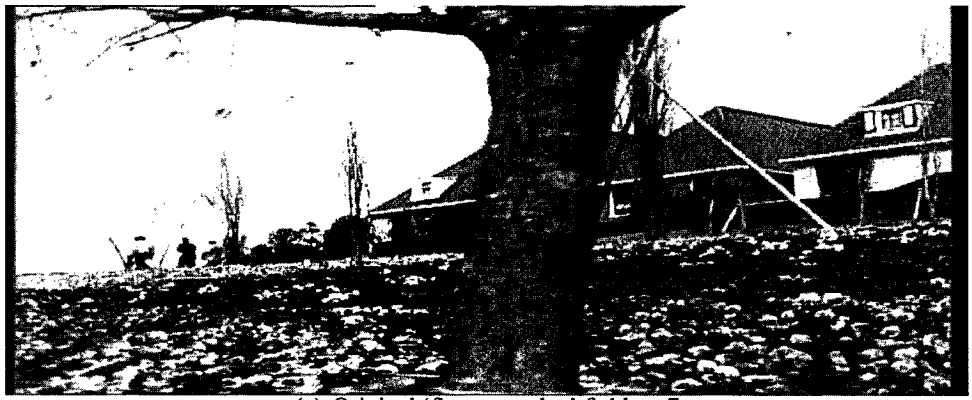

(a) Original 'flower garden' field no.7

(b) Field corrupted by AWGN (PSNR=25 dB)

(c) Field recovered by 3D rational filter

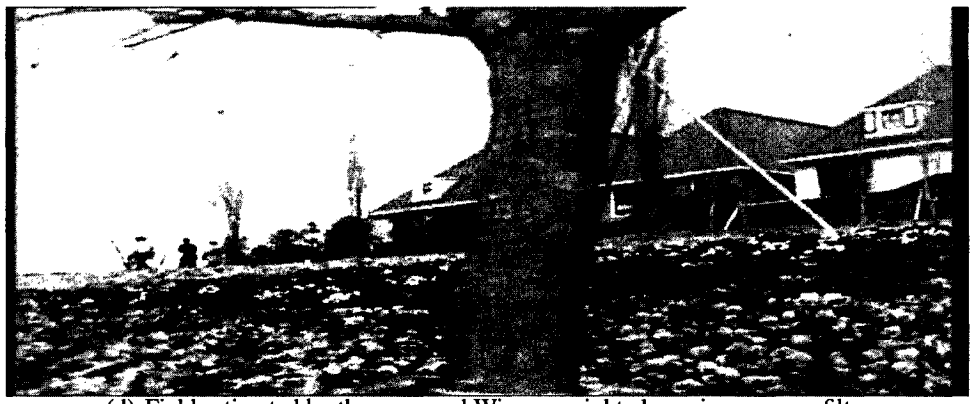

(d) Field estimated by the proposed Wiener-weighted running average filter

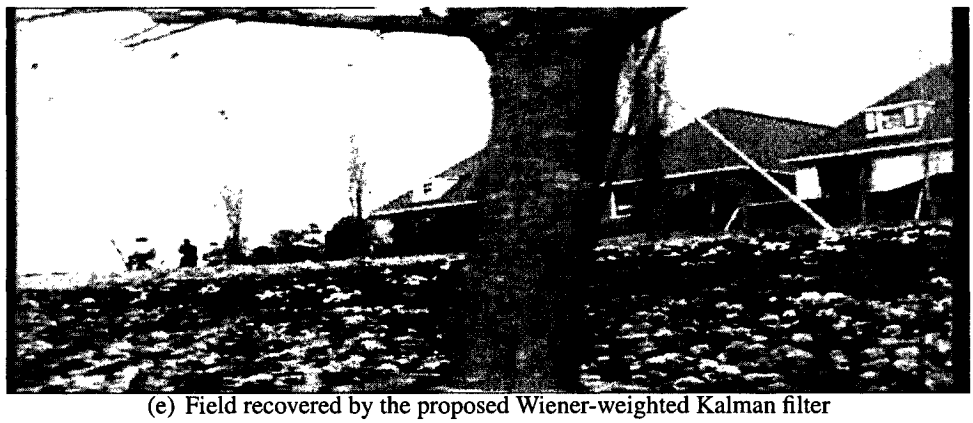

(e) Field recovered by the proposed Wiener-weighted Kalman filter

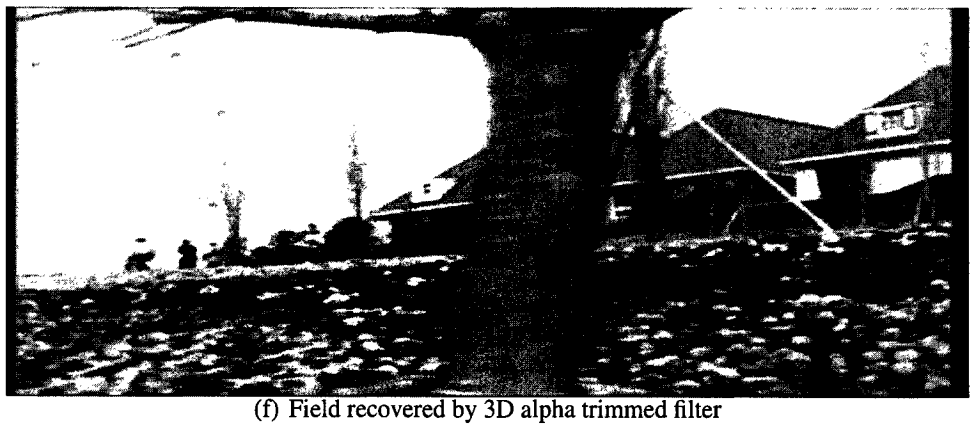

(f) Field recovered by 3D alpha trimmed filter

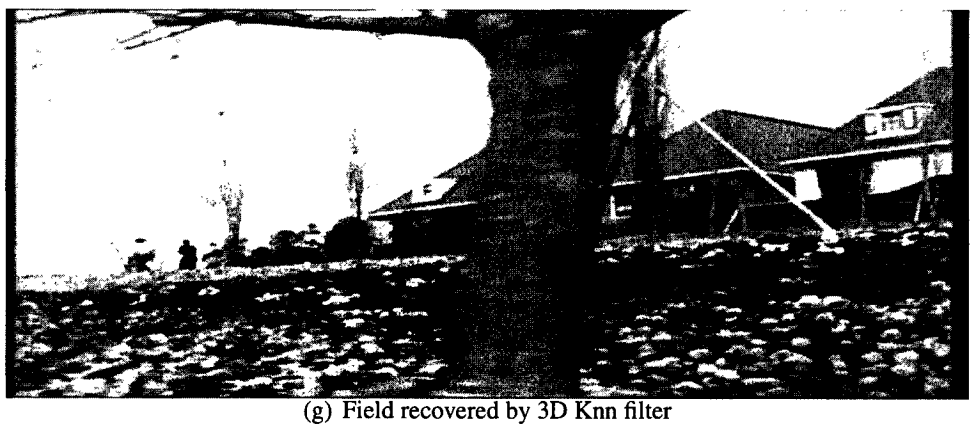

(g) Field recovered by 3D Knn filter

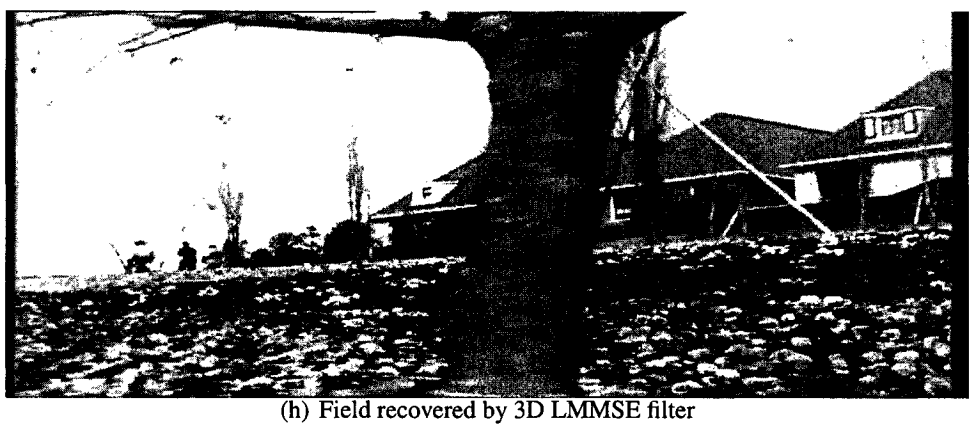

(h) Field recovered by 3D LMMSE filter

(i) Field recovered by 3D AWA filter

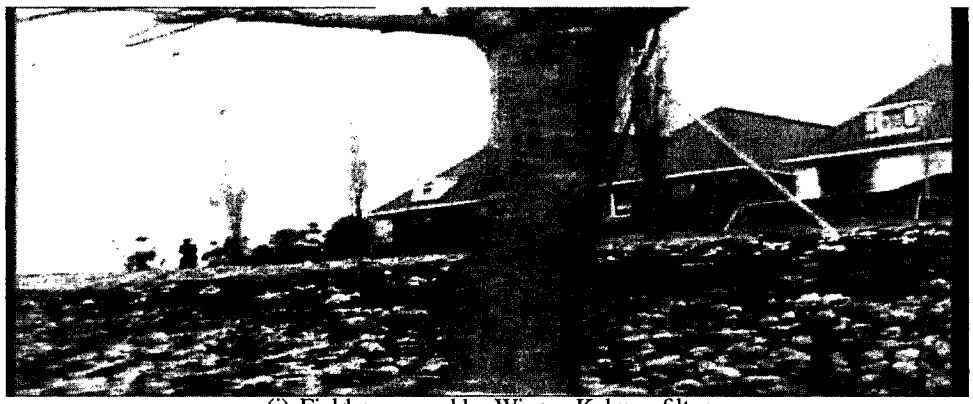

(j) Field recovered by Wiener-Kalman filter

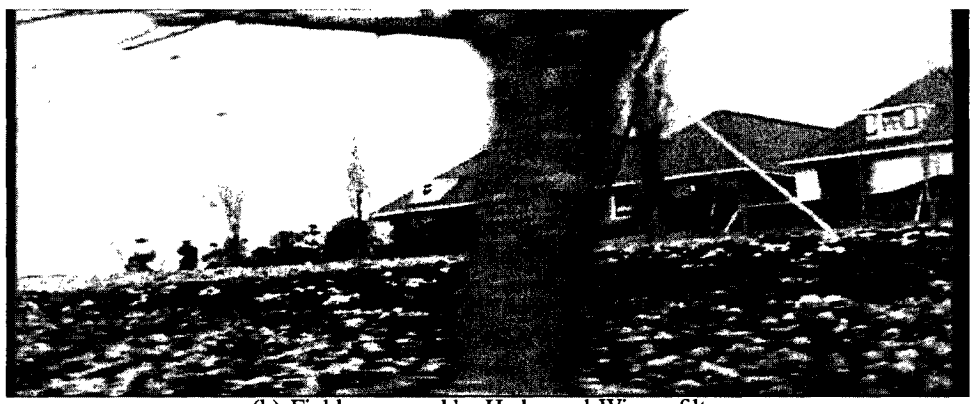

(k) Field recovered by Hadamard-Wiener filter

Figure 4.3: Qualitative performance of the various filters using the 'Flower Garden' test sequence

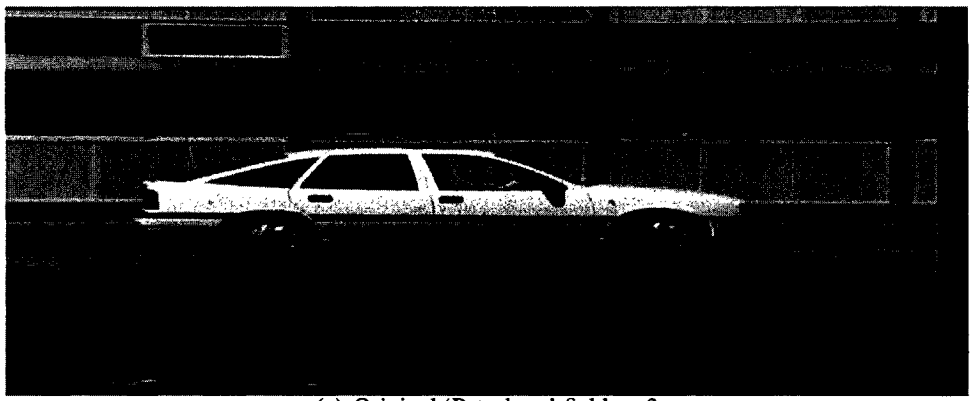

(a) Original 'Patrol car' field no.3

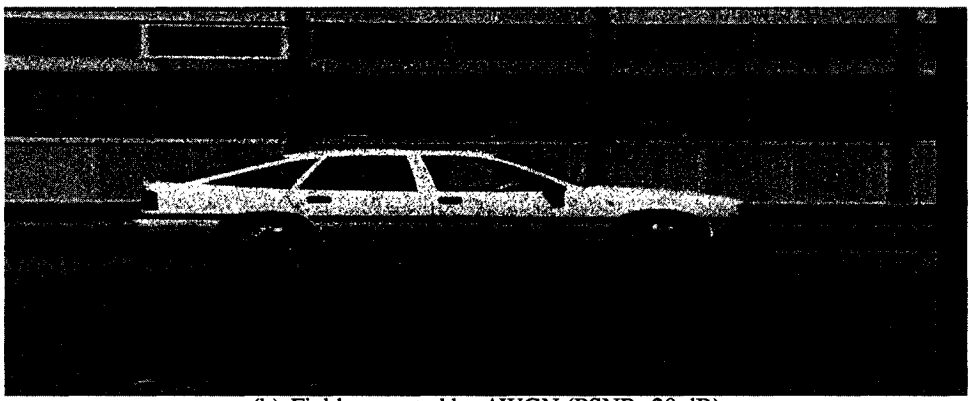

(b) Field corrupted by AWGN (PSNR=20 dB)

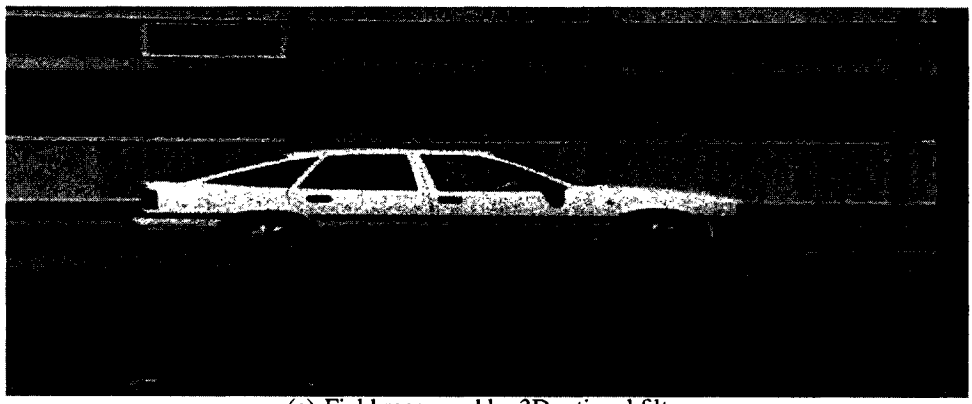

(c) Field recovered by 3D rational filter

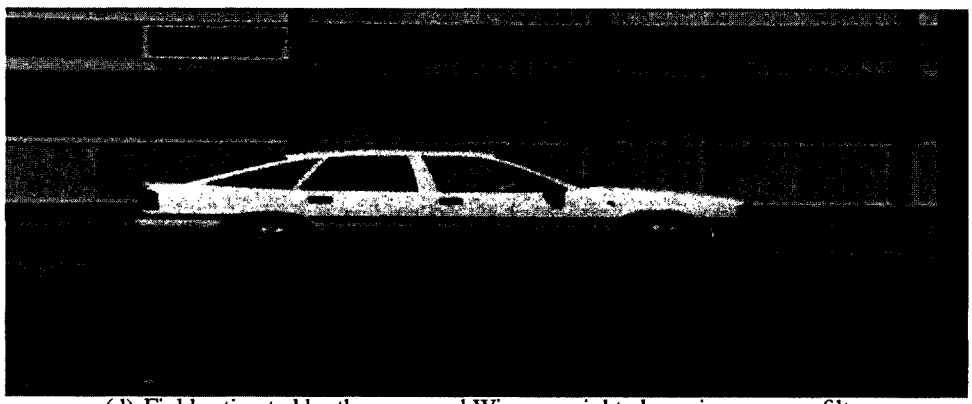

(d) Field estimated by the proposed Wiener-weighted running average filter

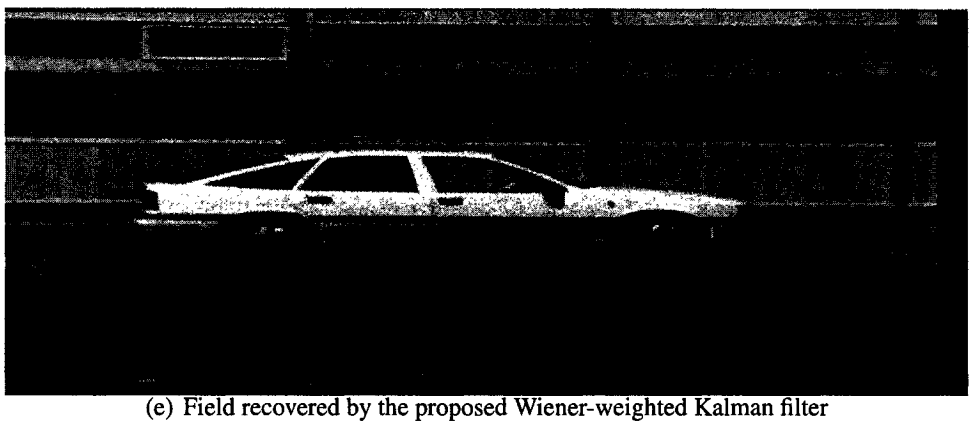

(e) Field recovered by the proposed Wiener-weighted Kalman filter

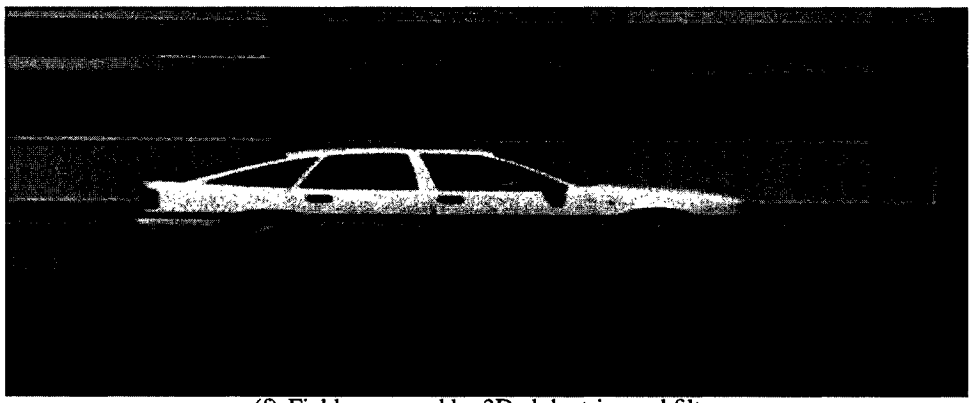

(f) Field recovered by 3D alpha trimmed filter

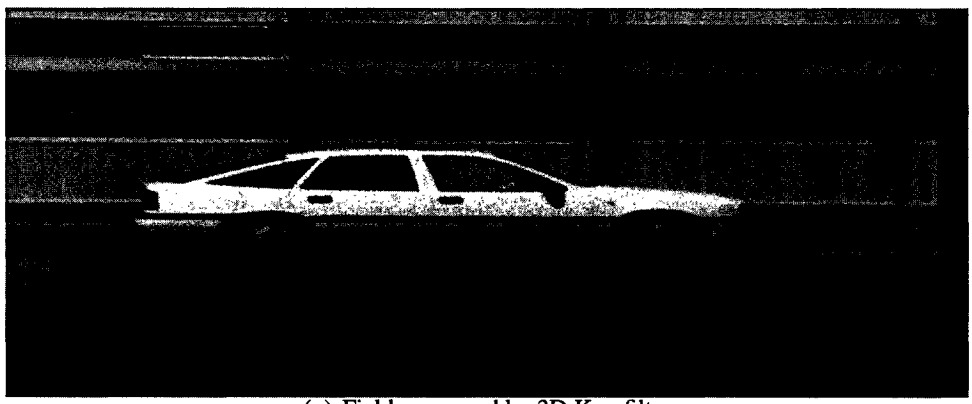

(g) Field recovered by 3D Knn filter

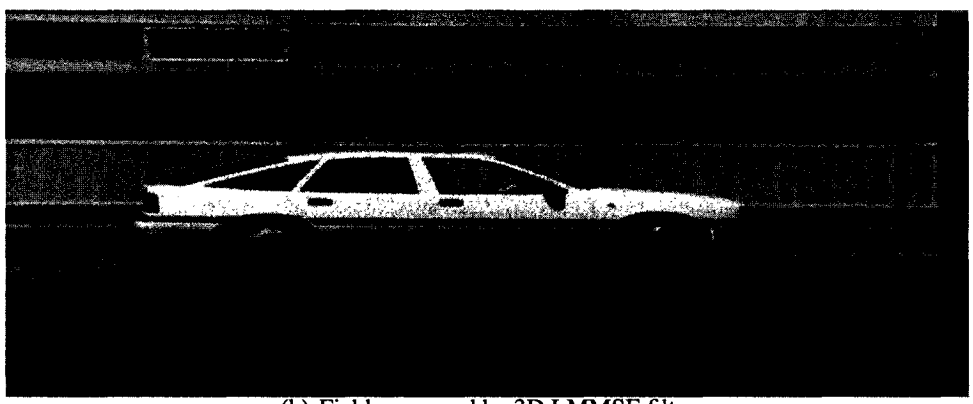

(h) Field recovered by 3D LMMSE filter

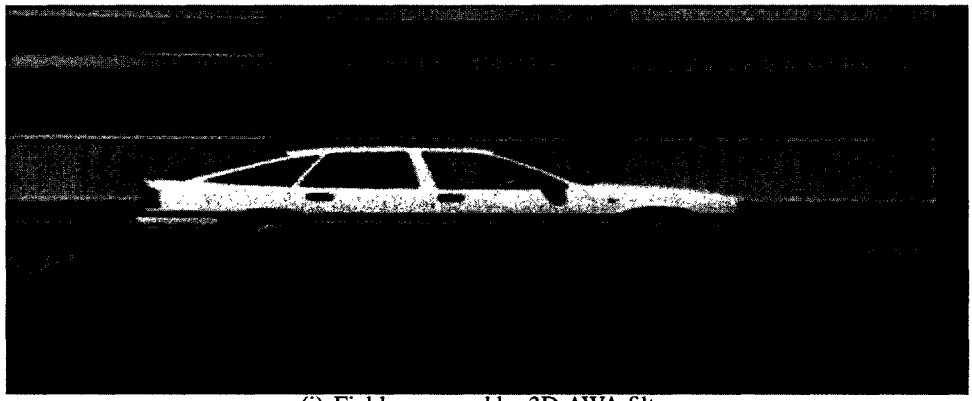

(i) Field recovered by 3D AWA filter

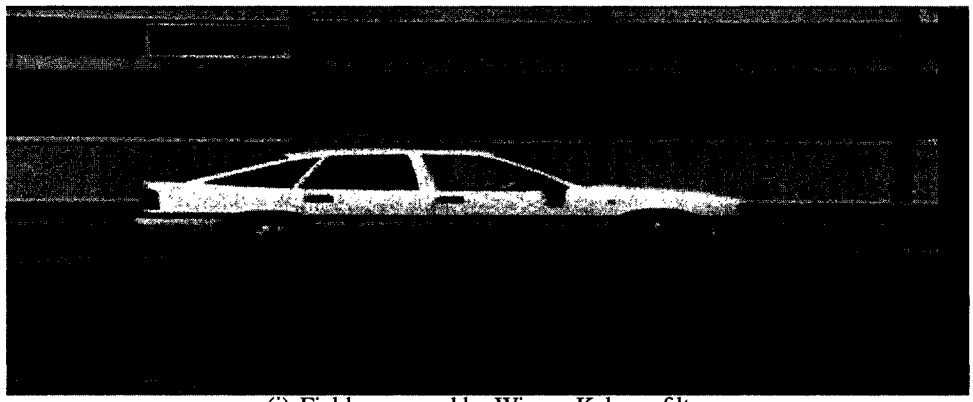

(j) Field recovered by Wiener-Kalman filter

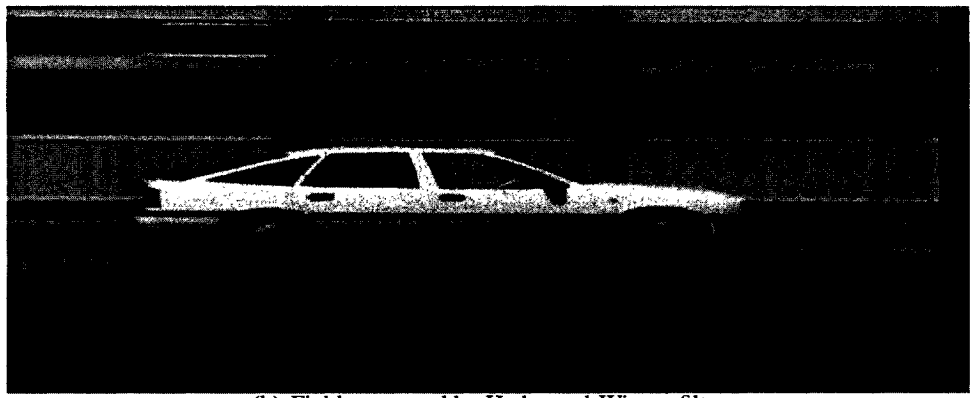

(k) Field recovered by Hadamard-Wiener filter

Figure 4.4: Qualitative performance of the various filters using the 'Patrol Car' test sequence

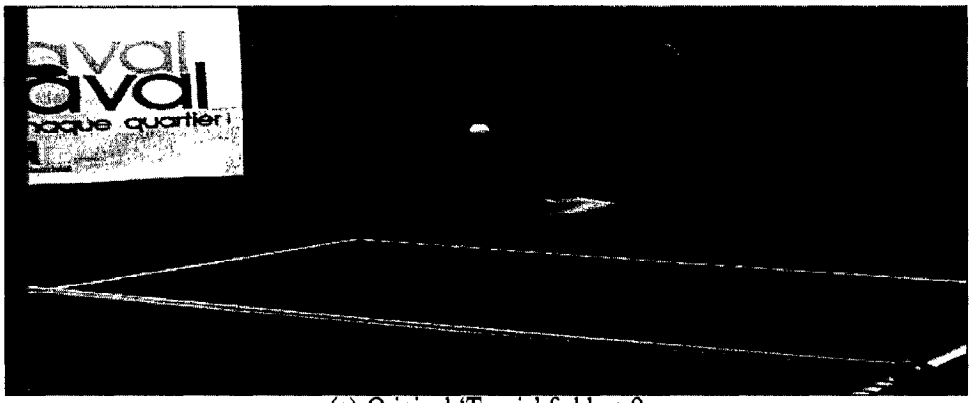

(a) Original 'Tennis' field no.9

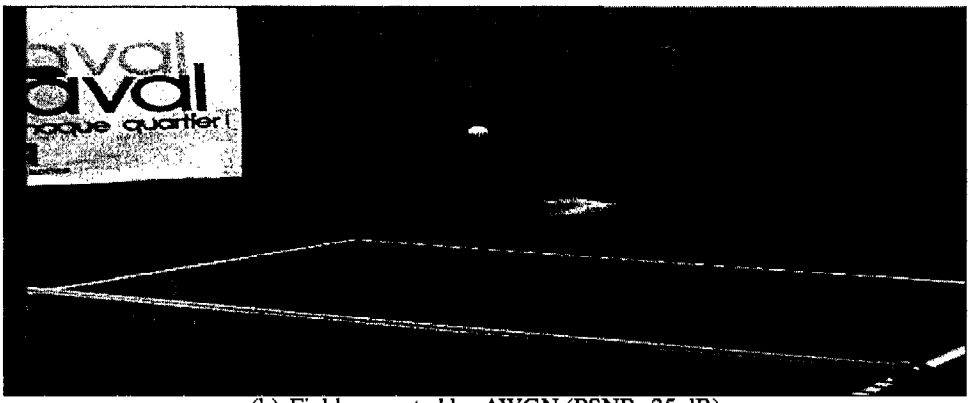

(b) Field corrupted by AWGN (PSNR=25 dB)

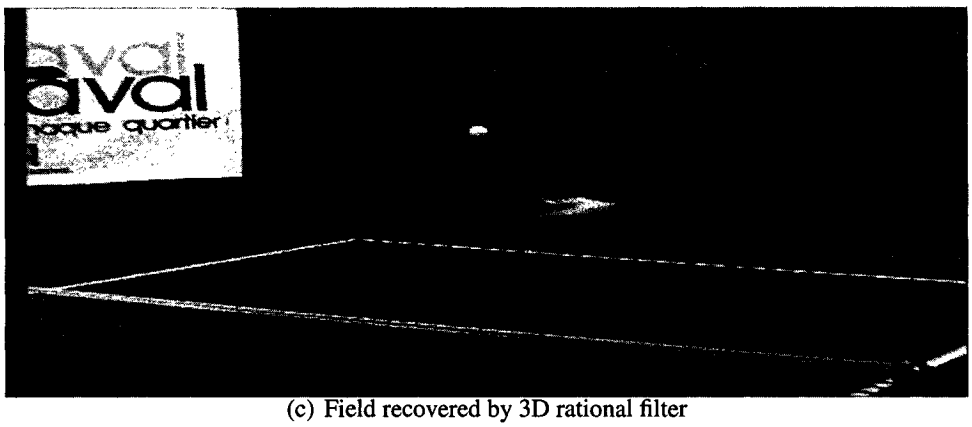

(c) Field recovered by 3D rational filter

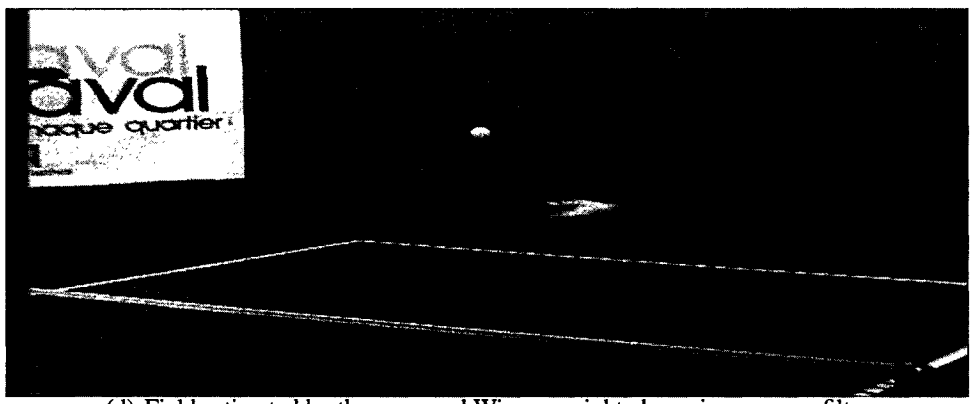

(d) Field estimated by the proposed Wiener-weighted running average filter

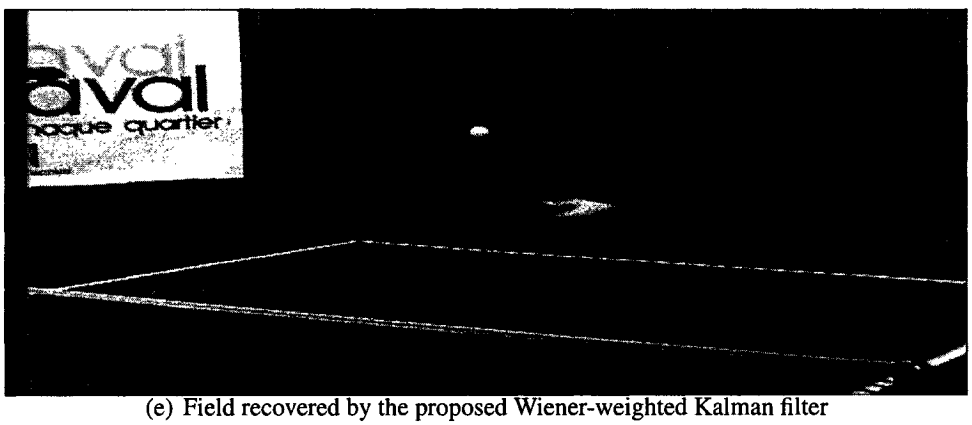

(e) Field recovered by the proposed Wiener-weighted Kalman filter

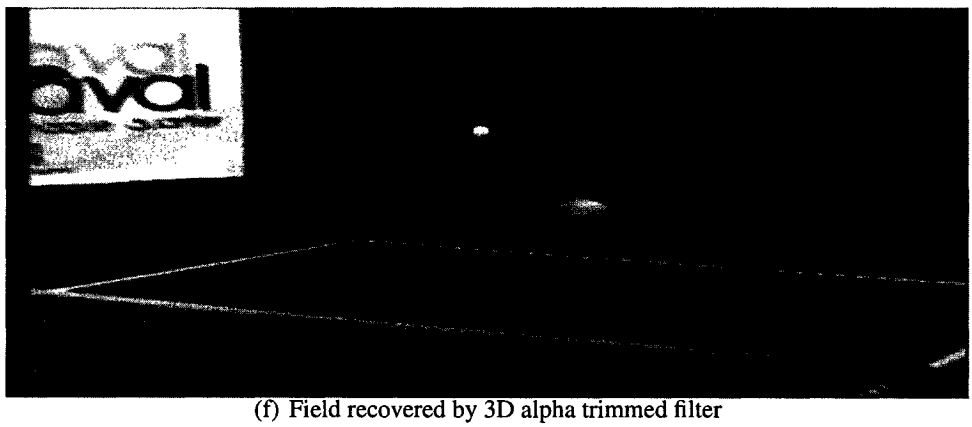

(f) Field recovered by 3D alpha trimmed filter

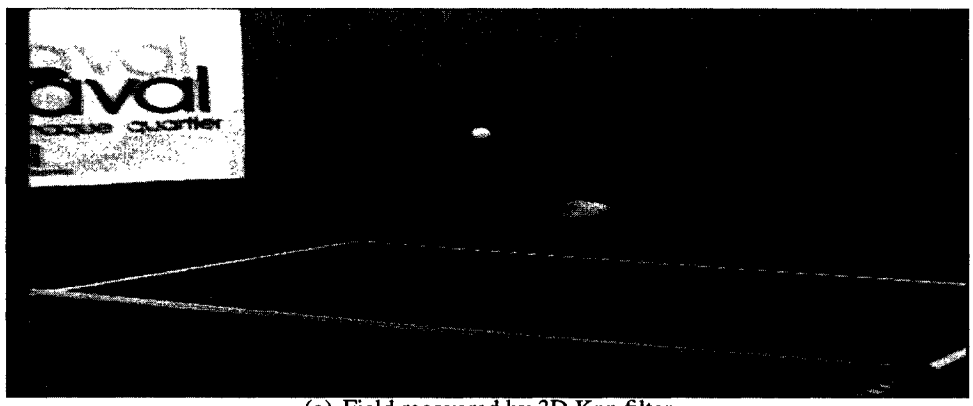

(g) Field recovered by 3D Knn filter

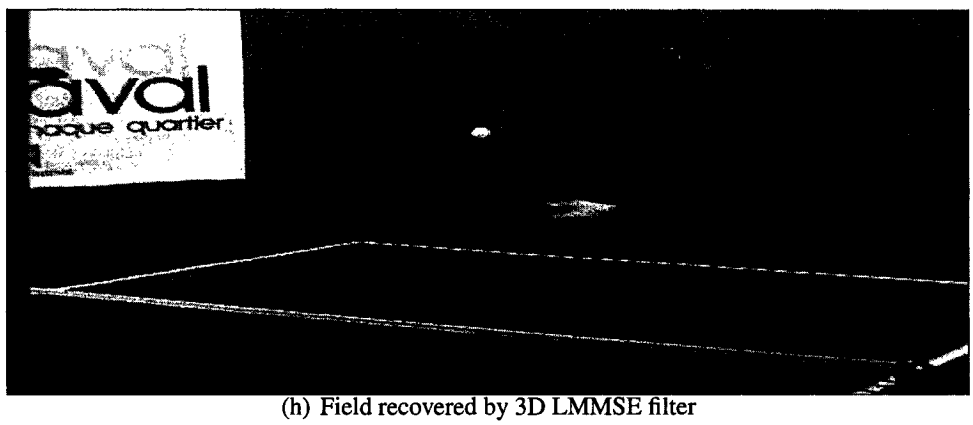

(h) Field recovered by 3D LMMSE filter

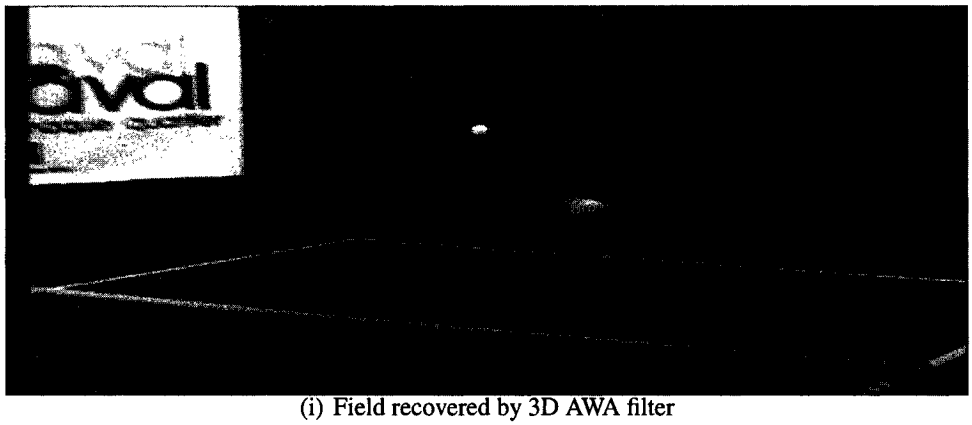

(i) Field recovered by 3D AWA filter

(j) Field recovered by Wiener-Kalman filter

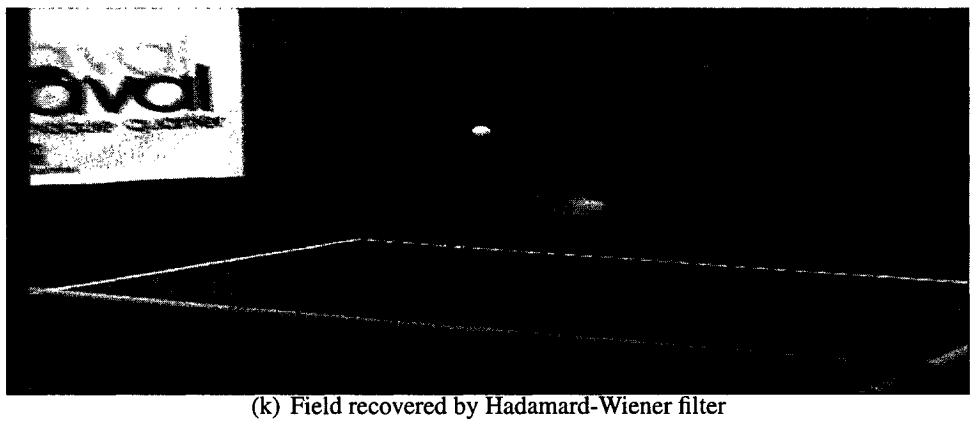

(k) Field recovered by Hadamard-Wiener filter

Figure 4.5: Qualitative performance of the various filters using the 'Tennis' test sequence

Table 4.3 gives the time required by the filters to process a frame (or field) of a video as a measure of their performance. The original videos considered are the same as in the previous two tables. The simulations were carried out using MATLAB on a windows machine with a 2.5 Ghz processor. It is seen from the Table 4.3 that the proposed filters are as fast as the 3D rational filter, that is known to be real-time implementable, and much faster than the other six filters. This is due to the fact that the process of motion estimation and compensation needed for these six filters is not required for the 3D rational filter or the proposed filters.

Figures 4.6-4.8 show the PSNR curves for the various noisy videos and those recovered by the different filters. The original videos considered in these figures are respectively the 'Patrol Car', 'Flower Garden' and 'Susie' sequences. The PSNR is calculated for each frame (or field) of the video and plotted against the frame (or field) number to get the PSNR curves. It is evident that the performance of the proposed filters is about the same as that of the others

TABLE 4.1

PSNRI OBTAINED BY USING THE VARIOUS FILTERS TO REDUCE AWGN IN VIDEOS WHEN THE INPUT TO THE FILTER HAS A PSNR OF 20 DB

Sequences→ Filters ↓	MA [CIF] dB	CG [CIF] dB	FG [PAL] dB	PC [PAL] dB	SU [PAL] dB	TN [PAL] dB
3D αTrimmed filter	11.27	1.336	2.495	3.5	10.756	3.431
3D Knn filter	8.825	3.217	4.208	5.057	8.745	4.98
3D LMMSE filter	11.114	3.921	4.99	5.984	11.385	7.396
3D AWA filter	10.763	2.095	2.799	3.903	10.535	4.59
Wiener-Kalman filter	11.625	4.473	3.929	6.807	11.265	6.338
Hadamard-Wiener filter	13.471	4.168	3.321	4.21	13.919	5.053
3D Rational filter	7.612	1.06	1.065	3.508	7.793	3.756
Wiener-weighted running average filter	12.258	4.162	5.59	8.104	11.643	8.593
Wiener-weighted Kalman filter	12.363	3.996	5.44	8.052	11.973	8.445

TABLE 4.2

PSNRI OBTAINED BY USING THE VARIOUS FILTERS TO REDUCE AWGN IN VIDEOS WHEN THE INPUT TO THE FILTER HAS A PSNR OF 25 DB

Sequences→ Filters ↓	MA [CIF] dB	CG [CIF] dB	FG [PAL] dB	PC [PAL] dB	SU [PAL] dB	TN [PAL] dB
3D αTrimmed filter	8.248	-3.682	-2.406	-1.386	7.467	-1.433
3D Knn filter	7.812	-1.221	0.178	1.18	7.437	0.988
3D LMMSE filter	9.422	1.679	3.223	4.261	9.726	5.276
3D AWA filter	7.765	-2.936	-2.183	-0.999	7.392	-0.226
Wiener-Kalman filter	10.187	-0.248	-0.219	3.733	9.533	2.722
Hadamard-Wiener filter	11.366	-0.653	-1.514	-0.664	11.671	0.194
3D Rational Filter	5.791	-3.446	-3.482	-0.571	5.98	-0.29
Wiener-weighted running averaging filter	10.466	-0.509	2.027	5.319	10.382	5.893
Wiener-weighted Kalman filter	10.381	-0.713	1.906	5.241	10.3	5.794

TABLE 4.3

TIME TAKEN BY THE VARIOUS FILTERS TO PROCESS A FRAME (OR FIELD) IN ORDER TO REDUCE AWGN IN VIDEOS

Sequences→ Filters ↓	MA [CIF] Sec/frame	CG [CIF] Sec/frame	FG [PAL] Sec/field	PC [PAL] Sec/field	SU [PAL] Sec/field	TN [PAL] Sec/field
3D αTrimmed filter	5.17 + $2C_T$	3.94 + $2C_T$	10.92 + $2P_T$	11.135 + $2P_T$	9.06 + $2P_T$	10.395 + $2P_T$
3D Knn filter	18.97 + $2C_T$	15.75 + $2C_T$	40.08 + $2P_T$	41.04 + $2P_T$	33.425 + $2P_T$	39.61 + $2P_T$
3D LMMSE filter	21.11 + $2C_T$	16.83 + $2C_T$	42.63 + $2P_T$	43.035 + $2P_T$	35.6 + $2P_T$	42.97 + $2P_T$
3D AWA filter	6.30 + $2C_T$	5.27 + $2C_T$	14.8 + $2P_T$	14.9 + $2P_T$	12.79 + $2P_T$	15.285 + $2P_T$
Wiener-Kalman Filter	3.2 + C_T	2.74 + C_T	6.575 +P_T	6.575 +P_T	5.86 +P_T	6.595 +P_T
Hadamard-Wiener filter	51.11 + $2C_T$	47.07 + $2C_T$	101.24 + $2P_T$	102.11 + $2P_T$	95.59 + $2P_T$	97.75 + $2P_T$
3D Rational filter	3.29	2.67	6.905	7.395	5.72	7.055
Wiener-weighted running averaging filter	3.4	2.75	6.74	6.63	5.9	6.64
Wiener-weighted Kalman filter	3.13	2.69	6.565	6.545	5.835	6.515

NOTE:
$C_T = 210$ seconds/frame stands for time required for motion estimation and compensation in a CIF format video.
$P_T = 575$ seconds/field stands for time required for motion estimation and compensation in a PAL format video.

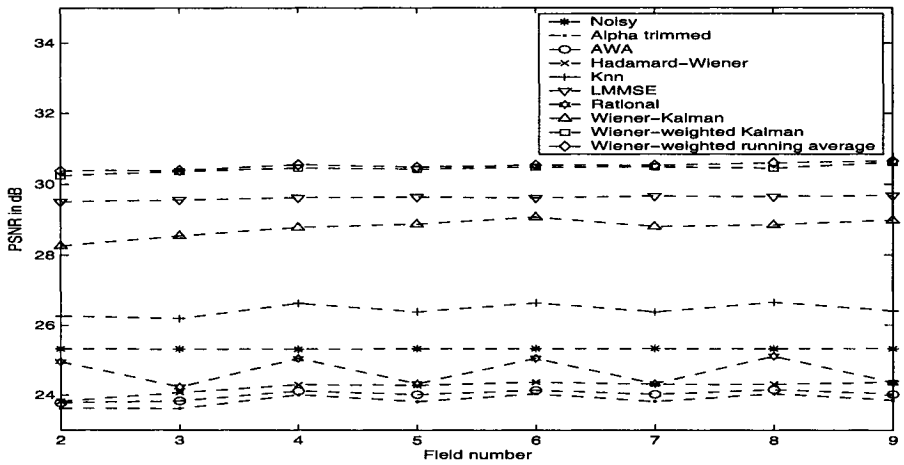

Figure 4.6: PSNR curves for various video filters using 9 consecutive frames of the 'Patrol Car' sequence

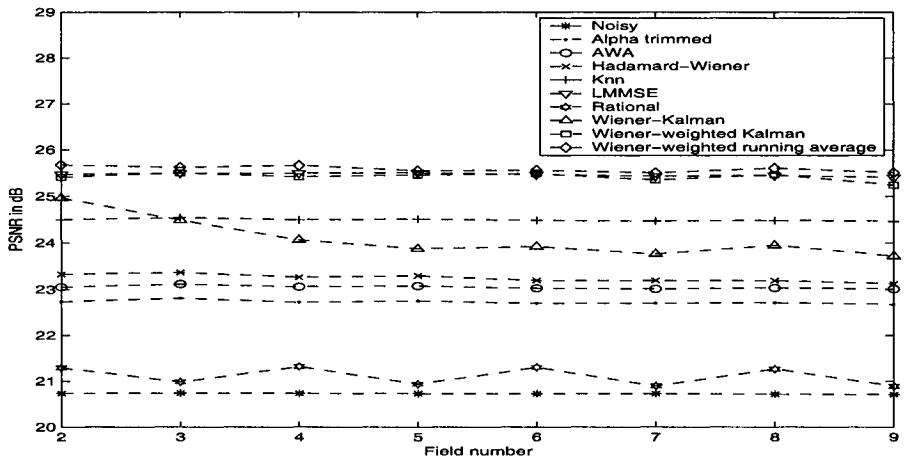

Figure 4.7: PSNR curves for various video filters using 9 consecutive frames of the 'Flower Garden' sequence

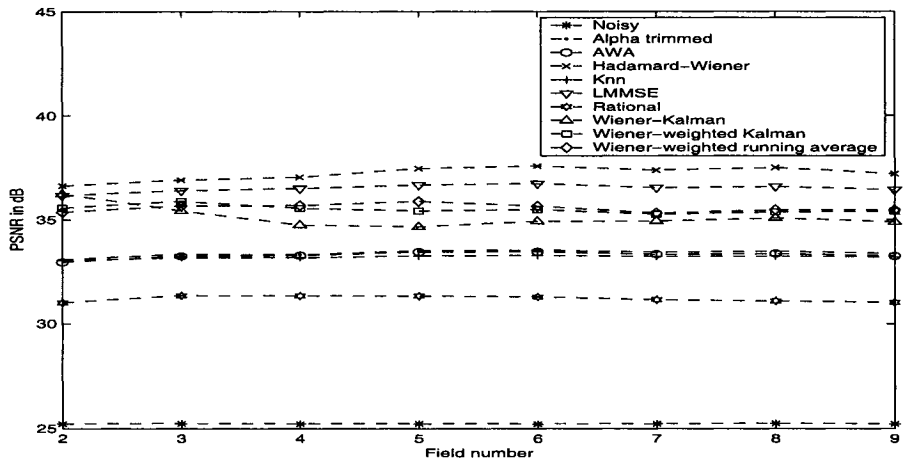

Figure 4.8: PSNR curves for various video filters using 9 consecutive frames of the 'Susie' sequence

4.5 Summary

In this chapter, we have proposed two novel fast filters to reduce AWGN in videos. These filters consists of a spatial estimation part and a temporal estimation part along with a change detection technique to detect the interframe motion, thus avoiding the complex method of motion estimation and compensation. The final estimate is obtained by an adaptive combination of the spatial and the spatiotemporal estimates of the uncorrupted signal. A detailed study of the quantitative and qualitative performance of the proposed filters in reducing AWGN in videos has been carried out and compared to that of other existing filters. It has been shown that the proposed filters outperform the others both in terms of the noise reduction capability and the processing time.

Chapter 5

Reduction of Speckle in Videos using an Unbiased Homomorphic System

5.1 Introduction

Speckle corruption is unavoidable in videos which are generated using coherent imaging systems. As mentioned in Chapter 4, such systems are used to generate videos for military, commercial and medical applications. In this chapter, the problem of reducing the speckle in videos is considered [49, 37]. To the best knowledge of the author, such a problem has been considered only in [41] and [50]. The authors in [41], have dealt with the problem of reducing the noise that could be signal independent or signal dependent. They have shown that in either case the Hadamard transform could be applied in the temporal direction to the corrupted signal to remove the correlation between the successive frames, followed by the use of the edge-adaptive Wiener filter to smooth the frames. In [50], a homomorphic system has been used to reduce the speckle from a video. After the forward homomorphic transform, the discrete cosine transform is applied in the temporal direction followed by the application of the edge-adaptive Wiener filter to each frame. Both these schemes work on the motion compensated frames and use a motion estimation and compensation technique.

In this chapter, we propose a fast system to reduce the speckle in videos. The speckle corruption in a frame of the video is considered to be independent that of other frames. As speckle is a type of multiplicative noise, the structure of the unbiased homomorphic system proposed in Chapter 2 is used. According to the properties of speckle presented in Chapter 3, the problem of speckle reduction in a video is essentially a problem of reducing the AWGN after the forward homomorphic transform, where the speckle noise is assumed to be white. We use the structure of the fast filters proposed in Chapter 4 (see Figure 4.1) to reduce the AWGN. The spatial filter applied to each frame is the MM-filter proposed in Chapter 3. We use the 1D weighted running average filter that was introduced in Chapter 4 as the temporal filter. The weights of this running average filter is based on the interframe motion, which is detected using a change detection algorithm. It should be noted that the proposed filter has a low computational complexity, since motion estimation and compensation is avoided. This low complexity of the filter might facilitate its real-time implementation, which is required in cases such as in coherent imaging system mounted on an airborne vehicle. Finally, the backward homomorphic transform is applied followed by the bias compensation proposed in Chapter 2 to obtain the unbiased estimate of the uncorrupted signal.

The organization of the chapter is as follows. In Section 5.2, the proposed system to reduce speckle in videos is presented. In Section 5.3, the performance of the proposed system is studied and compared with that of the schemes presented in [41] and [50].

5.2 A Technique to Reduce Speckle in Videos

When images are produced by a coherent imaging system at certain intervals of time, it forms an image sequence, i.e., a video. In general, it is assumed that the interval is high enough that we can assume the speckle corruption in any frame is uncorrelated with that of any other frame [51]. In this section, an algorithm to reduce speckle in videos is proposed.

Each frame in the video is corrupted by a speckle (lognormally distributed multiplicative noise) and the speckle corruption in a filter window is modelled as

$$as(i) = \theta \cdot \eta s(i) \tag{5.1}$$

where $\eta s(i)$ is a unit-mean lognormally-distributed white noise, θ the uncorrupted original signal and $as(i)$ the corrupted signal. The first operation is to perform the natural logarithmic transform of the observed corrupted signal. Applying natural logarithm to both sides of (5.1), we have

$$y(i) = x + \eta(i) \tag{5.2}$$

Equation (5.2) is equivalent to (2.36) given in Chapter 2, where $x = \ln \theta + m$, m being the mean of $\ln \eta s(i)$. The zero-mean white noise $\eta(i)$ has a Gaussian distribution. The MM-filter proposed in Chapter 3, which reduces noise effectively without blurring the edges, is used as the spatial filter applied on the video frames to get the spatial estimate of x. The spatial estimate is given by

$$\hat{x}^s = \sum_{j=1}^{r} \gamma(j) y_{(j)} \tag{5.3}$$

where j gives the position of an element in the array obtained by arranging the r samples of y within the filter window in an ascending order, i.e., $y_{(1)} < y_{(2)} < \ldots\ldots < y_{(r)}$ and γ is an array of r elements, which are the coefficients of the MM-filter. The coefficients of this MM-filter are based on the Criterion 1 presented in Section 3.3.1, as it is the simplest of the three criteria and results in a low complexity filter. Thus, the coefficients are given by

$$\gamma = \frac{\alpha \gamma_{mean} + \beta \gamma_{median}}{\alpha + \beta} \tag{5.4}$$

where γ_{mean} represents the coefficients of the sample mean estimator, γ_{median} those of the sample median estimator and the weights α and β are given by

$$\alpha = \sigma^2 \textbf{ and } \beta = \frac{1}{\sigma^2} - 1 \tag{5.5}$$

In (5.5), σ^2 is the estimated variance (normalized with respect to the maximum greyscale value, 255) of the Gaussian noise in a frame.

Next, the spatially filtered frames are processed using a temporal filter. Hence, the estimate obtained after the temporal filtering is the spatiotemporal estimate. The temporal filter considered here is the 1D weighted running average filter introduced in Section 4.3 and repeated for convenience. The update equations of the filter are given by

Initialization:

$$\hat{x}^t_{-1}(i,j) = \hat{x}^s_0(i,j) \tag{5.6}$$

Updates:

$$\begin{aligned} d_n(i,j) &= \text{nrm}[\hat{x}^s_n(i,j) - \hat{x}^t_{n-1}(i,j)] \\ \hat{x}^t_n(i,j) &= \frac{(1 - d_n(i,j)) \cdot (\hat{x}^t_{n-1}(i,j)) + \hat{x}^s_n(i,j)}{1 + 1 - d_n(i,j)} \\ \hat{x}^t_{n+1}(i,j) &= \hat{x}^t_n(i,j) \end{aligned} \tag{5.7}$$

where $\hat{x}^s_n$ denotes the spatial estimate of the $(n+1)^{th}$ frame, $\hat{x}^t_n$ the spatiotemporal estimate of the $(n+1)^{th}$frame, and nrm$[A]$ stands for the normalization of the elements of the array A with respect to the largest element.

Next, the criterion described in Section 4.3.4 is used to adaptively combine the estimates $\hat{x}^t_n$ and $\hat{x}^s_n$ to obtain the final estimate $\hat{x}_n$ of x_n. The combination is done based on the amount of interframe motion present and the amount of noise corrupting the frame. The

estimate $\hat{x}_n$ is given by (4.33) and repeated below:

$$\hat{x}_n(i,j) = \frac{K^2\text{VAR}[d_n]}{K^2\text{VAR}[d_n] + \text{VAR}[\eta_n]} \cdot \hat{x}_n^s(i,j) + \frac{\text{VAR}[\eta_n]}{K^2\text{VAR}[d_n] + \text{VAR}[\eta_n]} \cdot \hat{x}_n^t(i,j) \quad (5.8)$$

where $K = \frac{(352)(288)}{S_1 S_2}$, η_n is the AWGN corrupting the $(n+1)^{th}$ frame, $S1 \times S2$ is the size of the video frames, and VAR(A) stands for the variance of the random variable A normalized with respect to the maximum greyscale value of 255.

Once the estimate $\hat{x}_n$ is obtained, the estimate of the original signal θ_n, the $(n+1)^{th}$ frame of the video, can be obtained by applying exponentiation. But, this estimate would have a biased mean as explained in Sections 2.5.2 and 2.5.3. Hence, the bias compensation technique suggested in Section 2.5.3 is used to get the unbiased estimate $\hat{\theta}_n$ of θ_n. The overall algorithm to reduce speckle in videos is given in Figure 5.1.

5.3 Performance Analysis and Discussion

In this section, the performance of the proposed filter is studied and compared to the Hadamard-Wiener filter and the homomorphic DCT-Wiener filter given in [41] and [50], respectively. These two existing filters are motion compensated ones and as in Chapter 4, the motion estimation technique used here is the exhaustive block matching algorithm (EBMA) [8]. We use the ENL described in Chapter 3, to quantify the amount of speckle corrupting a frame of a video given as a input to the filters.

The signal to mean square error ratio (SMSER) is also used to measure the amount of speckle corruption in a video. The SMSER of a video is given by

$$\text{SMSER} = 10 \log \frac{\psi_{avg}^2}{\sigma_e^2} \text{ dB} \quad (5.9)$$

where

$$\sigma_e^2 = \frac{1}{J} \sum_k \sum_{m,n} (\psi(m,n,k) - \gamma(m,n,k))^2 \quad (5.10)$$

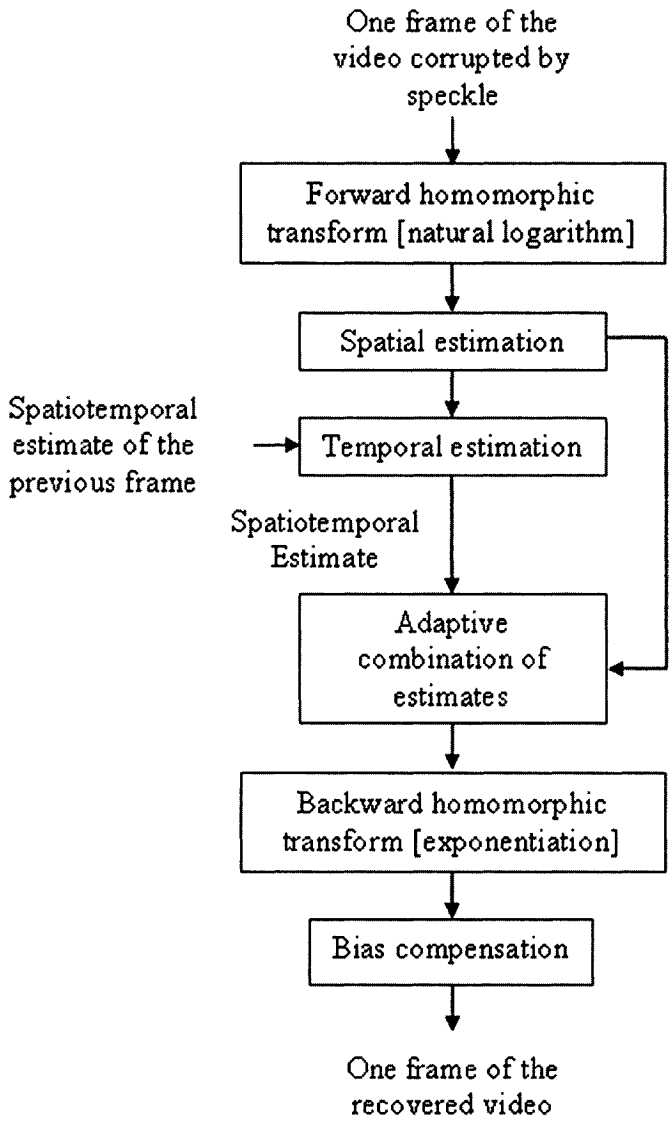

Figure 5.1: The proposed algorithm to reduce speckle in videos

$$\psi_{avg}^2 = \frac{1}{J}\sum_k \sum_{m,n} (\psi(m,n,k))^2 \tag{5.11}$$

In the above, σ_e^2 is the MSE between the original signal γ and the corrupted signal ψ, and J is the total number of pixels in the video.

Both qualitative and quantitative performance of the various filters are considered in this section. The quantitative measures used are as follows:

(1) Time taken by the various filters to process a frame of the video.

(2) The improvement in the SMSER (SMSERi), which is the difference between the SMSERs of the recovered and corrupted videos.

Figures 5.2-5.4 present the visual performance of the various filters in reducing speckle. In these figures, the frames are corrupted by combining the original signal with the speckle by using pixel-wise multiplications. The original uncorrupted videos considered are a few almost speckle-free SAR videos which we refer to as the 'DC south', the 'DC north' and 'Gibson west' sequences. Similar results are obtained using videos that are generated by coherent imaging systems having an unknown amount of speckle, and these are shown in Figures 5.5 and 5.6.

Table 5.1 gives the time required for processing a frame using the various filters. Tables 5.2-5.4 give the SMSERi results of the various filters in reducing speckle from videos. The SMSER of the recovered video is calculated using (5.9), where ψ is now the recovered video. Tables 5.2, 5.3 and 5.4 respectively correspond to the performance of the various filters when the ENL values of the are 2, 5 and 10.

Figures 5.7-5.9, show the SMSER curves for the various noisy videos and those recovered by the different filters. The SMSER is calculated for each frame of the video and plotted against the frame number to get the SMSER curves.

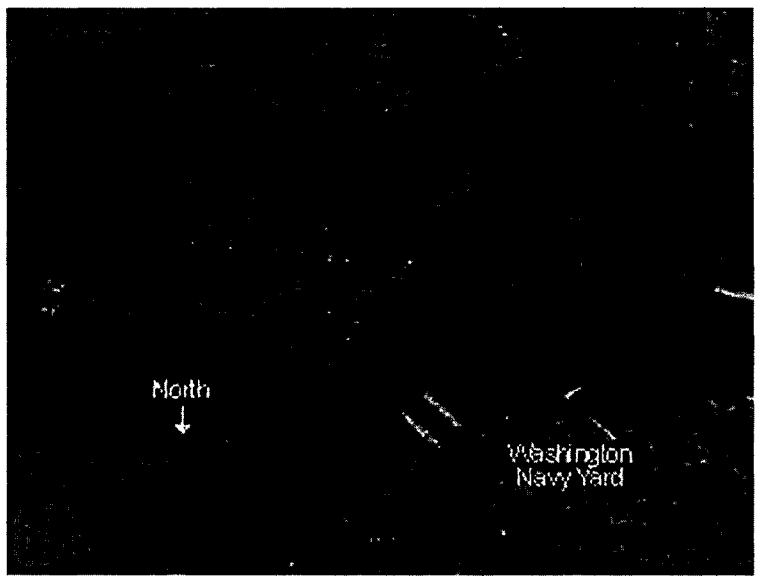

(a) Original 'DC south' frame no.5

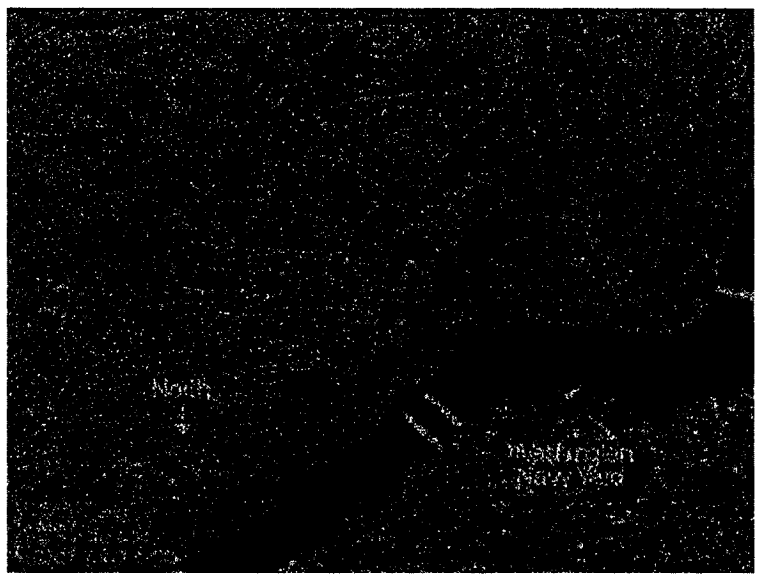

(b) Frame corrupted by speckle (ENL=2)

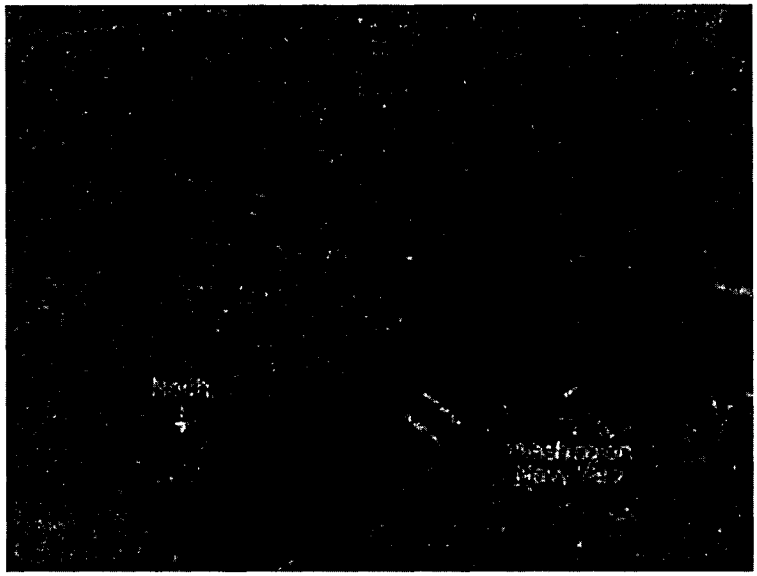

(c) Frame recovered by the proposed system

(d) Frame recovered by Hadamard-Wiener filter

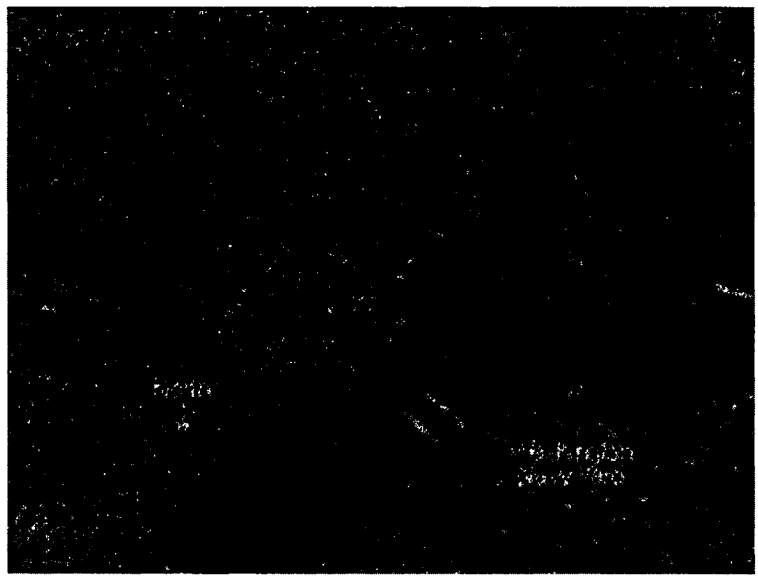

(e) Frame recovered by homomorphic DCT-Wiener filter

Figure 5.2: Qualitative performance of the various filters using 'DC south' sequence

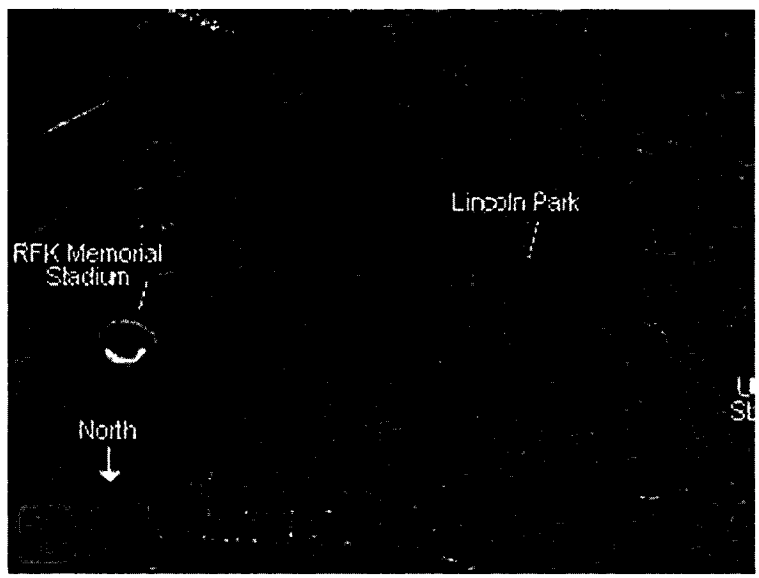

(a) Original 'DC north' frame no.6

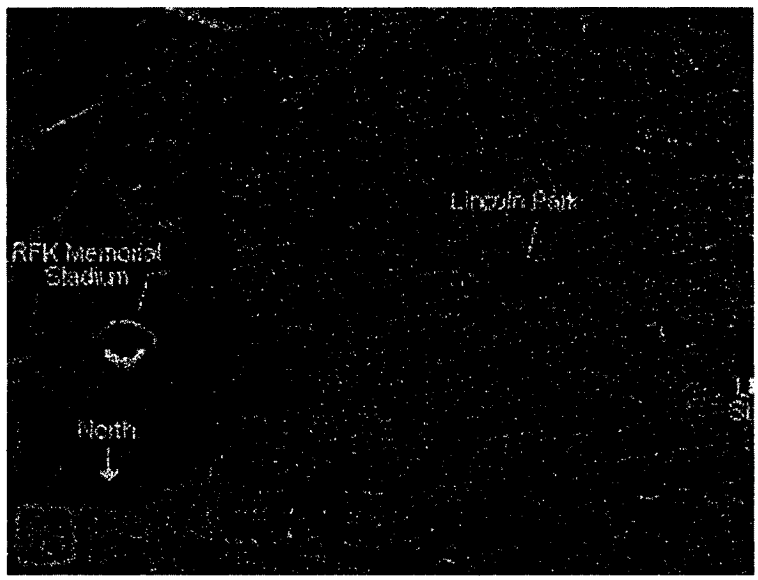

(b) Frame corrupted by speckle (ENL=5)

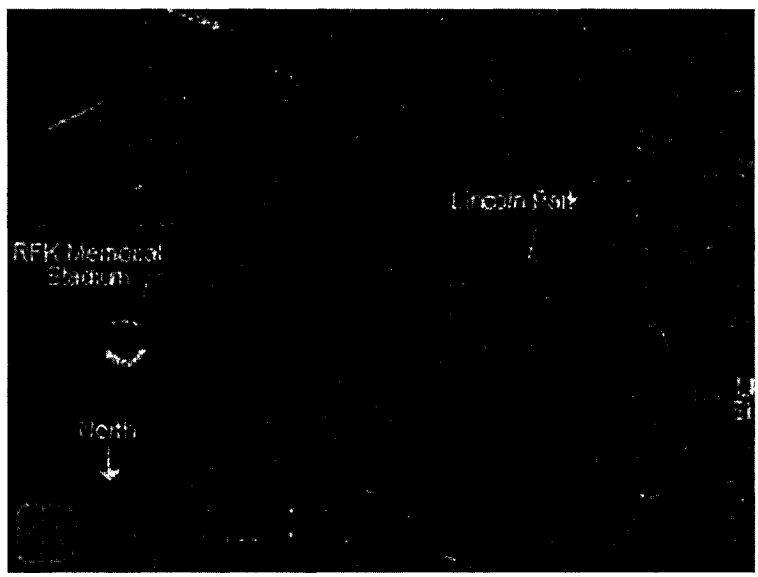

(c) Frame recovered by the proposed system

(d) Frame recovered by Hadamard-Wiener filter

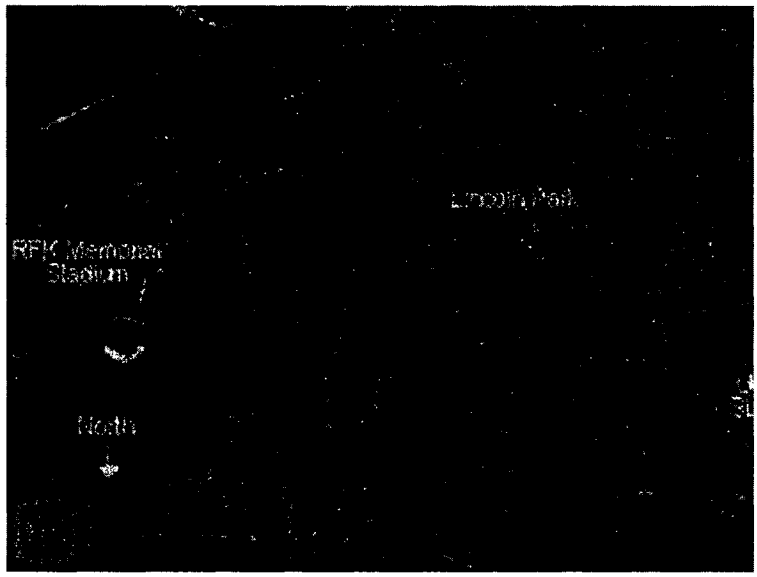

(e) Frame recovered by homomorphic DCT-Wiener filter

Figure 5.3: Qualitative performance of the various filters using 'DC north' sequence

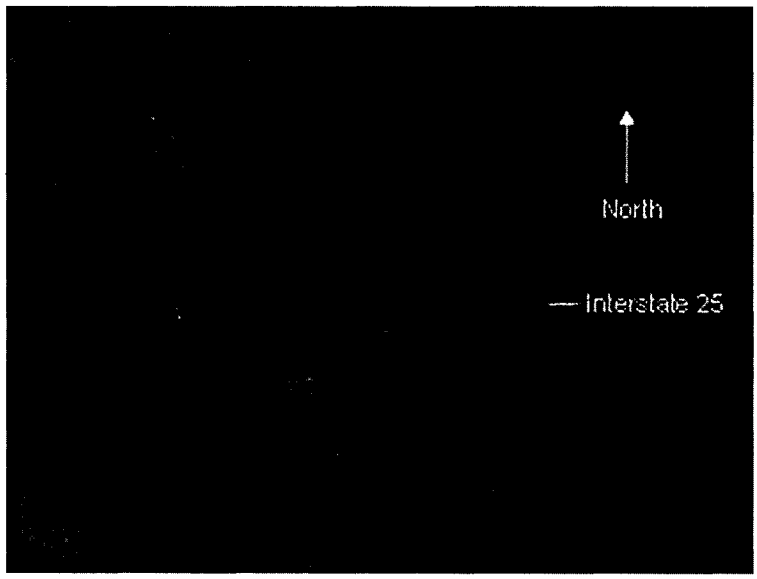

(a) Original 'Gibson west' frame no.7

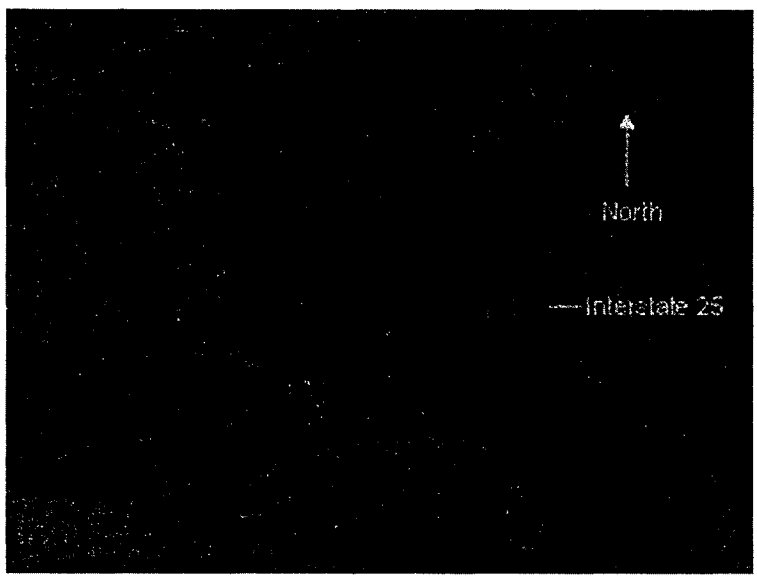

(b) Frame corrupted by speckle (ENL=10)

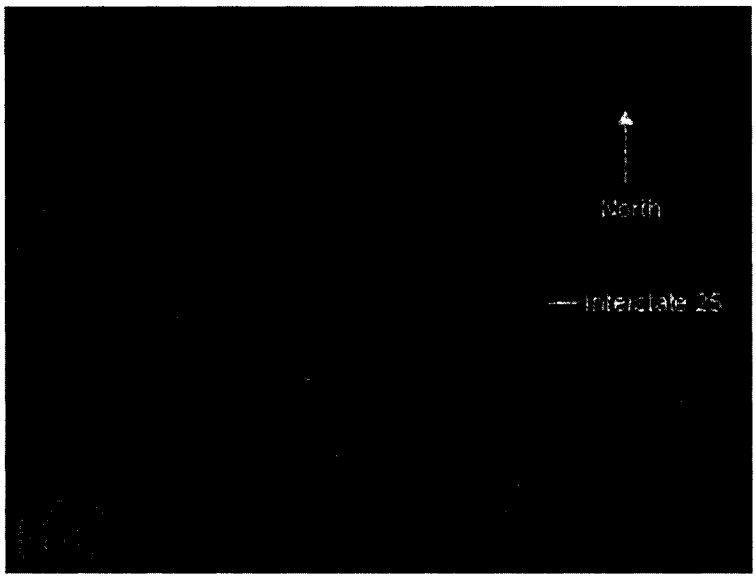

(c) Frame recovered by the proposed system

(d) Frame recovered by Hadamard-Wiener filter

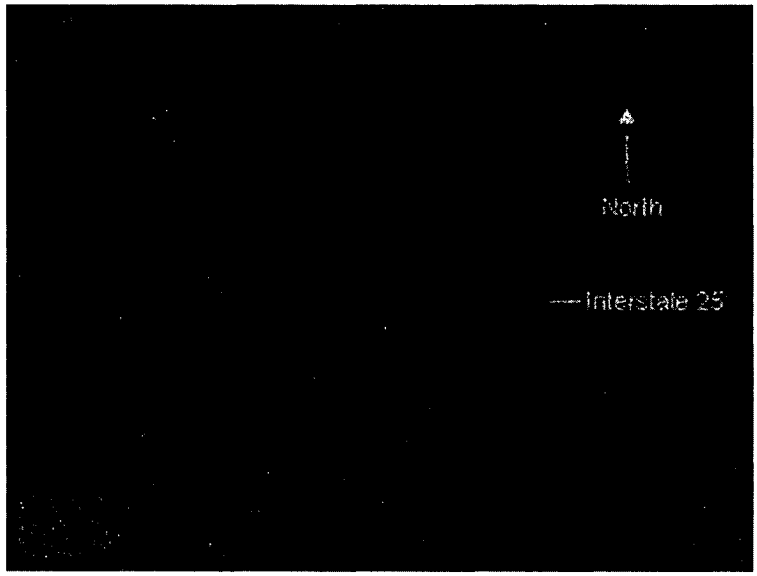

(e) Frame recovered by homomorphic DCT-Wiener filter

Figure 5.4: Qualitative performance of the various filters using 'Gibson west' sequence

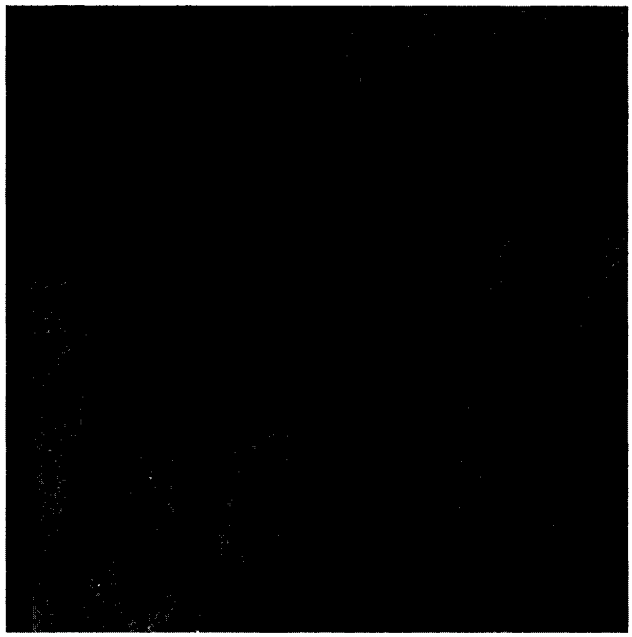

(a) Frame no.5 of a video captured by a coherent system

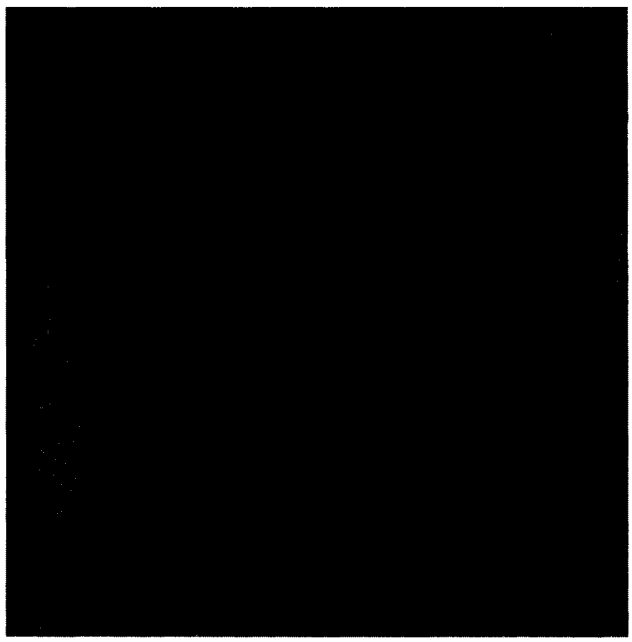

(b) Frame recovered by the proposed system

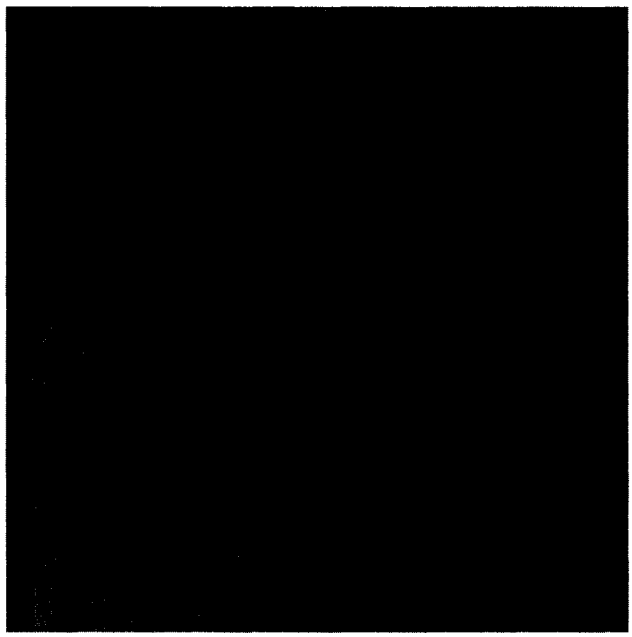

(c) Frame recovered by Hadamard-Wiener filter

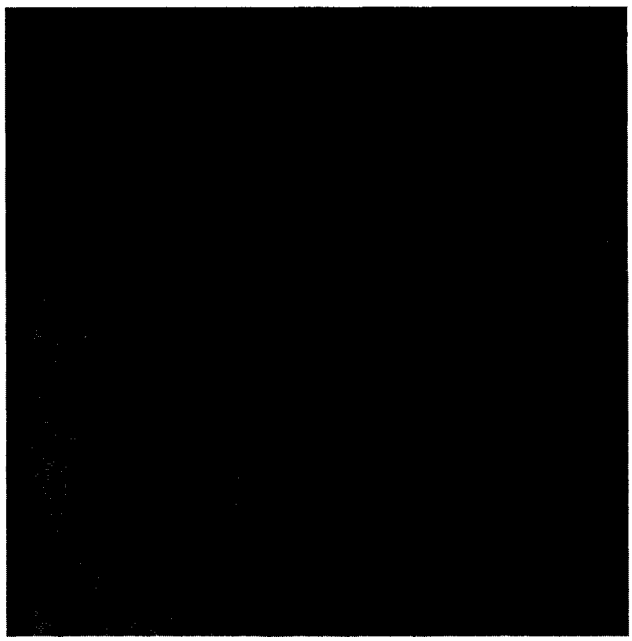

(d) Frame recovered by homomorphic DCT-Wiener filter

Figure 5.5: Qualitative performance of the various filters using a sequence corrupted by speckle of unknown ENL

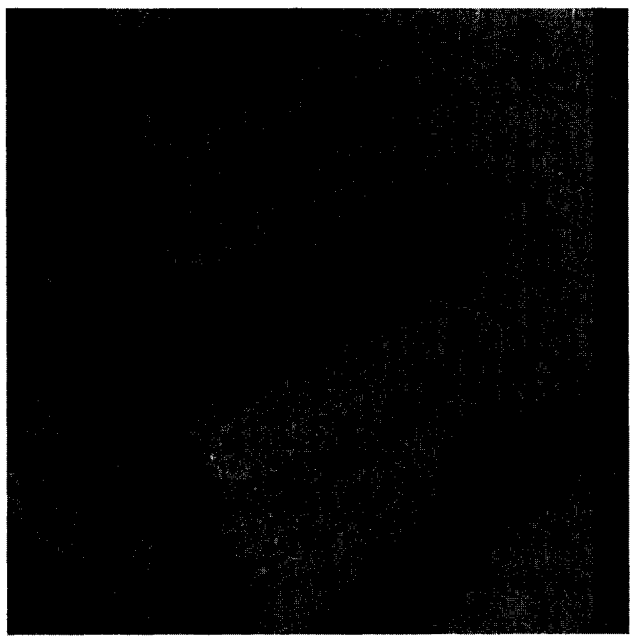

(a) Frame no.7 of a video captured by a coherent system

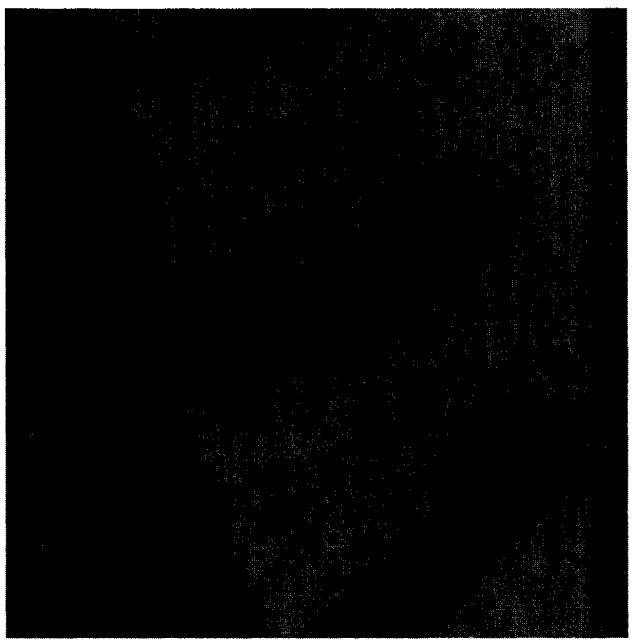

(b) Frame recovered by the proposed system

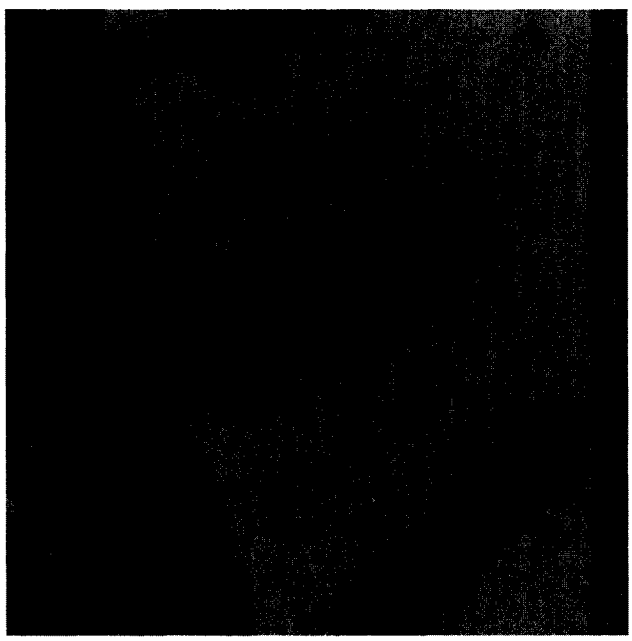

(c) Frame recovered by Hadamard-Wiener filter

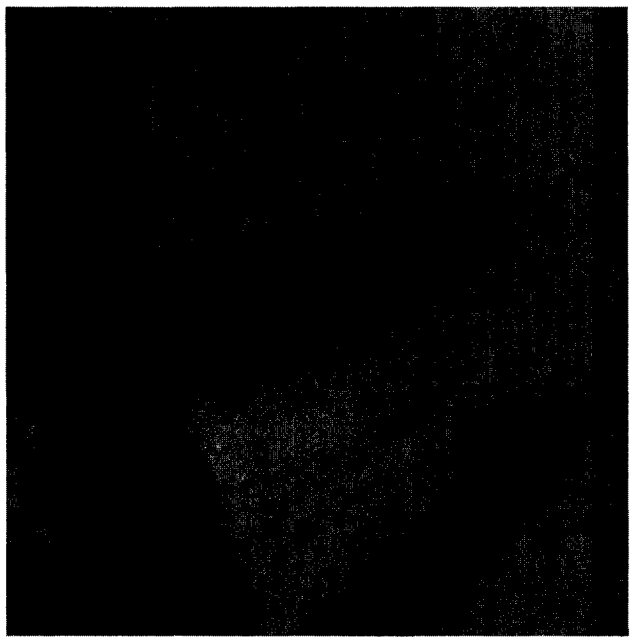

(d) Frame recovered by homomorphic DCT-Wiener filter

Figure 5.6: Qualitative performance of the various filters using a sequence corrupted by speckle of unknown ENL

TABLE 5.1

TIME TAKEN BY THE VARIOUS FILTERS TO PROCESS A FRAME IN ORDER TO REDUCE SPECKLE IN VIDEOS

Sequences→ Filters ↓	DC south $\frac{\text{Sec}}{\text{frame}}$	DC north $\frac{\text{Sec}}{\text{frame}}$	Gibson west $\frac{\text{Sec}}{\text{frame}}$
The proposed homomorphic MM-weighted running average filter	5.484	5.524	5.522
Hadamard-Wiener filter	470.771	471.802	472.617
Homomorphic DCT -Wiener filter	137.153	136.74	138.55

TABLE 5.2

SMSERI OBTAINED BY USING THE VARIOUS FILTERS TO REDUCE SPECKLE IN VIDEOS WHEN THE ENL OF THE INPUT IS 2

Sequences→ Filters ↓	DC south dB	DC north dB	Gibson west dB
The proposed homomorphic MM-weighted running average filter	10.2408	10.1168	10.5733
Hadamard-Wiener filter	7.3878	6.0857	6.8178
Homomorphic DCT -Wiener filter	8.374	7.5345	7.79

TABLE 5.3

SMSERI OBTAINED BY USING THE VARIOUS FILTERS TO REDUCE SPECKLE IN VIDEOS WHEN THE ENL OF THE INPUT IS 5

Sequences→ Filters ↓	DC south dB	DC north dB	Gibson west dB
The proposed homomorphic MM-weighted running average filter	9.7328	9.0204	9.818
Hadamard-Wiener filter	4.4075	2.9502	4.0643
Homomorphic DCT -Wiener filter	6.5944	5.4522	6.3288

TABLE 5.4

SMSERI OBTAINED BY USING THE VARIOUS FILTERS TO REDUCE SPECKLE IN VIDEOS WHEN THE ENL OF THE INPUT IS 10

Sequences→ Filters ↓	DC south dB	DC north dB	Gibson west dB
The proposed homomorphic MM-weighted running average filter	8.6731	7.6825	8.9481
Hadamard-Wiener filter	1.9273	0.3827	1.6508
Homomorphic DCT -Wiener filter	5.6407	3.4776	4.8906

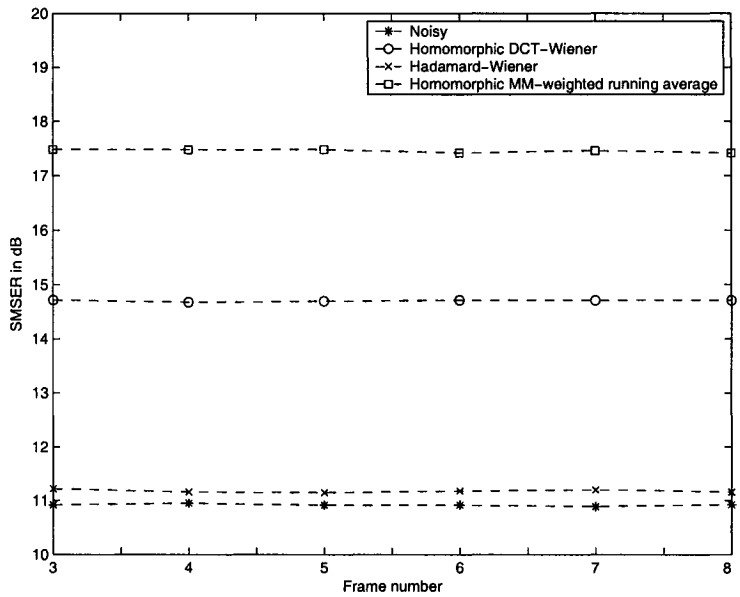

Figure 5.7: SMSER curves for various video filters to reduce speckle using 6 consecutive frames of the 'DC north' sequence

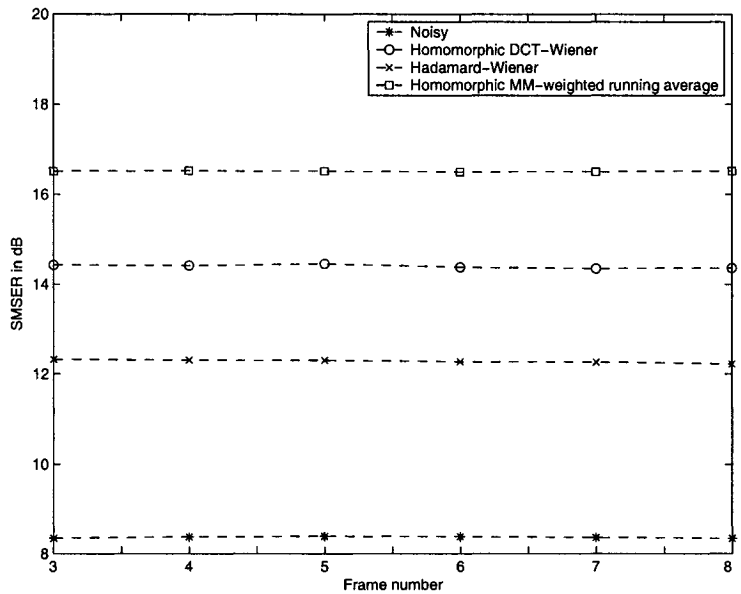

Figure 5.8: SMSER curves for various video filters to reduce speckle using 6 consecutive frames of the 'DC south' sequence

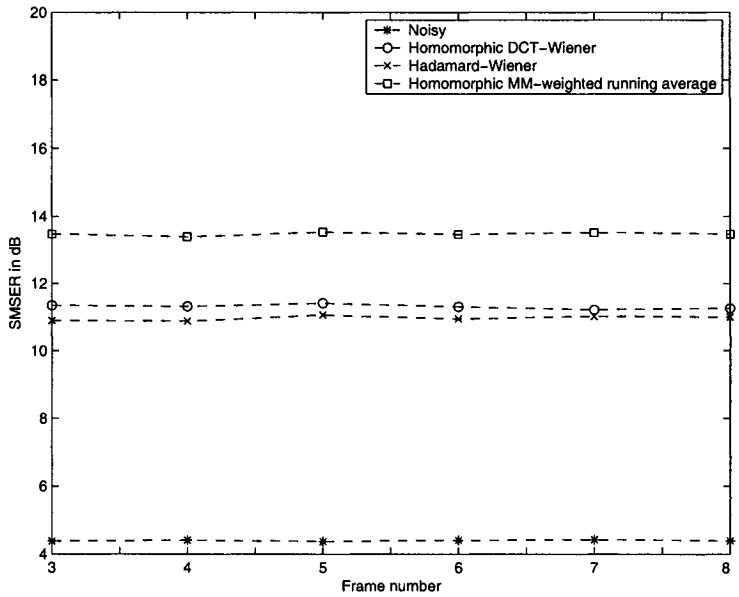

Figure 5.9: SMSER curves for various video filters to reduce speckle using 6 consecutive frames of the 'Gibson west' sequence

The performance of the homomorphic DCT-Wiener filter, even though satisfactory, tends to leave behind noise at the edges. Tables 5.2-5.4 and Figures 5.7-5.9 show that its performance is consistently below that of the proposed one. Although the performance of the Hadamard-Wiener filter with respect to noise reduction is satisfactory, it suffers from the disadvantage that the edges are heavily blurred indicating the filter to be highly sensitive to the errors in motion estimation. It is evident from the various tables and figures that, on a overall basis, the proposed system outperforms the other two both on qualitative and quantitative bases

The most attractive feature of the proposed system is its processing speed. It is evident from Table 5.1, that the proposed system is far ahead in simplicity when compared to the other two filters. This low complexity of the filter could facilitate its implementation in a real time environment.

5.4 Summary

In this chapter, we have proposed a fast unbiased homomorphic system to reduce speckle in videos. A filter, which uses the MM-filter and the 1D weighted running average filter for the spatial and temporal estimation, respectively, is used within an unbiased homomorphic system to achieve the speckle reduction. A study of the quantitative and qualitative performance of the proposed system has been carried out and compared to that of the other existing filters. It has been shown that the proposed system outperforms the others both in terms of the noise reduction capability and the processing time.

Chapter 6

Concluding Remarks

6.1 Conclusions

Multiplicative noise corrupting a signal makes the easily implementable linear systems not suitable for the reduction of such a noise. Nonlinear systems, especially homomorphic systems where a suitable filter is used between the natural logarithm function and the exponentiation, have the potential to deal with the multiplicative noise more effectively. The primary contribution of this thesis has been the development of an order statistics-based unbiased homomorphic system to reduce multiplicative noise.

First, the sample function weighted order (SFWO) filter has been generalized by relaxing the symmetry condition of the probability density function (PDF) of the noise. Then, this generalized SFWO (GSFWO) filter, whose design is based on the PDF of the multiplicative noise, has been used within a homomorphic system to reduce the multiplicative noise. It has been shown that the output from such a homomorphic system is biased, and hence, a suitable bias compensation technique has been proposed. The qualitative and quantitative performance of the proposed system in reducing the multiplicative noise has been studied and compared with that some of the other existing schemes. The proposed system has been found to perform better than the others irrespective of the nature of the

PDF of the multiplicative noise.

The problem of reducing speckle, which is a particular type of multiplicative noise, has been considered next. An unbiased homomorphic system to reduce speckle in images has been proposed. The speckle has been assumed to be white noise with a lognormal distribution. Hence, the application of the natural logarithm function on the speckle transforms it into an additive white Gaussian noise (AWGN). A new filter called the mean median (MM) filter has been proposed to reduce the AWGN in images. The estimation of the original signal by the MM-filter has been carried out by a suitable combination of the mean and median estimates. It has been shown that a combination of these would provide a better estimate than the minimum mean square (MMSE) optimal mean filter, when the signal to the filter is not constant within the filter window. Three criteria have been proposed to combine the mean and median estimates judiciously. The quantitative and the qualitative performance of the MM-filter in reducing the AWGN have been studied and compared with those of the mean filter and the edge-adaptive Wiener filter. The MM-filter is then used within the unbiased homomorphic system instead of the GSFWO filter to reduce the speckle. The quantitative and qualitative performance of the proposed system to reduce the speckle has been analysed and compared with that of some of the existing schemes. It has been found that the proposed system performs better than the others in terms of noise reduction capability and the processing time.

The problem of reducing the AWGN in videos has been considered next and two new filters have been proposed. The two filters use the edge-adaptive Wiener filter as the spatial estimator; however, they differ in the way the temporal estimation has been carried out. In one of them, the temporal estimation is based on the scalar Kalman filter, whereas in the other it is based on the running average filter. A change detection technique has been used to measure the interframe motion in lieu of the commonly applied and complex motion estimation and motion compensation technique. The quantitative and the qualitative results of the proposed filters in reducing the AWGN have been studied and compared with that

of some of the existing ones. The proposed filters have been found to have a significantly high processing speed and to perform better than the others in reducing the AWGN.

Finally, reduction of the speckle noise in videos has been investigated. For this purpose the MM-filter has been used as the spatial estimator within the unbiased homomorphic system. The temporal estimator used in the system is based on the running average filter. The quantitative and the qualitative performance of the proposed system has been studied and compared with that of the two existing ones. The proposed system has been found to perform significantly better in terms of noise reduction and processing speed.

6.2 Scope For Further Investigation

In this thesis, it has been shown that, while reducing an AWGN, a combination of the mean and the median estimates gives a better estimate of the original signal than the MMSE optimal mean filter, when the signal to the filter within the filter window is not constant. It would be desirable to investigate if an optimal combination of the mean and median estimates could be found based on the characteristics of the noise and the uncorrupted signal.

A study on the possible extension of the proposed system to reduce speckle in videos in reducing in videos the multiplicative noise, with PDFs other than the lognormal distribution, could be undertaken.

Finally, it could be worthwhile implementing the proposed filters in VLSI.

Appendix A

This appendix contains the names and the corresponding functions of the MATLAB files used in this thesis and available in a CD-ROM.

- ungsfwo.m → Implementation of the GSFWO filter-based unbiased homomorphic system
- kuan.m → Implementation of the Kuan filter to reduce a multiplicative noise
- hmean.m → Implemetation of the sample mean filter-based homomorphic system
- hmedian.m → Implementation of the sample median filter-based homomorphic system
- hwiener.m → Implementation of the edge-adaptive Wiener filter-based homomorphic system to reduce a multiplicative noise
- uhmean.m → Implemetation of the sample mean filter-based unbiased homomorphic system
- uhmedian.m → Implementation of the sample median filter-based unbiased homomorphic system
- uhwiener.m → Implementation of the edge-adaptive Wiener filter based unbiased homomorphic system

- lnweight.m → Determination of the co-efficients of the GSFWO filter when the multiplicative noise has a lognormal distribution
- gweight.m → Determination of the co-efficients of the GSFWO filter when the multiplicative noise has a Gaussian distribution
- uweight.m → Determination of the co-efficients of the GSFWO filter when the multiplicative noise has a uniform distribution
- fom.m → Calculation of the FOM value
- lf.m → Implementation of the Lee filter
- kf.m → Implementation of the Kuan filter to reduce speckle
- ff.m → Implementation of the Frost filter
- gf.m → Implementation of the gamma filter
- hawf.m → Implementation of the edge-adaptive filter-based homomorphic system to reduce speckle
- hmmfc1.m → Implementation of the MM-filter-based unbiased homomorphic system where the MM-filter is based on Criterion 1.
- hmmfc2.m → Implementation of the MM-filter-based unbiased homomorphic system where the MM-filter is based on Criterion 2.
- hmmfc3.m → Implementation of the MM-filter-based unbiased homomorphic system where the MM-filter is based on Criterion 3.
- mmfc1.m → Implementation of the MM-filter based on Criterion 1.
- mmfc2.m → Implementation of MM-filter based on Criterion 2.
- mmfc3.m → Implementation of the MM-filter based on Criterion 3.

- meanf.m → Implementation of the sample mean filter
- awf.m → Implementation of the edge-adaptive Wiener filter
- rat.m → Implementation of the rational filter
- wwraf.m → Implementation of the Wiener-weighted running average filter
- wwwkf.m → Implementation of the Wiener-weighted scalar Kalman filter
- atf.m → Implementation of the α-trimmed filter
- knn.m → Implementation of the K nearest neighborhood filter
- awa.m → Impelementation of the adaptive weighted averaging filter
- wkf.m → Implementation of the Wiener-Kalman filter
- hadw.m → Implementation of the Hadamard-Wiener filter
- ebma.m → Implementation of the exhaustive block matching algorithm for motion estimation
- mcp.m → Implementation of the motion compensation algorithm
- uhmmwwraf.m → Implementation of the MM-filter and weighted running average filter based unbiased homomorphic system
- dctw.m → Implementation of the DCT-Wiener filter

References

[1] I. Pitas and A. N. Venetsanopoulis, Nonlinear Digital Filters: Principles and Applications, Norwell, MA: Kluwer, 1990.

[2] J. Astola and P. Kousmanen, Fundamentals of Nonlinear Digital Filtering, Boca Raton, FL: CRC, 1997.

[3] R. W. Hamming, Digital Filters, 2nd ed., Englewood Cliffs, NJ : Prentice-Hall, Prentice-Hall signal processing series, 1983.

[4] A. K. Jain, Fundamentals of digital image processing, Prentice hall information and system science series, 1989.

[5] R. Öten and R. J. P. de Figueiredo, "Sampled-function weighted order filters", IEEE Transaction on Circuits and Systems II: Analog and Digital Signal Processing, Vol. 49, No. 1, pp. 1-10, January 2002.

[6] L. Gagnon and A. Jouan, "Speckle filtering of SAR images - A comparative study between complex wavelet-based and standard filters", Department of R&D, Lockheed Martin, Canada, 1997.

[7] S. J. Lim, Two-Dimensional Signal and Image Processing, Englewood Cliffs, NJ: Prentice Hall, 1990.

[8] Y. Wang, J. Ostermann and Y.-Q. Zhang, Video Processing and Communications, Prentice Hall Signal Processing Series, 2002.

[9] E. Hervet, R. Fjortoft, P. Marthon and A. Lopes, "Comparison of wavelet-based and statistical speckle filters", EUROPTO conference on SAR Image Analysis, Modeling, and Techniques, Barcelona, Spain, Vol. SPIE 3497, September 1998.

[10] L. Gagnon, H. Oppenheim and P. Valin, "R&D activities in airborne SAR image processing/analysis at Lockheed Martin, Canada - R&D department", Lockheed Martin Canada, Montréal, Canada, 1998.

[11] D. Kuan, A. Sawchuk, T. Strand and P. Chavel, "Adaptive restoration of images with speckle", IEEE Transactions on Acoustics, Speech, and Signal Processing, Vol. 35, No. 3, pp. 373-383, March 1987.

[12] V. S. Frost, J. A. Stiles, K. S. Shanmugan and J. C. Holtzman, "A model for radar images and its application to adaptive digital filtering of multiplicative noise", IEEE Transactions on Pattern Analysis and Machine Intelligence, vol. PAMI-4, pp. 157-166, 1982.

[13] J. S. Lee, "Speckle analysis and smoothing of synthetic aperture radar images", Computer Graphics and Image Processing, vol. 17, pp. 24-32, 1981.

[14] A. Lopes, E. Nezry, R. Touzi, H. Laur, "Structure detection and statistical adaptive speckle filtering in SAR images", International Journal of Remote Sensing, Vol. 14, No. 9, pp. 1735-1758, June 1993.

[15] D. Sen, M. N. S. Swamy and M. O. Ahmad, "Order statistics-based unbiased homomorphic system to reduce multiplicative noise", in the proceedings of European Signal Processing Conference, 2005.

[16] D. Sen, M. N. S. Swamy and M. O. Ahmad, " Unbiased homomorphic system and its application in multiplicative noise reduction", under preparation for a journal submission.

[17] R. C. Gonzalez and R. E. Woods, Digital Image Processing, Second Edition, Pearson Education, 2002.

[18] F. Mosteller, "On some useful inefficient statistics", Annals of Mathematics and Statistics, Vol. 17, pp. 377-408, 1946.

[19] G. Gregorcic, "The singular value decomposition and the pseudoinverse", Department of Electrical Engineering, University College Cork, Ireland, 2001.

[20] C. S. Cleghorn, "Application of generalized inverses and circulant matrices to iterated functions on integers", Department of Mathematics, Angelo State University, San Angelo, Texas, U.S, 2001.

[21] S. M. Kay, Fundamentals of Statistical Signal Processing, Estimation Theory: Prentice Hall Signal Processing Series, 1993.

[22] H. L. Van Trees, Detection, Estimation and Modulation Theory - Part I, John Wiley and Sons, 2001.

[23] A. Papoulis and S. U. Pillai, Probability, Random Variables, and Stochastic Processes, Fourth edition, McGrawHill, 2002.

[24] D. Kuan, A. Sawchuk, T. Strand and P. Chavel, "Adaptive noise smoothing filter for images with signal-dependent noise", IEEE Transactions on Pattern Analysis and Machine Intelligence, Vol. PAMI-7, pp. 165-177, March 1985.

[25] J. W. Turkey, "Nonlinear (nonsuperposable) methods for smoothing data", in Cong. Rec. EASCON' 74, pp. 673, 1974.

[26] V. Wanpiyarat, D. Buapradupkul and S. Chutirattanaphan, "Potential use of airborne Synthetic Aperture Radar to monitor agricultural land uses - A case study in Thailand", Office of soil survey and land use planning, Department of land development, Bangkok, Thailand, 1997.

[27] Sandia national laboratories, U.S.A. (http://www.sandia.gov/RADAR).

[28] J. W. Goodman, Speckle phenomenon in optics: theory and applications, 2004.

[29] D. Sen, M. N. S. Swamy and M. O. Ahmad, "An unbiased homomorphic system to reduce speckle in images", submitted to European Conference on Circuit Theory and Design, 2005.

[30] I. E. Abdou, W. K. Pratt, "Quantitative Design and Evaluation of Enhancement/Thresholding Edge Detectors". Proc. IEEE, Vol. 67, pp. 753-763, 1979.

[31] P. J. Huber, Robust Statistics, Wiley Series in Probability and Mathematical Statistics, John Wiley & Sons, Inc., 1981.

[32] S. M. Stigler, "The asymptotic distribution of the trimmed mean", Annals of Statistics, Vol. 1, No. 3, pp. 472-477, 1973.

[33] M. Stevens, Dave Dominy and Stuart young, Real time SAR processing in GEDAE, THALES group, 2004.

[34] I. D. Scherson, Sandeep Sen, "Parallel Sorting in two-dimensional VLSI models of computation", IEEE Transaction on Computers, Vol. 38, No. 2, Febraury 1989.

[35] V. Zlokolica, W. Philips and D. Van De Ville, "Robust non-linear filtering for video processing", 14th International Conference on Digital Signal Processing, Vol. 2, pp. 571-574, 1-3 July 2002.

[36] D. Sen, M. N. S. Swamy and M. O. Ahmad, " Fast AWGN reduction in videos using change detection", under preparation for a conference submission.

[37] D. Sen, M. N. S. Swamy and M. O. Ahmad, " Novel techniques to reduce AWGN and speckle in videos", under preparation for a journal submission

[38] F. Cocchia, S. Carrato and G. Ramponi, "Design and real-time implementation of a 3-D rational filter for edge preserving smoothing", IEEE Transactions on Consumer Electronics, Vol. 43, No. 4, pp. 1291-1300, November 1997.

[39] M. K. Ozkan, M. I. Sezan and A. M. Tekalp, "Adaptive motion-compensated filtering of noisy image sequences", IEEE Transactions on Circuits and Systems for Video Technology, Vol. 3, No. 4, pp. 277-290, August 1993.

[40] R. Dugad and N. Ahuja, "Video denoising by combining Kalman and Wiener estimates", International Conference on Image Processing, Vol. 4, pp. 152-156, 24-28 October 1999.

[41] K. J. Boo and N. K. Bose, "A motion-compensated spatio-temporal filter for image sequences with signal-dependent noise", IEEE Transactions on Circuits and Systems for Video Technology, Vol. 8, No. 3, pp. 287-298, June 1998.

[42] M. Ceccarelli and A. Petrosino, "High performance motion analysis for video restoration", 14th International Conference on Digital Signal Processing, Vol. 2, pp. 689-692, 1-3 July 2002.

[43] E. Cheever, "The scalar Kalman filter", Swarthmore College, Pennsylvania, U.S.A. (http://www.swarthmore.edu/NatSci/echeeve1/Ref/Kalman/ScalarKalman.html).

[44] G. Welch and G. Bishop, "An introduction to Kalman filter", TR 95-041, Department of Computer Science, University of North Carolina, USA, 2004.

[45] J. Kneip, S. Bauer, J. Vollmer, B. Schmale, P. Kuhn and M. Reissmann, "The MPEG-4 video coding standard-a VLSI point of view", IEEE Workshop on Signal Processing Systems, pp. 43-52, 8-10 October 1998.

[46] L. Li and M. K. H. Leung, "Robust change detection by fusing intensity and texture differences", Proceedings of the 2001 IEEE Computer Society Conference on Computer Vision and Pattern Recognition, Vol. 1, pp. I-777 - I-784, 8-14 December 2001.

[47] I. Niemeyer, M. Canty and D. Klaus, "Unsupervised change detection techniques using multispectral satellite images", Geoscience and Remote Sensing Symposium, Vol. 1, pp. 327-329, 28 June-2 July, 1999.

[48] M. I. Sezan, M. K. Ozkan, and S. V. Fogel, "Temporally adaptive filtering of noisy image sequences using a robust motion estimation algorithm", IEEE international conference on Acoustics, Speech and Signal Processing, Toronto, Canada, pp. 2429-2432, May 1991.

[49] D. Sen, M. N. S. Swamy and M. O. Ahmad, "A homomorphic system to reduce speckle in videos", in the proceedings of International Geoscience and Remote Sensing Symposium, 2005.

[50] D. Coltuc, E. Trouve, F. Bujor, N. Classeau and J. P. Rudant, "Time-space filtering of multitemporal SAR images", Geoscience and Remote Sensing Symposium, Vol. 7, pp. 2909-2911, 24-28 July 2000.

[51] A. N. Evans and M. S. Nixon, "Temporal methods for ultrasound speckle reduction", In Proceedings of Seminar on Texture Analysis in Radar and Sonar, pp. 1/1-1/6, 1993.